STUDIES ON PRIMATE EXTRASTRIATE VISUAL CORTEX

I. THE INTERHEMISPHERIC CONNECTIONS OF VISUAL CORTEX IN THE OWL MONKEY, AOTUS TRIVIRGATUS, AND THE BUSHBABY, GALAGO SENEGALENSIS

II. A FUNCTIONAL LOCALIZATION OF NEURONAL RESPONSE PROPERTIES IN EXTRASTRIATE CORTEX OF THE OWL MONKEY, AOTUS TRIVIRGATUS

Thesis by

William Thomas Newsome III

In Partial Fulfillment of the Requirements

For the Degree of

Doctor of Philosophy

California Institute of Technology

Pasadena, California

1980

(Submitted August 15, 1979)

ACKNOWLEDGEMENTS

I would like to express sincere gratitude to three persons in particular who have contributed greatly to my development as a neurobiologist during the years of work toward this thesis. My advisor, Dr. John Allman, was constantly involved in all stages of the work presented in this thesis, and I am indebted to him for his generous sharing of ideas and insight, for many hours of personal instruction and training and for use of his laboratory facilities. I am grateful to Dr. David Van Essen for his sure guidance and thoughtful advice during the conception, execution and interpretation of the interhemispheric connections study, and for the unlimited use of his histology facilities which I enjoyed. I also express my deep appreciation to Dr. James Baker whose day-to-day advice and assistance covered the spectrum of problems encountered by a graduate student - faculty committees, technical quandaries, photography, figure-drawing, writing, post-doc applications, etc.

The work presented in Chapter II is the result of a collaborative effort, and I warmly acknowledge the full participation of Dr. James Baker and Mr. Steve Petersen in all aspects of the study. The excitement and drudgery of long recording sessions, the pleasure and frustration of data analysis, and the consumption of vast quantities of beer were shared experiences in a rewarding research effort. In addition, I thank Mr. Francis Miezin for the design and implementation of the computer programs which enabled us to perform the quantitative studies.

I also thank Dr. James Hudspeth for helpful advice and encouragement during some of the tougher months of my thesis work. Dr. Hudspeth's perspicacity and magnanimity in his sharing of microscope facilities, medical advice and scatological taunts were most appreciated. Dr. Henry Lester should know that the hours he spent teaching to me the basics of cellular neurophysiology are neither unremembered nor unappreciated. Drs. Brockes, Konishi and Pettigrew have

made valuable contributions to my graduate experience as they have served on my thesis committee.

I am particularly grateful to my wife, Zondra, for the common life which I have been privileged to share with her over the last six years. The meaningful and growing relationship we have had during this time has greatly enhanced all my efforts as a scientist and as a person. I am also profoundly indebted to my parents whose love and sacrifice have, in large measure, afforded me the opportunity to develop my mind and talents to such a degree.

Finally, I tip my hat to the men and women of Fleming House who have done their utmost to keep me from becoming overly toadly during these years of thesis work.

The financial assistance of the Danforth and Spencer Foundations, the McCallum and Weigle Funds, and NIH Grant NS00178 to J. M. Allman is gratefully acknowledged. The patience and skill of Connie Katz of the Division of Biology typing pool greatly smoothed the typing and final preparation of this thesis.

ABSTRACT

Anatomical techniques have been used to map within visual cortex the pattern of degenerating axonal terminals produced by surgical section of the splenium of the corpus callosum in the owl monkey, Aotus trivirgatus, and the bushbaby, Galago senegalensis. To the extent to which degenerating callosal terminals correspond to physiological representations of the visual vertical meridian, the pattern of interhemispheric connections can be used as a powerful aid in locating visual area boundaries. The goals of this study have been 1) to assess the degree of correspondence between degenerating callosal terminals and anatomically identifiable vertical meridian representations, and 2) to gain information concerning the existence and organization of as yet unknown extrastriate visual areas. In both the owl monkey and the bushbaby, a discrete band of degeneration corresponds precisely to the vertical meridian representation at the V1-V2 border, and a less precise increase in the density of axonal terminals corresponds to the vertical meridian representation of extrastriate area MT. A well-defined band of degeneration on the ventral surface of the owl monkey's cerebral hemisphere corresponds to a previously unknown vertical meridian representation which is shared by two newly defined extrastriate visual areas. Over much of areas DL and DI in the owl monkey, and in the region where the center-of-gaze representations of V2, DL and MT are in close proximity in both the owl monkey and the bushbaby, the pattern of callosal terminals is complex and has little value for determining precise areal boundaries.

The response properties of 275 single neurons from four extrastriate visual areas have been quantitatively studied in chronically prepared, sedated owl monkeys. During experimental sessions, computer controlled visual stimuli were presented to the animal while the computer recorded the responses of single

cortical neurons. The responses were stored on magnetic tape for later analysis. The major result of this study is the demonstration of a striking localization of direction-selective neurons to extrastriate area MT of the owl monkey. MT neurons responded maximally to stimuli tuned to a single optimal direction of motion whereas neurons of the medial third tier areas (DM, DI and M) responded maximally to oriented stimuli moving in either of two directions perpendicular to the optimal axis of orientation. Other differences were noted between neurons of MT and neurons of the medial third tier areas. A systematic difference exists in the tightness of tuning to the optimal direction of motion. Neurons in MT tended to be less well tuned to the optimal direction of motion than did neurons of the medial third tier areas. Neurons in MT also exhibited a different pattern of preferences for stimulus velocity than did neurons of the medial third tier areas. A distinct group of MT cells preferred velocities of 10-25 degrees/second, while neurons of the medial third tier areas had a broad distribution of preferred velocities ranging from 10-100 degrees/second. There was no systematic difference in tuning to preferred velocity for the two regions.

Table of Contents

GENERAL INTRODUCTION

Since Charles Bell and F. J. Gall first developed the notion in a systematic manner early in the nineteenth century, the doctrine of cerebral localization of function has been a dominant conceptual theme shaping the thrust of scientific brain research. Although their specific applications of the doctrine proved in some instances to be erroneous, their fundamental ideas concerning the localization of specific nervous functions to well-defined regions of the central nervous system were seminal and have in the intervening years inspired a prodigious amount of scientific research and debate, both for and against. General acceptance of the "localist" ideas was far from immediate. The suggestive work of a few isolated anatomists and brain surgeons notwithstanding, the dominant view of the times held that the brain was a unitary, homogeneous and indivisible mass subserving a unitary, indivisible soul. This "delocalist" view received influential scientific support from the widely acclaimed work of P. J. M. Fluorens. Fluorens, while recognizing the functional specialization of the three major divisions of the brain (brainstem, cerebellum, and cerebrum), held that his experiments on the behavioral effects of controlled cortical ablations demonstrated an absence of any localization of function within the organ of "perception and will"—the cerebral hemispheres. Thus, the principle of "functional equivalence" was reinforced as the prevalent view of cerebral function. Despite the dominating influence of Fluoren's work, the next fifty years witnessed a slowly growing momentum for acceptance of "localist" ideas due to the work of such independent-minded students of the brain as Baillarger, Bouillaud, Broca, Meynert and Hughlings Jackson. The localist ideas finally gained widespread respect, if not acceptance, with the discovery of the precentral motor area in the dog by Fritsch and Hitzig in 1870. Although formidable opposition was maintained in various circles for many years,

the overwhelming weight of ensuing anatomical, physiological and clinical work has demonstrated the power and essential correctness of the localist doctrine (for discussion see Polyak, 1957, and Diamond, 1979).

Identification of the occipital lobes as the cortical site of visual information processing followed quickly once localist thought became widespread. Gratiolet's early (1854) dissection experiments furnished evidence for the selective termination of an optic projection within the occipital lobes, but the idea did not gain wide acceptance until the results of clinical and anatomical studies by Munk, Ferrier, and Starr became well known. The accumulating evidence for localization of visual function to the occipital lobes became compelling with the myelogenetic studies of Flechsig. Flechsig, by studying the development of the myelin sheaths of various fiber tracts within the brain, was able to identify the primary cortical centers of vision, audition, and somesthesis in addition to other cortical areas. He also identified several "association" areas which presumably were involved in the elaboration and integration of the sensory information derived from the primary areas. Among these was a visual association area lying directly anterior to most of striate cortex, which Flechsig considered to be the substratum of higher visual functions (for references to Flechsig's work, see Polyak, 1957). Work by many scientists in the first half of the twentieth century established the striate cortex as the primary visual sensory area and elucidated the topographic nature of the representation of visual space within the primary area. However, knowledge of the surrounding visual "association" area progressed little beyond the general notions developed by Flechsig.

In the past thirty years, powerful new physiological and anatomical techniques have stimulated a wealth of experimental studies on the organization and function of the mammalian visual system. Some major functions of striate

cortex in the processing of visual information have become clear as a result of many intensive investigations, most notably those of Hubel and Wiesel (1977). Increasingly now attention is being given to the visual "association" area of Flechsig. Cortex lying in this region immediately anterior to striate cortex yields robust physiological responses to visual stimuli, and is now generally known as extrastriate visual cortex. The major task before the student of extrastriate cortex can once again be cast in the light of the doctrine of cerebral localization of function. What specific functions are performed in the interpretation of visual information by neural tissue in this region? Are particular functions localized to specific subareas within the region? How might the experimentalist reasonably subdivide extrastriate cortex into such functionally distinct units? Some tentative answers to each of these questions have begun to emerge, but much remains obscure.

The experimental studies reported in this thesis may be viewed within the historical perspective outlined in the preceding paragraphs. They were designed to advance our knowledge of the regional organization of primate extrastriate cortex and of the specific functions performed by particular regions. To this end, two primate species were chosen for investigation. The owl monkey, Aotus trivirgatus, is a small New World monkey which offers the advantages of 1) a relatively smooth cortex which greatly simplifies the experimental problems involved in its study, and 2) a decade of previous research by Allman and Kaas (1971a,b, 1974a,b, 1975, 1976) into the basic organization of its extrastriate cortex thus allowing the current investigations to ask relatively more advanced questions. The bushbaby, Galago senegalensis, is a small strepsirhine primate which also offers the advantages of a smooth brain and previous experimental study (Allman et al., 1973; Allman et al., 1979; Myerson et al., 1979). In addition, the bushbaby promises to be a species of particular evolutionary interest because the strepsirhine

primates have, in general, retained many features characteristic of primitive primate species (Hill, 1953; Allman, 1977).

The first study reported in this thesis is an investigation of the interhemispheric connections of visual cortex in the owl monkey and the bushbaby. The study of interhemispheric connections has proven useful in identifying boundaries of individual extrastriate areas in the macaque monkey (Zeki, 1969, 1970; Zeki and Sandeman, 1976; Van Essen and Zeki, 1978), and in my hands the technique has led to the tentative identification of two previously unknown extrastriate areas on the ventral surface of the owl monkey's occipital lobe. The second study reported in the thesis, performed in collaboration with other workers in John Allman's laboratory, employs the technique of single unit recording to assess the functional properties of neurons in identified extrastriate areas of the owl monkey's visual cortex. We have demonstrated a localization of functional properties to particular areas within extrastriate visual cortex.

REFERENCES

Allman, J. M. (1977). Evolution of the visual system in the early primates. In Progress in Psychobiology and Physiological Psychology, Vol. 7, eds. Sprague, J. M. and Epstein, A. N. New York: Academic Press.

Allman, J. M. and Kaas, J. H. (1971a). A representation of the visual field in the caudal third of the middle temporal gyrus of the owl monkey (Aotus trivirgatus). Brain Research **31**, 85-105.

Allman, J. M. and Kaas, J. H. (1971b). Representation of the visual field in striate and adjoining cortex of the owl monkey (Aotus trivirgatus). Brain Research **35**, 89-106.

Allman, J. M. and Kaas, J. H. (1974a). The organization of the second visual area (VII) in the owl monkey: A second order transformation of the visual hemifield. Brain Research **76**, 247-265.

Allman, J. M. and Kaas, J. H. (1974b). A crescent-shaped cortical visual area surrounding the middle temporal area (MT) in the owl monkey (Aotus trivirgatus). Brain Research **81**, 199-213.

Allman, J. M. and Kaas, J. H. (1975). The dorsomedial cortical visual area: A third tier area in the occipital lobe of the owl monkey (Aotus trivirgatus). Brain Research **100**, 473-487.

Allman, J. M. and Kaas, J. H. (1976). Representation of the visual field on the medial wall of occipital-parietal cortex in the owl monkey. Science **191**, 572-575.

Allman, J. M., Campbell, C. B. G. and McGinness, E. (1979). The dorsal third tier area in Galago senegalensis. Submitted for publication.

Allman, J. M., Kaas, J. H. and Lane, R. H. (1973). The middle temporal visual area (MT) in the bushbaby, Galago senegalensis. Brain Research **57**, 197-202.

Diamond, I. T. (1979). The subdivisions of neocortex: A proposal to revise the traditional view of sensory, motor, and association areas. In Progress in Psychobiology and Physiological Psychology, Vol. 8, eds. Sprague, J. M. and Epstein, A. N. In press.

Hill, W. C. O. (1953). Primates. Comparative Anatomy and Taxonomy. I. Strepsirhini. Edinburgh: University of Edinburgh Press.

Hubel, D. H. and Wiesel, T. N. (1977). Functional architecture of macaque monkey visual cortex. Proceedings of the Royal Society, London, Series B **198**, 1-59.

Myerson, J., Kaas, J. H. and Allman, J. M. (1979). The visuotopic organization of the geniculo-striate system in Galago senegalensis. In preparation.

Polyak, Stephen (1957). The Vertebrate Visual System. Chicago: University of Chicago Press.

Van Essen, D. C. and Zeki, S. M. (1978). The topographic organization of rhesus monkey prestriate cortex. Journal of Physiology (Lond.) **277**, 193-226.

Zeki, S. M. (1969). Representation of central visual fields in prestriate cortex of monkey. Brain Research **14**, 271-291.

Zeki, S. M. (1970). Interhemispheric connections of prestriate cortex of monkey. Brain Research **19**, 63-75.

Zeki, S. M. and Sandeman, D. R. (1976). Combined anatomical and electrophysiological studies on the boundary between the second and third visual areas of rhesus monkey cortex. Proceedings of the Royal Society, London, Series B **194**, 555-562.

I. THE INTERHEMISPHERIC CONNECTIONS OF VISUAL CORTEX IN THE OWL MONKEY, *AOTUS TRIVIRGATUS*, AND THE BUSHBABY, *GALAGO SENEGALENSIS*

INTRODUCTION

Allman and Kaas have performed an extensive series of topographic mapping studies of extrastriate visual cortex in the owl monkey (Allman and Kaas, 1971a,b, 1974a,b, 1975, 1976). These investigations have led to the identification of six extrastriate visual areas, at least five of which contain a complete representation of the contralateral visual hemifield. It seems likely that such discrete representations of the visual field indicate functional differences between the individual areas and should therefore be considered fundamental subunits of extrastriate cortex. The organization of these extrastriate visual areas of the owl monkey can be seen in Figure 1. The second visual area, V2, surrounds striate cortex, or V1, on the exposed surface of the occipital lobe, and these two areas share a common representation of the vertical meridian of the visual field. V2 is characterized by a split representation of the horizontal meridian (termed a second-order transformation of the visual field by Allman and Kaas, 1974a) such that the representation of the upper visual field in V2 is not physically continuous with the representation of the lower field beyond about five degrees of eccentricity. Anterior to V2 lies a third tier of visual areas each of which shares a partial representation of the horizontal meridian with V2. Anterior to one of the third tier areas, DL, lies yet another discrete visual area, MT. MT and DL are, respectively, first-order and second-order transformations of the visual field, and together they form a small mirror image of the V1-V2 region.

Another useful approach to the study of extrastriate cortex has been the study of the interhemispheric connections of the occipital lobe. The interhemispheric input to the occipital lobe may be visualized by staining serial sections for anterograde degeneration following transection of the splenium of the corpus callosum (Pandya et al., 1971). In a variety of mammals, the interhemispheric

Figure 1. Topographic organization of visual cortex in owl monkey as revealed by electrophysiological mapping studies of Allman and Kaas. At the top is a ventromedial view of the right hemisphere of the brain, at the bottom is a dorsolateral view of the whole brain. The visual field symbols on the perimeter chart are superimposed on the cerebral cortex to illustrate the representation of the visual field in the individual visual areas. The open circles symbolize representations of the vertical meridian, filled squares denote representations of the horizontal meridian, and the filled triangles locate representations of the periphery of the visual field. Pluses symbolize the upper visual field, minuses the lower field. Dashed lines are borders where visual field locations are represented other than the ones which are illustrated by symbols in the perimeter chart. The row of V's represents the approximate anterior border of visual cortex, and dotted lines broken by question marks are uncertain borders. (DI, dorsointermediate area; DL, dorsolateral crescent; IT, inferotemporal cortex; M, medial area; MT, middle temporal area; ON, optic nerve; OT, optic tectum; PP, posterior parietal cortex; T, tentorial area, as yet incompletely mapped; X, optic chiasm.) From Allman (1977).

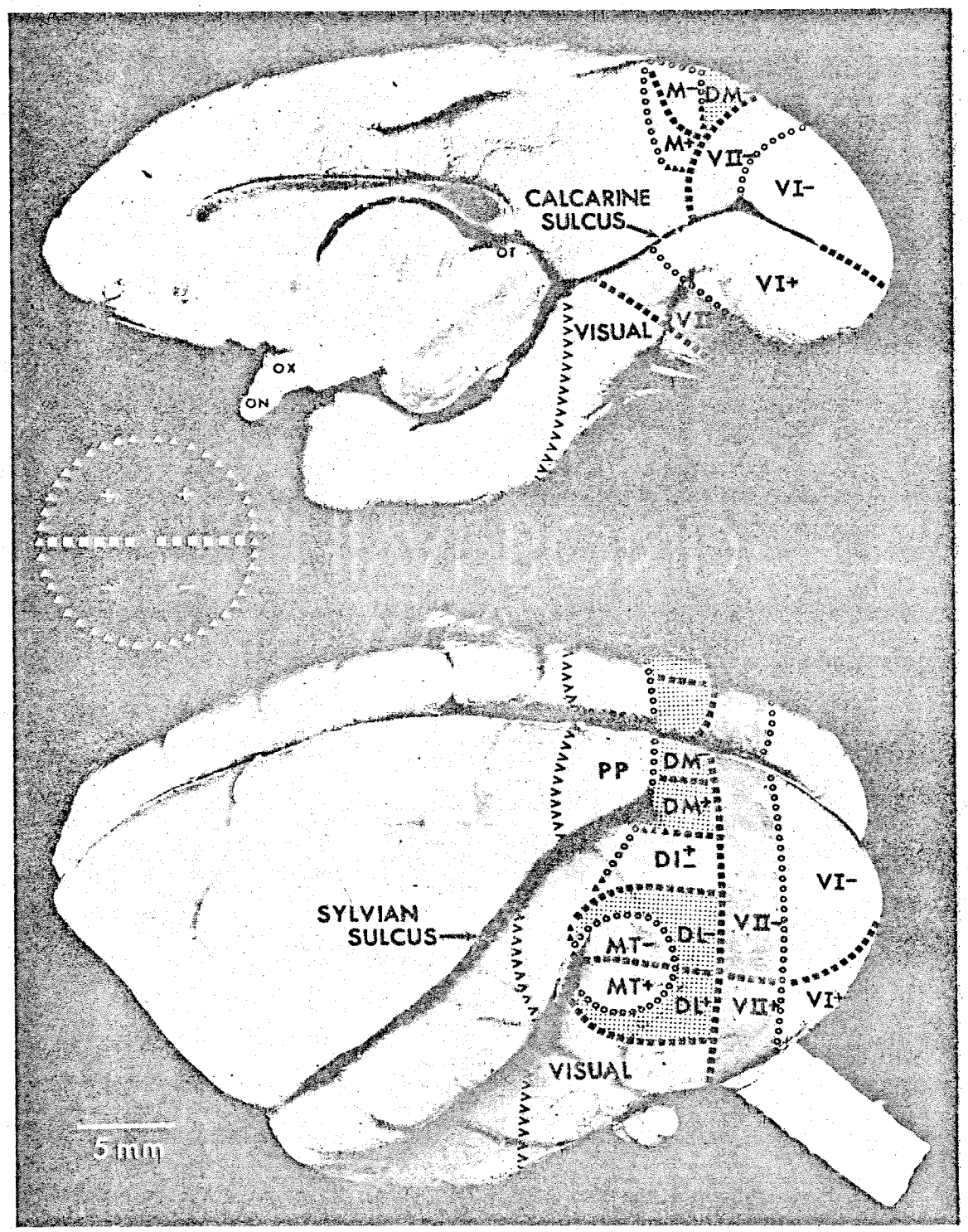
M−DM
M+
VII−
VI−
CALCARINE SULCUS
OT
VI+
VISUAL
VI
OX
ON
PP
DM−
DM+
DI±
VI−
SYLVIAN SULCUS
VII−
MT−
DL−
MT+
DL+
VII+
VI+
VISUAL
5 mm

input is of a patchy, nonhomogeneous nature such that it is possible to divide extrastriate cortex into areas possessing or areas lacking extensive callosal input. It has been demonstrated in raccoon (Ebner and Meyers, 1965), cat (Ebner and Myers, 1965; Shatz, 1977) and macaque monkey (Myers, 1962; Zeki, 1969, 1970) that a discrete band of callosal input is present at the striate-extrastriate boundary, a cortical site of the representation of the vertical meridian of the visual field. These observations have led to the idea that the fibers involved in the transmission of visual information between the hemispheres preferentially perform the task of creating a unified representation of the entire visual field by connecting the separate hemispheric half-field representations along the length of the vertical meridian. Electrophysiological evidence supporting this idea has come from two sources. Recordings within the corpus callosum of the cat have shown that only visual stimuli near the vertical meridian are capable of driving callosal fibers (Hubel and Wiesel, 1967). When direct retinothalamic input to a hemisphere is interrupted by cutting the ipsilateral optic tract, again, only vertical meridian stimulation is effective for obtaining visual cortical responses (Choudhury et al., 1965). Clinical observations of split-brain humans also support the notion of callosal connection of the visual vertical meridia (Mitchell and Blakemore, 1970). Studies of interhemispheric connections of somatosensory cortex in cat and raccoon (Ebner and Myers, 1965) and rhesus monkey (Pandya and Vignolo, 1968) demonstrate heavy callosal projections to cortical loci representing body surfaces near the midline (face, torso, tail), lighter projections to representations of intermediate surfaces, and no projections to representations of distal body surfaces (paw, hand, foot). This suggests that the role of the corpus callosum in uniting separate hemispheric representations of sensory surfaces along the midline may be general for various sensory modalities.

In a recent paper, Sanides (1978) compared the pattern of callosal inputs to extrastriate visual cortex in the cat with previous electrophysiologically-obtained topographic maps of the area (Tusa et al., 1978, 1979; Palmer et al., 1978) and concluded that at least a rough correspondence between vertical meridian representations and callosal inputs holds over a wide range of extrastriate cortex. The most extensive and informative investigations of callosal inputs to extrastriate cortex have been performed by S. M. Zeki and his colleagues in the macaque monkey (Zeki, 1969, 1970; Zeki and Sandeman, 1976; Van Essen and Zeki, 1978). Combined physiological and anatomical studies of a restricted portion of dorsal extrastriate cortex have demonstrated a reliable correspondence between a discrete patch of callosal input in the depths of the lunate sulcus and the vertical meridian representation shared by areas V3 and V3A, and also between callosal input to the anterior bank of the lunate sulcus and the vertical meridian representation forming the common boundary of areas V3A and V4. This correspondence may break down in the region of V4 on the prelunate gyrus where visual field topography becomes complex. These experiments have the virtue of providing both anatomical and physiological data on the same hemisphere so that precise comparisons between callosal input and visual field topography can be made. Thus, it appears that maps obtained by subdividing extrastriate cortex on the basis of interhemispheric connections may be congruent with maps obtained by electrophysiological mapping. To the extent that this is true, the pattern of interhemispheric connections becomes a powerful tool for identifying areal boundaries within extrastriate cortex.

In this chapter, I report a study of the interhemispheric connections of visual cortex in the owl monkey and in the bushbaby. This work was performed with two major goals in mind. First, since the owl monkey is the primate species in which the details of extrastriate topography have been most completely worked

out, this study should provide a valuable assessment of the overall utility of the callosal technique in subdividing extrastriate cortex. Second, it was hoped that information would be obtained concerning the existence and organization of as yet unmapped extrastriate areas.

METHODS

The splenium of the corpus callosum was transected in two adult owl monkeys and three adult bushbabies. The animals were anesthetized with ketamine HCl (Vetalar) and placed in a head holder. The scalp was longitudinally incised and deflected. An opening was made in the skull to expose the dorsal aspect of one cerebral hemisphere as far medial as the saggital sinus. Care was taken not to expose the opposite hemisphere at all. The dura mater was deflected and the exposed hemisphere was retracted slightly with a small spatula. The callosal transection was performed using a number eleven scalpel blade. The wound was closed, sutured and treated with a topical disinfectant (furazolidone). The animals were allowed a four-day survival period during which they received daily intramuscular administrations of an antibiotic, gentamicin sulfate (Gentocin, 0.75 mg/kg), and a dexamethasone solution (Azium, 0.3 mg/kg). At the time of sacrifice, the animals were deeply anesthetized with sodium pentobarbital (Nembutal, 40 mg/kg) and perfused through the heart with 10% formol-saline. The brains were removed, photographed, and equilibrated with 30% sucrose. The hemispheres which remained unexposed during the surgical procedure were blocked and the posterior blocks, including the visual cortices, were sectioned serially at 30 μm intervals in frozen sections. One section in eight was stained for cell bodies using a standard cresyl-violet procedure, one in eight for myelinated fibers using a modification of the Weigert technique, and one in eight for degenerating axons and terminals using a slight modification of the Wiitanen method (Wiitanen, 1969).

When viewed under the light microscope, degenerating fibers had a characteristic beaded appearance. Degenerating terminals appeared as a dust-like sprinkling of silver grains which was distinguishable from silver precipitates which occasionally formed around vascular tissue and cell bodies. In general, degenerating fibers predominated in the owl monkey material while the dust-like terminal degeneration was relatively more common in the bushbaby material. It is possible that this represents a geniune species difference in the reaction of degenerating tissue to the staining techniques here employed. However, it is also possible that the relative amounts of fiber and terminal degeneration are a function of post-lesion survival time, and that this function may differ for the two species.

Following transection of the splenium of the corpus callosum, degenerating axonal fibers and terminals can be seen across a broad expanse of the occipital, parietal and temporal lobes. The degeneration does not appear as a homogeneous projection to the entire region, but rather, appears in a characteristic patchy pattern which is reproducible in broad outline from animal to animal within a species. A particular patch of heavy degeneration may be separated by as little as 100 μm from an area of cortex which is entirely free of degeneration, but transitions in density of degeneration frequently take place in a more smoothly graded fashion. One should therefore remember that the discrete categories of degeneration density employed in composing the cortical reconstructions (see below) are an approximation of a pattern whose transitions are generally graded.

Cortical Reconstructions. Much of the owl monkey's visual cortex lies buried in the depths of the calcarine sulcus, and small portions of it lie in cortex of the superior temporal and Sylvian sulci. Thus, it was advantageous to display the experimentally-determined pattern of interhemispheric connections on two-dimensional reconstructions of the occipital lobe so that the total pattern could

be viewed. To this end, a simple method was devised for representing the cortical surface on a flattened out, two-dimensional map. The method is illustrated in Figure 2. A drawing of a particular frontal section was made, and data from adjacent Nissl-, myelin- and degeneration-stained sections were pooled on the drawing in the manner illustrated in step 1 of Figure 2. The density of degeneration at all points on the section was characterized as heavy (solid black), moderate (large dots), light (small dots), or absent. Examples of each category are given in the micrographs in Plate 1. Cytoarchitectonic boundaries of V1 were transferred to the drawing from the Nissl section, and myeloarchitectonic boundaries of the extrastriate area, MT, were transferred from the adjacent myelin-stained section (Allman and Kaas, 1971a). Cytoarchitectonic layer IV was denoted in the drawing by the dashed line. Several useful surface morphological features were also marked in the composite drawing (see step 1, Figure 2). These were the upper and lower lips of the calcarine sulcus, the point at which the dorsal hemispheric surface turns onto the medial wall of the hemisphere (termed the medial hemispheric convexity, MHC), and the point at which the lateral hemispheric surface turns into the ventral hemispheric surface (termed the lateral hemispheric convexity, LHC). In step 2 (Figure 2), the layer IV contour was clipped at the fundus of the calcarine sulcus and lifted from the section drawing as though it were a string. All information concerning degenerating fibers, architectonic boundaries and surface morphological features was retained by appropriate marks on the isolated layer IV contour. The layer IV contour was then straightened except for the folds representing the Sylvian and superior temporal sulci, and laid onto a two-dimensional surface in alignment with similar layer IV contours from previous sections (step 3, Figure 2). The serial side-by-side placement of adjacent layer IV contours generated a two-dimensional representation of the cortical surface which displayed the pattern

Figure 2. Method for constructing a simple two-dimensional map of owl monkey visual cortex. Step 1. Histological data and surface morphological markers (see text) from adjacent sections are pooled on a frontal section drawing. V1 and MT are identified by architectonic criteria, and the density of degeneration is determined from Wiitanen-stained sections. Cortical layer IV, identified in Nissl-stained sections, is represented by the dashed line. Step 2. The layer IV contour is cut at the fundus of the calcarine sulcus and lifted from the section as though it were a string. All histological and morphological data are retained by the appropriate symbols on the contour line. Step 3. The final reconstruction is formed as successive layer IV contours at 240 μm intervals are aligned side-by-side on a two-dimensional surface. Heavy degeneration is represented by solid black areas, moderate degeneration by the large dots and light degeneration by the small dots. Grey-shaded regions are two architectonically identifiable visual areas, V1 and MT (see text). (CS, calcarine sulcus; LHC, lateral hemispheric convexity; MHC, medial hemispheric convexity; MT, middle temporal area; SS, Sylvian sulcus; STS, superior temporal sulcus; V-1, the first visual area, or striate cortex; X, site where layer IV contour is cut.)

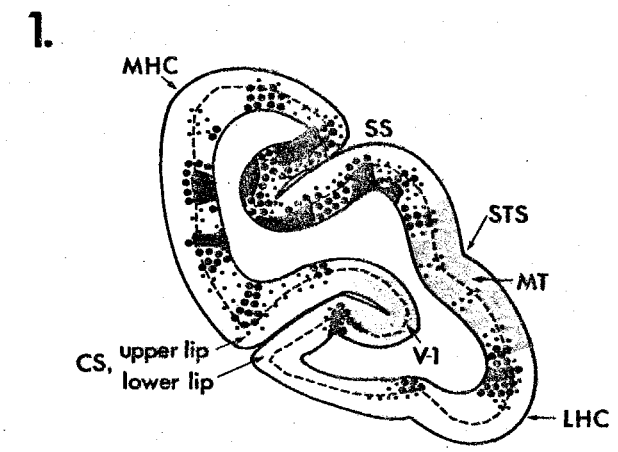
1.
MHC
SS
STS
MT
CS, upper lip
lower lip
V-1
LHC

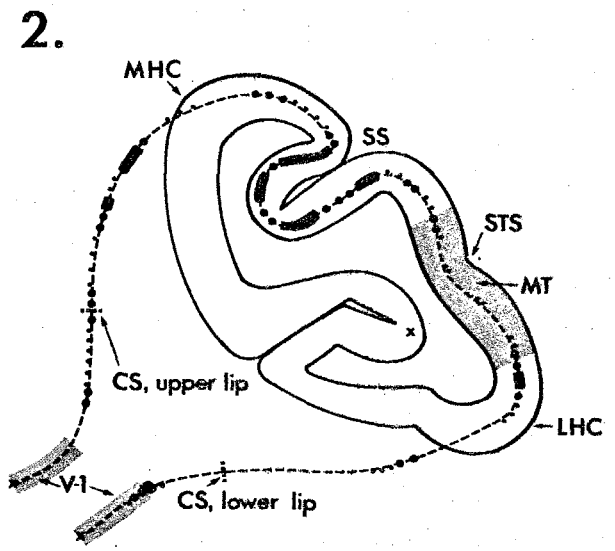
2.
MHC
SS
STS
MT
CS, upper lip
LHC
V-1
CS, lower lip

5mm

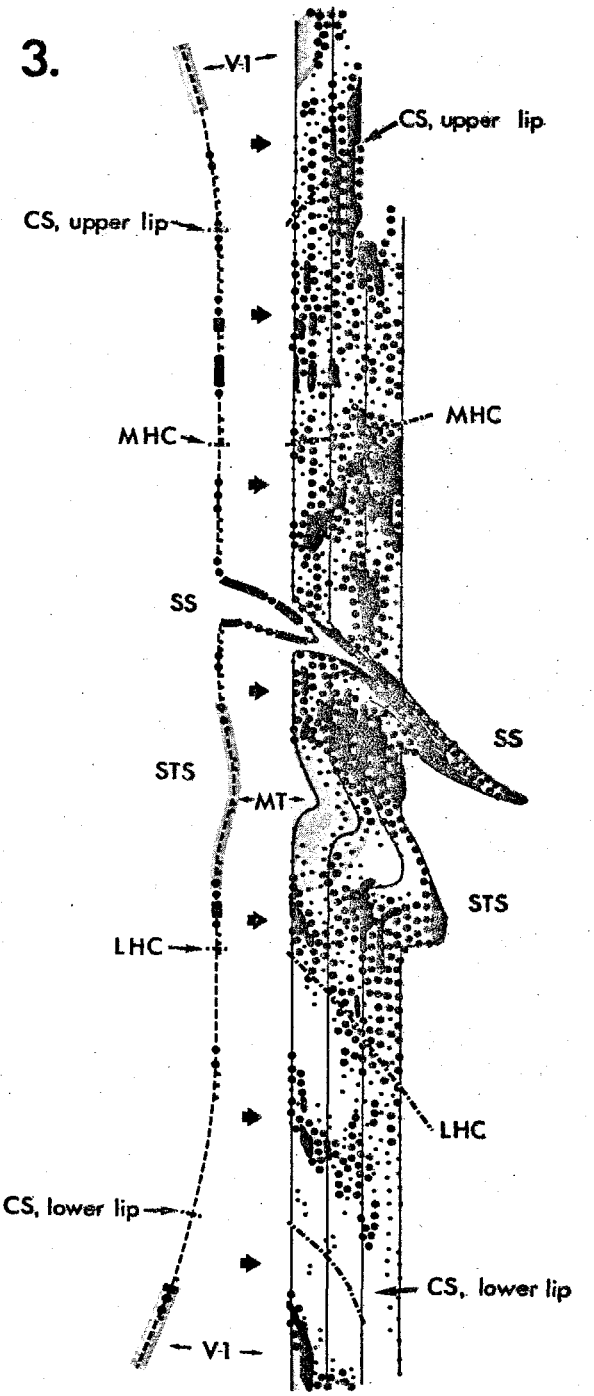
3.
V-1
CS, upper lip
CS, upper lip
MHC
MHC
SS
SS
STS
MT
STS
LHC
LHC
CS, lower lip
CS, lower lip
V-1

Plate 1. Examples of the classes of degeneration density employed in reconstructing the pattern of interhemispheric connections. The degeneration resulted from surgical section of the splenium of the corpus callosum. A, light degeneration; B, moderate degeneration; C, heavy degeneration.

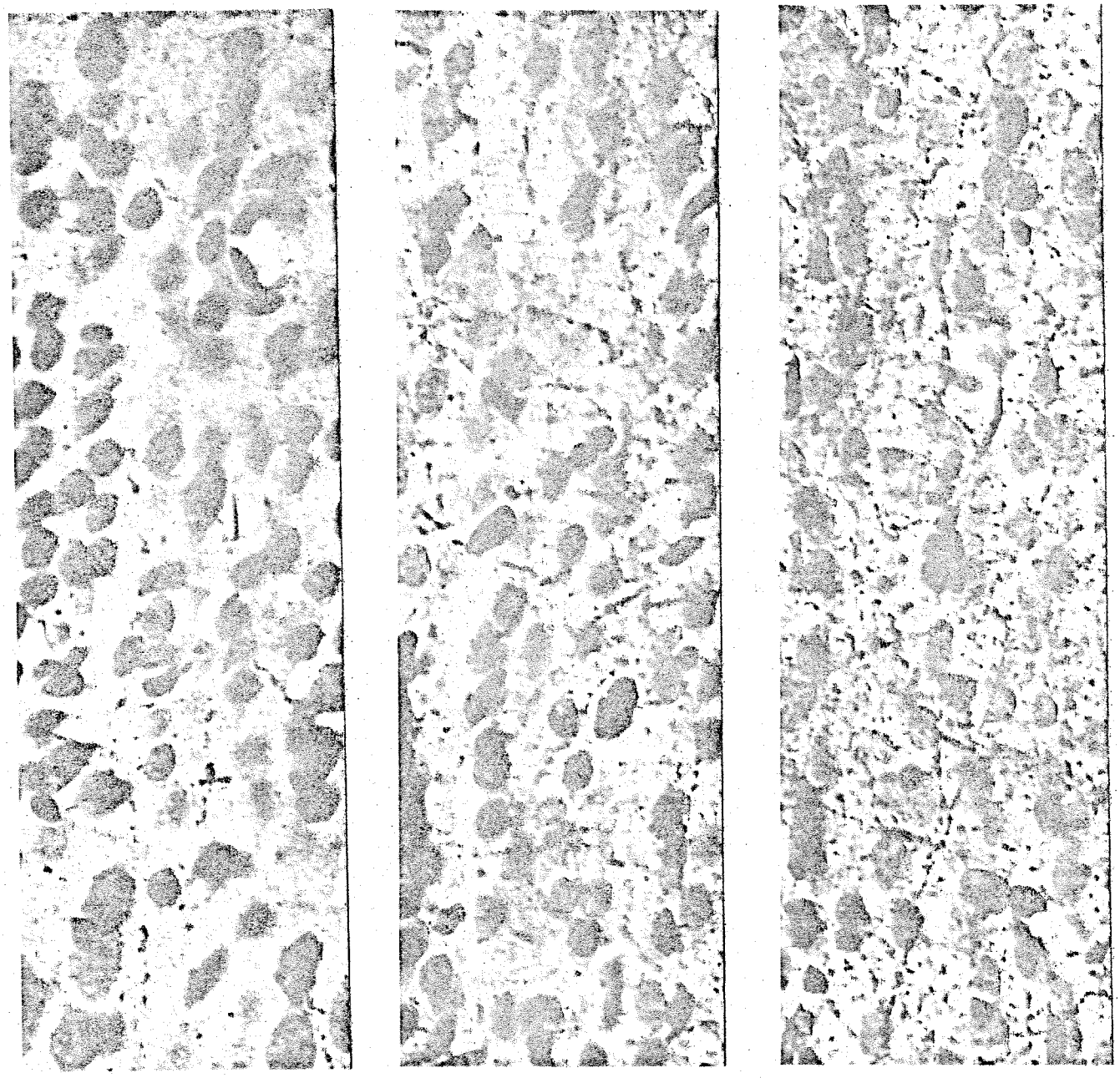

A B C

of interhemispheric connections in relation to architectonically-identified visual areas and the relevant surface morphological features. The serial layer IV contours used in making the reconstructions were separated by 240 μm.

One such reconstruction of owl monkey visual cortex is shown in Figure 3. The continuous lines running from top to bottom are representative layer IV contours with more posterior sections found to the left of the map. The broken lines on the map represent the surface morphological features described above. The contour lines which terminate at top and bottom against the solid black boundary line represent layer IV contours which were arbitrarily cut at the fundus of the calcarine sulcus. Thus, the solid black boundary line at the top of the cortical reconstruction represents a line of cortex running along the fundus of the calcarine sulcus. Because the three-dimensional cortical surface was effectively "cut" along this line during the unfolding procedure, each point on the fundus is represented twice on the map—once on the upper border of the map, and again at the corresponding point on the lower border. Thus, cortex on the upper bank of the calcarine sulcus is represented from the top of the map to the broken line which marks the upper lip of the calcarine sulcus. Similarly, cortex on the lower bank of the calcarine sulcus is represented from the bottom of the map to the broken line which marks the lower lip of the calcarine sulcus. Moving from top to bottom on the map, a contour line "emerges" from the calcarine sulcus at the upper lip, traverses the medial wall of the hemisphere up to the medial hemispheric convexity, and then crosses the dorsal and lateral surfaces of the hemisphere up to the lateral hemispheric convexity (see Figure 2). After "rounding" the lateral hemispheric convexity, the contour line crosses the ventral surface of the hemisphere and re-enters the calcarine sulcus at the lower lip.

The two-dimensional maps thus obtained are simple, flattened out versions of complicated three-dimensional surfaces, and some distortions in point-to-point cortical distances have occurred, particularly at the edges of the maps and in regions of high curvature. However, we believe that the maps presented here are easily comprehensible and are useful for viewing the general pattern of interhemispheric connections over the whole of visual cortex.

Physiology. Some physiological data are presented for the purpose of comparison with the interhemispheric connections pattern on the ventral surface of the occipital lobe. The techniques involved are standard electrophysiological mapping techniques which have been detailed elsewhere (Allman and Kaas, 1971a).

RESULTS

In both the owl monkey and the bushbaby, the best opportunity for assessing the degree of congruence of vertical meridian representation and callosal connections is afforded by the existence of two visual areas whose boundaries can be identified anatomically and thus compared precisely with patches of degeneration. Previous work (Allman and Kaas, 1971a,b, 1976b; Allman et al., 1973) has shown that in both species, V1 is identical with the anatomically-identifiable striate cortex, and that extrastriate area MT is identical with a region of heavily myelinated cortex on the lateral surface of the hemisphere. These studies have also shown that the greatest extent of the boundaries of both of these areas is devoted to the representation of the vertical meridian (see Figures 6, 7, 10 and 11). Thus, at least two regions of vertical meridian representation can be located precisely with anatomical methods and compared to the pattern of callosal degeneration seen on adjacent sections in the same hemisphere.

In extrastriate cortex dorsal to MT, a representation of the vertical meridian exists at the anterior border of extrastriate areas DM and M (see Figure 1). We are not able to make a precise comparison of callosal input and vertical meridian representation in this region since these borders cannot be reliably located with anatomical techniques. However, a general idea of the relation between visual field topography and callosal input to this region can be obtained by comparing maps of visual topography generated by electrophysiological experiments with maps of interhemispheric connections generated by anatomical experiments (see Figures 6, 7, 10 and 11). In extrastriate cortex ventral to MT, electrophysiological mapping data are incomplete in the owl monkey and nonexistent in the bushbaby. It is therefore likely that the pattern of interhemispheric connections in this region provides information concerning the organization of extrastriate cortex which exceeds that presently available from electrophysiology.

In the first section of the results, the pattern of interhemispheric connections for the owl monkey is described for each of the cortical regions mentioned above. In the second section, similar data from the bushbaby are examined.

Owl Monkey. In regions in which callosal fibers terminate, degenerating axons and terminals are generally observed coursing upward from white matter and terminating predominantly in cortical layers IV, V, and VI. Degeneration frequently appears in the supragranular layers, but it is always reduced in intensity from that appearing immediately beneath in the lower three layers. The patchy nature of the callosal inputs is usually more distinct in layer IV than in the infragranular layers. This is due to the fact that the callosal inputs to layer VI, especially, tend to spread out over a wider area than do the inputs to layer IV.

Reconstructions of the callosal input to visual cortex in two owl monkey hemispheres are shown in Figures 3 and 4. The hemisphere illustrated in Figure 4

Figure 3. A two-dimensional reconstruction of visual cortex showing the pattern of degeneration caused by transection of the splenium of the corpus callosum (owl monkey 78-3). Heavy degeneration is represented by the solid black areas, moderate degeneration by the large dots and light degeneration by the small dots. Grey-shaded areas are two architectonically identifiable visual areas, V1 and MT. The broken lines represent surface morphological features (see text) as labeled. The solid black lines running from top to bottom are representative layer IV contours. Layer IV contours which terminate against the solid black line surrounding the posterior portion of the reconstructed area were cut at the fundus of the calcarine sulcus and therefore are continuous contours. Contours which terminate in regions marked by asterisks were discontinuous since they ended within the calcarine sulcus at the juncture of neocortex with the hippocampal formation. A discrete band of degeneration is congruent with the vertical meridian representation at the V1-V2 border. An increase in the density of degenerating terminals corresponds to the vertical meridian representation at the MT border. The solid arrow indicates a small, degeneration-free region of cortex on the medial wall of the hemisphere which may be the site of the medial visual area, M (see text). Note the well-defined strip of degeneration on the ventral surface of the hemisphere (open arrows). Abbreviations are the same as in Figure 2.

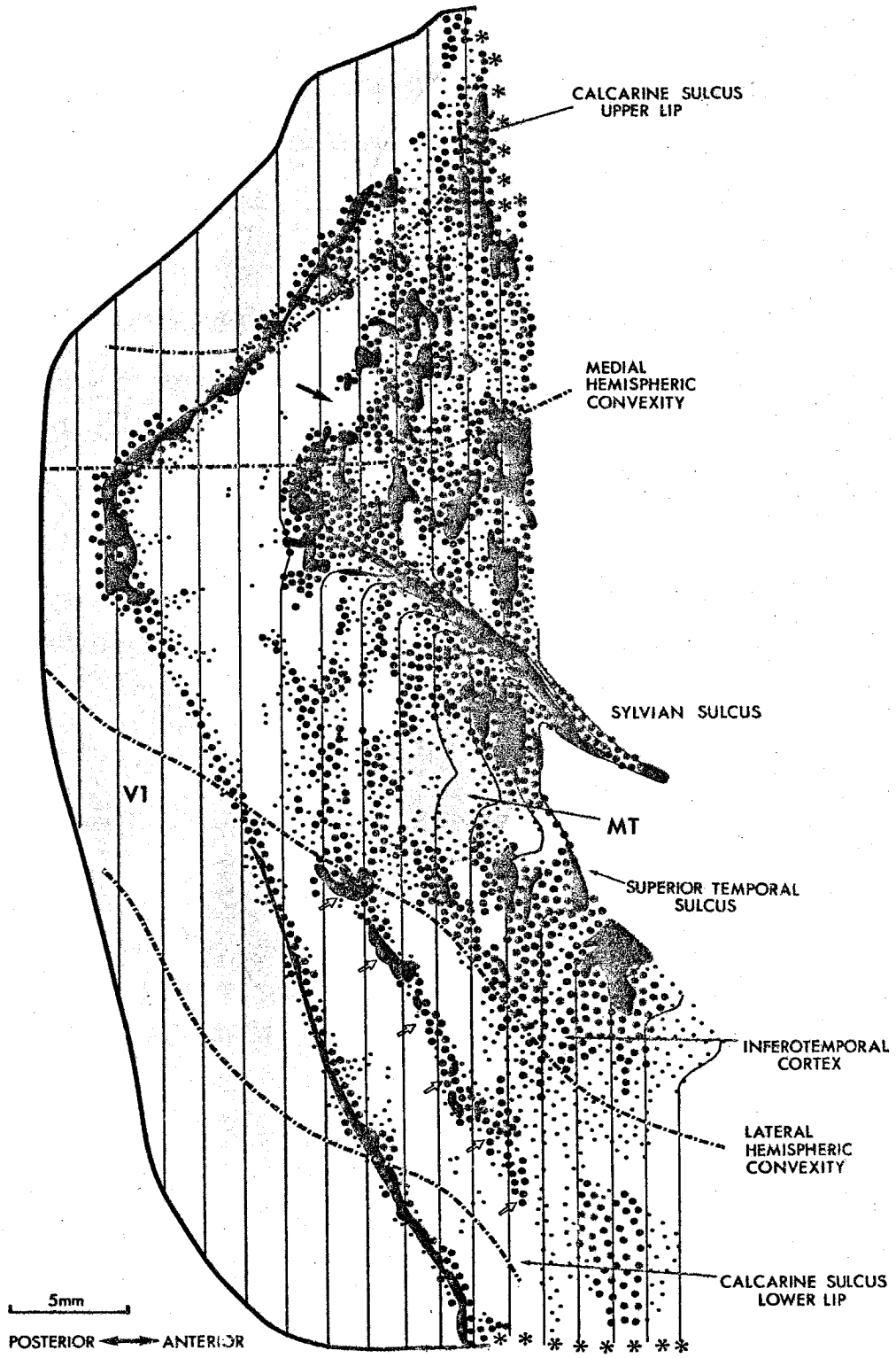
CALCARINE SULCUS
UPPER LIP
MEDIAL
HEMISPHERIC
CONVEXITY
SYLVIAN SULCUS
V1
MT
SUPERIOR TEMPORAL
SULCUS
INFEROTEMPORAL
CORTEX
LATERAL
HEMISPHERIC
CONVEXITY
CALCARINE SULCUS
LOWER LIP
5mm
POSTERIOR ANTERIOR

Figure 4. Reconstruction of visual cortex illustrating the pattern of degeneration caused by transection of the splenium of the corpus callosum (owl monkey 78-4). The splenium of the corpus callosum was only partially sectioned resulting in degeneration over the dorsal half of visual cortex only. Once again, a discrete band of degeneration is congruent with the vertical meridian representation at the V1-V2 border. The proliferation of callosal terminals associated with the vertical meridian representation of MT is also seen. The solid arrow indicates a small, degeneration-free region of cortex on the medial wall of the hemisphere which may be the site of the medial visual area, M (see text). Symbols and abbreviations are the same as for Figure 3.

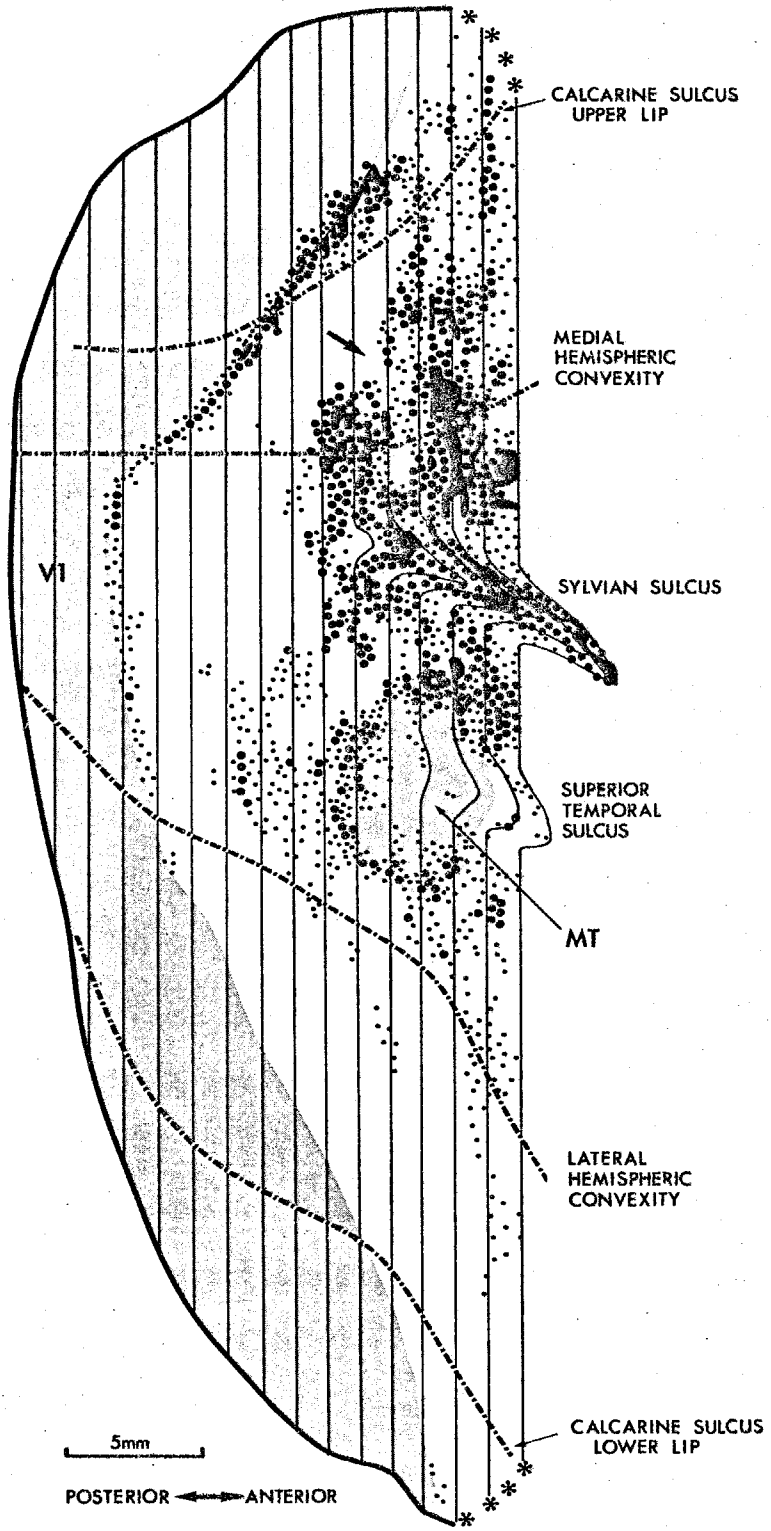
CALCARINE SULCUS
UPPER LIP
MEDIAL
HEMISPHERIC
CONVEXITY
V1
SYLVIAN SULCUS
SUPERIOR
TEMPORAL
SULCUS
MT
LATERAL
HEMISPHERIC
CONVEXITY
CALCARINE SULCUS
LOWER LIP
5mm
POSTERIOR ANTERIOR

is from a brain in which the splenium of the corpus callosum was only partially sectioned, resulting in degeneration within the dorsal half of visual cortex only. The most obvious patch of degeneration in both of these reconstructions lies along most of the boundary of striate cortex, which is the site of the common vertical meridian representation for V1 and V2. This narrow band of degeneration which runs along the V1-V2 boundary is interrupted only in a restricted portion of cortex, on the upper bank of the calcarine sulcus, which has been shown to be the physiological site of representation of the visual field periphery for V1 (Allman and Kaas, 1971b). Thus, there is a striking correlation between vertical meridian representation and callosal inputs for at least one cortical locus. Occasionally, small "fingers" of degeneration which are continuous with the narrow band of input at the V1-V2 border invade the interior of V2 for a distance of up to 2 mm. Similar "fingers" have also been observed invading V2 from the V1-V2 border in the macaque monkey (Van Essen and Zeki, 1978). Their functional significance remains obscure in both species.

The band of callosal input to the V1-V2 vertical meridian representation lies predominantly on the V2 side of the striate boundary, but frequently ventures a short distance into V1 (see Figures 3 and 4). The laminar arrangement of this extension into V1 is different from that observed anywhere else in visual cortex. Immediately on the V2 side of the border, the callosal input has the typical appearance described above. Fibers course up from white matter and terminate largely in layers IV, V, and VI, and a few fibers extend into the supragranular layers. However, at the level of layer IVb (Gennari's stripe) on the striate side of the border, some fibers appear to make a sharp turn and course tangentially into striate cortex for 0.2 to 1 mm along layer IVb, thus forming a kind of "shelf" of input along the striate boundary. Frequently a spreading of callosal input into

striate cortex in layer VI may also be seen, but a continuous coursing of fibers from layer VI to layer IVb on the striate side of the boundary of sufficient density to account for the striking presence of degeneration in layer IVb is rarely seen. The reason for this exception to the general laminar arrangement of callosal inputs is unclear.

The second cortical vertical meridian representation which can be located with some precision using the anatomical methods of this study lies in extrastriate visual cortex at the boundary between areas MT and DL (see Figure 1). A glance at the callosal inputs to area MT in Figures 3 and 4 shows the correlation of degeneration with vertical meridian representation to be looser than is the case at the V1-V2 boundary, but to exist nevertheless. A comparison of the inputs to MT in Figures 3 and 4 also reveals the existence of considerable individual variation in the tightness of the correlation from one animal to the next. In Figure 3, callosal input exists over much of the interior of MT, but a definite proliferation of callosal terminations can be seen as one approaches the MT-DL boundary. In Figure 4, the callosal input to MT is restricted much more closely to the region of vertical meridian representation. In both figures, an attenuation of callosal input is evident at the most anterior part of the MT boundary in the superior temporal sulcus where the visual field periphery is located. A correlation between vertical meridian representation and more dense callosal inputs thus holds for this anatomically-identifiable vertical meridian representation although the correlation is less impressive than that at the V1-V2 boundary.

Further examination of Figure 3 reveals a complex pattern of callosal input to extrastriate cortex outside MT. However, it is evident that a striking difference exists in the pattern of interhemispheric connections of extrastriate cortex dorsal to MT (toward the top of the map) and the pattern ventral to MT

(toward the bottom of the map). In contrast to the intricate moasic of degenerating terminals present dorsally, the ventral pattern is dominated by a narrow, 10-15 mm long band of degeneration which begins in or near extrastriate area DL at the lateral hemispheric convexity and runs anterio-medially across the ventral surface of the hemisphere and closely approaches (in one case enters) the lower bank of the calcarine sulcus (see open arrows, Figure 3). This ventral band of callosal input separates two regions of entirely degeneration-free cortex, and is the best defined patch of callosal input observed in visual cortex, except for the band at the V1-V2 border. The presence of such a strikingly well-organized strip of callosal input on the ventral surface of the hemisphere suggests the existence of an as yet unmapped vertical meridian representation at this site. This vertical meridian representation could be the anterior boundary of a third tier extrastriate area which shares a common representation of the horizontal meridian posteriorly with V2. This hypothesized ventral vertical meridian representation could also be the posterior boundary of another extrastriate visual area which lies in the region of degeneration-free cortex anterior to the ventral strip of degeneration. While no complete electrophysiological map of visual topography in this region exists, some recordings from ventral extrastriate cortex were made during the course of experiments designed for the study of other regions of extrastriate cortex (Allman and Kaas, unpublished observations). It is informative to examine some of these data to see whether they are consistent with the scheme of ventral extrastriate organization deduced from the pattern of callosal inputs.

Figure 5 compares the pattern of callosal inputs to ventral extrastriate cortex with physiological recordings made in the same area in a different experiment. A ventral view of a hemisphere on which the pattern of ventral callosal connections has been represented is shown in Figure 5A. Figure 5B is a ventral

Figure 5. Comparison of anatomical results with physiological data for the ventral surface of owl monkey visual cortex. A. The pattern of degeneration on the ventral surface of owl monkey 78-3. Heavy degeneration is solid black, moderate degeneration is represented by the large dots, and light degeneration by the small dots. B. Electrophysiological recording sites (1-11) on the ventral surface of owl monkey 72-343 (Allman and Kaas, unpublished observations). Open circles denote the vertical meridian representations and the closed squares signify the horizontal meridian representation. Dashed lines represent uncertain boundaries. C. Receptive fields for recording sites 1-11 (B and D). The black receptive field is in V1, the grey-shaded receptive fields are in V2 and the unshaded receptive fields are in VP and VA. D. Parasagittal section showing electrode tracks for recording sites 1-11 in B. Shaded areas are V2. Note the progression of receptive fields from the horizontal meridian (recording site 5) at the V2-VP border to the vertical meridian (recording site 8) at the VP-VA border. The vertical meridian representation at site 8 appears to correspond to the patch of callosal degeneration on the ventral surface in A. (OD, optic disk; VA, ventral anterior area; VP, ventral posterior area; V1, first visual area, or striate cortex; V2, second visual area.)

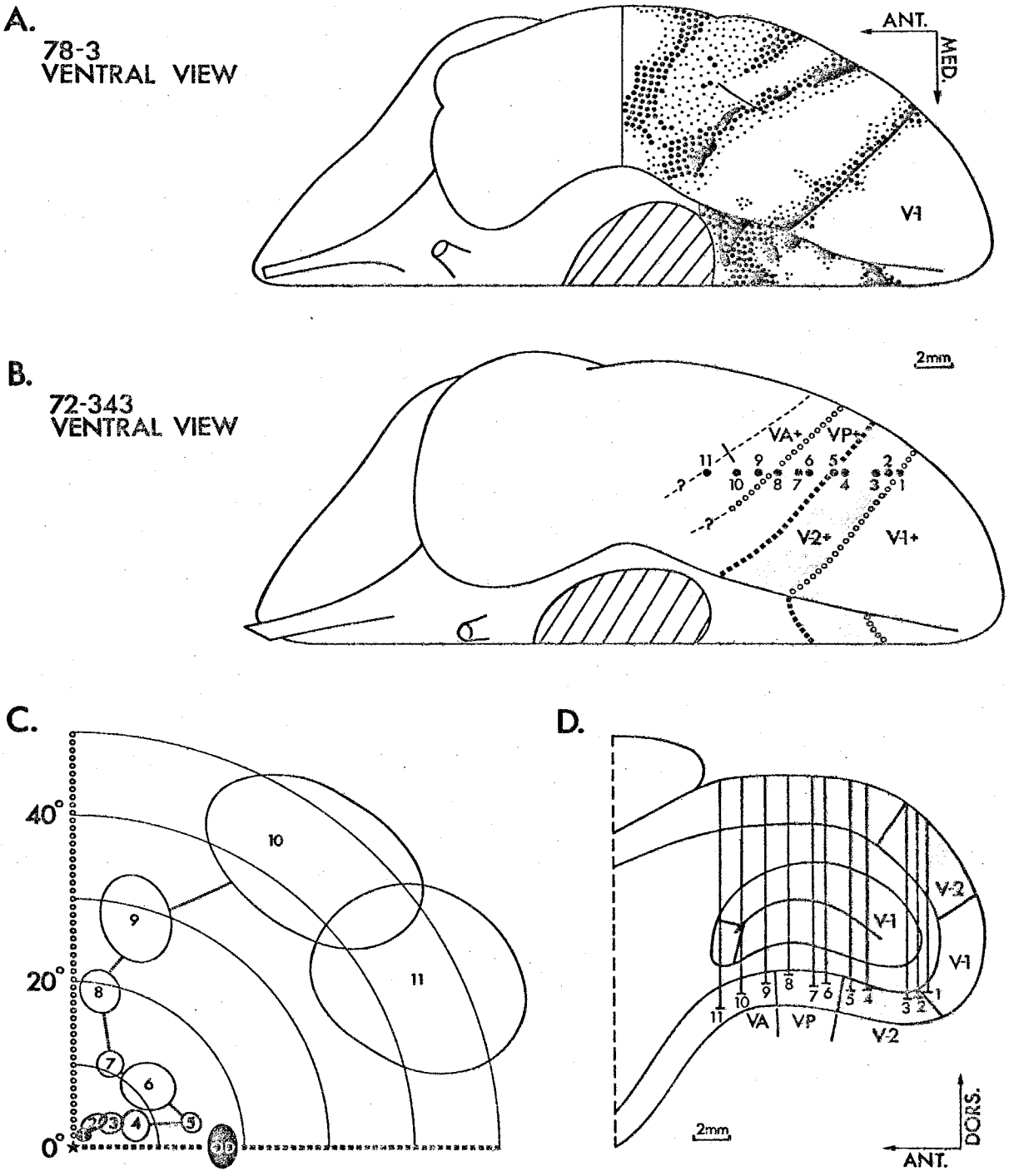
A.
78-3
VENTRAL VIEW
ANT.
MED.
V1
B.
72-343
VENTRAL VIEW
2mm
VA+
VP+
11
10
9
8
7
6
5
4
3
2
1
V2+
V1+
C.
40°
20°
0°
10
9
8
7
6
5
4
3
2
1
11
D.
V-2
V-1
V-1
11
10
9
8
7
6
5
4
3
2
1
VA
VP
V-2
2mm
DORS.
ANT.

view of a hemisphere in which an anterior-posterior row of eleven physiological recording sites was made on the ventral surface beginning in striate cortex and extending as far anterior as visual responses could be obtained (Allman and Kaas, unpublished observations). Figure 5D illustrates a reconstruction in the parasagittal plane of the electrode tracks whose ventral recording sites are illustrated in 5B. The electrode entered the dorsal surface of visual cortex and penetrated through the cortex of the calcarine sulcus to the cortex of the ventral surface. The recording sites 1-11 illustrated in 5D are the same recording sites 1-11 illustrated in 5B. In Figure 5C, the visual receptive fields recorded at each site 1-11 are illustrated. Posteriorly, recording site 1 in striate cortex yields a small receptive field in the upper visual field near the center-of-gaze, as would be expected from the known visual topography of V1 (Allman and Kaas, 1974a). Recording sites 2-5 are located in V2 and yield receptive fields which form a progression from the center-of-gaze to a point several degrees eccentric on the horizontal meridian. Once again, this is consistent with the known visual topography of V2 (Allman and Kaas, 1974a). Proceeding further into extrastriate cortex, recording sites 6-8 form a regular progression from the horizontal meridian back to the vertical meridian. This is consistent with the scheme deduced from the callosal connections above. Recording sites 6-8 are located in a third tier visual area anterior to V2 which shares a horizontal meridian representation with V2 and has its vertical meridian representation congruent with the strip of callosal degeneration anteriorly. Proceeding still further into extrastriate cortex, recording sites 9-11 move away from the vertical meridian back into the periphery of the visual field. This is consistent with the idea developed from the callosal connections that yet another extrastriate visual area lies in the degeneration-free cortex anterior to the ventral strip of degeneration and shares a common representation of the vertical meridian with the third tier extrastriate area of recording sites 6-8.

Physiological data similar to those illustrated in Figure 5 have been obtained in other experiments where recordings were made on the ventral surface. Although the several recordings do not yield a complete map of the ventral extrastriate cortex, all the data are consistent with the picture of ventral extrastriate organization proposed above. In addition, the combined physiological recordings indicate that the center-of-gaze is represented laterally toward the lateral convexity, and the visual periphery is represented medially toward the calcarine sulcus. We have assigned the names "ventral anterior" (VA) and "ventral posterior" (VP) to the two extrastriate visual areas now thought to exist on the ventral surface. Their location and what is known of their organization are shown in Figures 6 and 7. It should be emphasized that our knowledge of the organization of these areas is still incomplete and may be modified with the acquisition of additional data. Several questions in particular remain outstanding. No physiological recordings have been made from the most medial extent of these areas near the calcarine sulcus, and it is not clear exactly where the medial boundary of these areas should be drawn. Likewise, no physiological recordings have been made from the most lateral portions of these areas where they perhaps abut the dorsolateral area, DL, on the lateral surface of the hemisphere. Thus, it is not certain where the lateral boundaries should be drawn. Of more importance is the fact that all receptive fields thus far recorded from VA and VP are located in the upper half of the visual field. The observation that receptive fields approach the center-of-gaze as recording sites proceed laterally leads one to expect a lower field representation to exist even further laterally beyond the center-of-gaze representation. Although the lateral boundary of these areas is not yet defined, recordings have been made far enough laterally to warrant the conclusion that if a lower field representation exists, it must be extremely compressed in comparison to the upper field representation.

Extrastriate cortex dorsal to MT (upper half of Figures 3 and 4) is a particularly difficult region to interpret due to 1) the intricate arrangement of the dense callosal input to the region, and 2) the fact that vertical meridian representations in the region (DM and M, see Figure 1) cannot be independently located by architectonic criteria. However, a general idea of the relation between visual field topography and the pattern of interhemispheric connections in the region can be obtained by comparing maps of visual field topography generated by electrophysiological experiments with maps of interhemispheric connections generated by anatomical experiments.

Inspection of the maps in Figures 3 and 4 reveals a complex arrangement of callosal inputs to the dorsal half of extrastriate visual cortex. The most prominent feature of the pattern of callosal input to this region is a locus of heavy degeneration situated in the posterior termination of the Sylvian sulcus on the dorsal hemispheric surface (see Figures 3 and 4). This locus of degeneration extends medially across the medial hemispheric convexity and terminates just onto the medial wall of the hemisphere. Further anterior on the dorsal surface, heavy and moderate degeneration is present throughout most of the cortex buried in the Sylvian sulcus. An intricate mosaic of heavy, moderate, and light degeneration is observed in posterior parietal cortex between the Sylvian sulcus and the medial hemispheric convexity. This mosaic of callosal inputs extends medially across the hemispheric convexity and covers the medial wall of the hemisphere at this more anterior level. The resulting overall pattern of callosal input on the medial wall of the hemisphere, therefore, consists of a broad expanse of complex input covering the wall anteriorly, and a region of dense to moderate input terminating just onto the wall posteriorly. Partially separating these two regions of callosal degeneration is a small, degeneration-free region of cortex, indicated by the solid arrow in

Figures 3 and 4, which may be the site of the medial extrastriate visual area, M (see below).

In dorsal extrastriate cortex lying lateral to the Sylvian sulcus (toward the lateral hemispheric convexity), we once again see a complex arrangement of callosal inputs. A region of heavy-to-moderate degeneration is located between the Sylvian sulcus and MT, and this degeneration is continuous with callosal input to the MT border. Posterior to MT, extensive callosal connections exist in cortex between MT and V1. These connections closely approach, but do not join, the band of degeneration at the V1-V2 border. This contrasts to the situation posterior to the Sylvian sulcus, where a wide region of degeneration-free cortex is interposed between extrastriate callosal input and V1-V2 border input.

An informative comparison between the pattern of callosal projections to dorsal extrastriate cortex and the known visual topography of the region can be made by comparing pictures of intact hemispheres on which the respective data have been represented. Such data are presented in Figures 6 and 7. While comparisons between the topographic and anatomical data cannot be precise due to the composite nature of both representations, certain conclusions can be drawn.

The map of visual field topography (see Figures 1 and 6) indicates the existence of a continuous vertical meridian representation beginning lateral to the Sylvian sulcus at the anterior boundary of DM and DI and running posteriomedially past the posterior termination of the Sulvian sulcus to the medial hemispheric convexity. Near the medial hemispheric convexity, this vertical meridian representation in area DM joins the vertical meridian representation of area M which then proceeds anteriorly along the convexity for a short distance before making a near-right-angle turn and proceeding down the medial wall of the hemisphere. Thus, the vertical meridian representation on the medial wall of the

Figure 6. Two dorsolateral views of the right hemisphere of an owl monkey brain. The top figure illustrates the topographic organization of visual cortex. The dashed lines ventral to DL are uncertain boundaries. The bottom figure shows the pattern of callosal degeneration over the expanse of cortex for which the topographic organization is shown at the top. The shaded area at the occipital pole is striate cortex (V1), the shaded area on the lateral surface in extrastriate cortex is MT. The large dots signify heavy and moderate degeneration, the small dots denote light degeneration. The solid black line shows the anterior extent of the reconstruction. Note the discrete band of degeneration at the V1-V2 border and the thickening of degeneration at the MT border. (TP, temporoparietal cortex; all other symbols and abbreviations are the same as for Figure 1.)

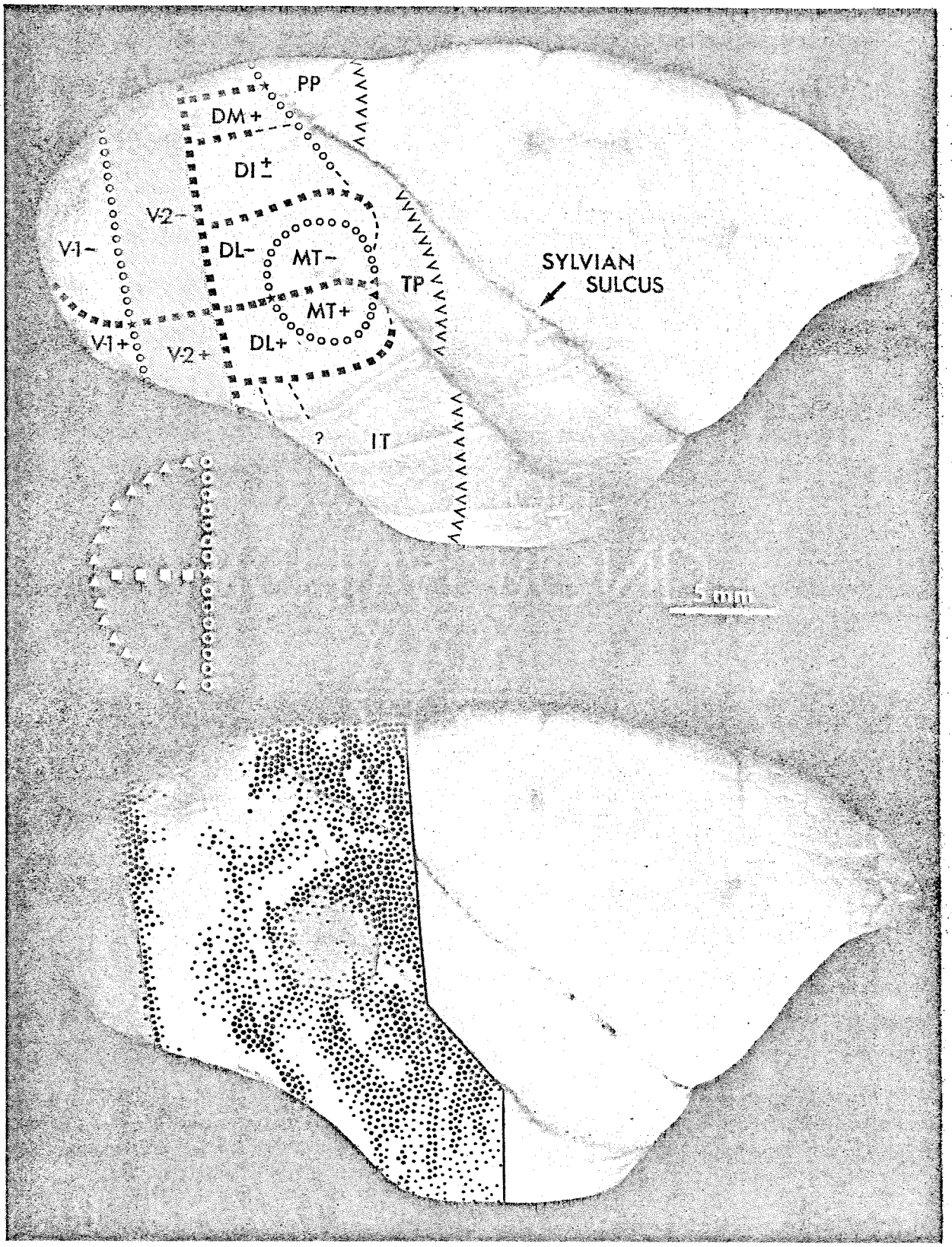
PP
DM+
DI ±
V2−
V1−
DL−
MT−
MT+
TP
SYLVIAN
SULCUS
V1+
V2+
DL+
?
IT
5 mm

Figure 7. Two ventromedial views of the left hemisphere of an owl monkey brain. The top figure illustrates the topographic organization of visual cortex, including the newly discovered areas, VA and VP (see text). The dashed lines represent uncertain boundaries. The bottom figure shows the pattern of callosal degeneration over the expanse of cortex for which the topographic organization is shown at the top. The shaded area at the occipital pole is striate cortex (V1). Note the correspondence between the vertical meridian representation of VA and VP with the prominent band of degeneration lying anteriorly on the ventral surface of the hemisphere. (CC, corpus callosum; VA, ventral anterior area; VP, ventral posterior area; all other symbols and abbreviations are the same as in Figure 1.)

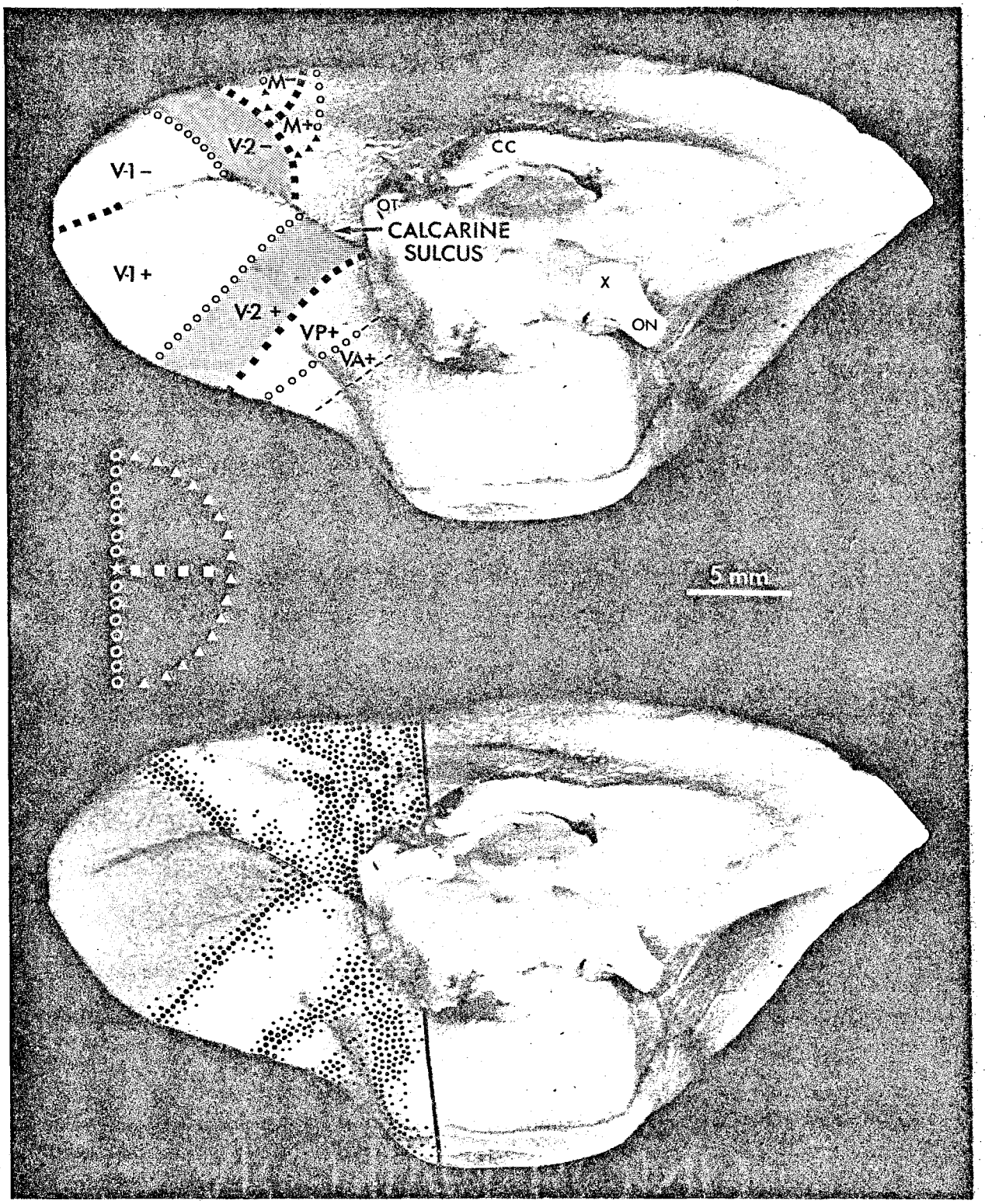
M−
M+
V-2 −
V-1 −
CC
QT
CALCARINE
SULCUS
V-1 +
X
ON
V-2 +
VP+
VA+
5 mm

hemisphere forms an "L-shaped" configuration which resembles the pattern of callosal inputs to the region. It is therefore possible that the interior of the medial visual area, M, in which the visual field away from the vertical meridian is represented, lies in the previously described degeneration-free region of cortex which is located between major sites of callosal degeneration on the medial wall. Similarly, it is possible that the dense callosal input at the posterior termination of the Sylvian sulcus is roughly congruent with the vertical meridian representation in DM. If so, the interior of area DM occupies an expanse of degeneration-free cortex immediately posterior to the patch of degeneration. While combined anatomical and physiological experiments on the same hemisphere would be required to test these hypotheses precisely, the data discussed above are suggestive.

In the region of dorsal extrastriate cortex lateral to the Sylvian sulcus, the pattern of callosal connections bears little resemblance to the pattern of visual area boundaries which exists in the region. Anteriorly, the degeneration which is continuous with that at the MT boundary clearly covers the "wing" area of DL. The area of callosal input which is located posterior and dorso-posterior to MT occupies much of the interior of areas DI and DL (see Figure 6). Although the presence of this input may not be entirely inconsistent with the notion of vertical meridian representation (see Discussion), the presence of such a broad expanse of complex callosal connections over a region of cortex known to contain several closely apposed visual areas makes the task of correlating the pattern of callosal projections with currently known visual area boundaries exceedingly difficult in this region.

Results: Bushbaby. In the bushbaby the degeneration resulting from transection of the splenium of the corpus callosum has a similar laminar arrangement to that found in the owl monkey. The callosal inputs course upward from white

matter and terminate largely in layers IV, V, and VI. Degeneration is frequently seen in layers II and III, but always less densely than in the lower three layers. Once again, degeneration tends to spread out over a wider area in layer VI, thus making the callosal patches better defined in layer IV.

Reconstructions of the pattern of callosal projections to visual cortex in two bushbabies are shown in Figures 8 and 9. Once again, although the callosal inputs are quite complex, similarities can be seen between the overall pattern of inputs in the different animals. As in the owl monkey, the two regions where precise comparisons of vertical meridian representation and callosal projections can be made are in two anatomically-identifiable visual areas, V1 and MT. Examination of Figures 8 and 9 reveals that the pattern of callosal projections to the vertical meridian representation in each of these areas is quite similar to the pattern seen in the owl monkey. A narrow band of degeneration is seen along the length of the V1-V2 border, except on the upper bank of the calcarine sulcus and part of the lower bank of the calcarine sulcus where the visual field periphery of V1 is represented (Myerson et al., 1979). Unlike that in the owl monkey, the laminar arrangement of callosal input to the V1-V2 border in the bushbaby is in every way typical of the laminar arrangement of callosal input over the rest of the visual cortex. Once again, the bulk of the degeneration is on the V2 side of the boundary, but the degeneration which spills over into V1 is present throughout cortical layers IV, V, and VI, and occasionally II and III as well. There is no "shelf" of input to V1 in the bushbaby as was described earlier for the owl monkey.

In area MT, a relatively more crude, but nevertheless distinct increase in the density of callosal degeneration corresponds to the vertical meridian representation at the boundary of the area. The only part of the MT boundary where

Figure 8. A two-dimensional reconstruction of the visual cortex of the bushbaby showing the pattern of degeneration caused by transection of the splenium of the corpus callosum (bushbaby 78-1). A discrete band of degeneration is congruent with the vertical meridian representation at the V1-V2 border, and an increase in the density of callosal terminals corresponds to the vertical meridian representation at the MT border. No obvious homologue of the owl monkey "ventral strip" is present. Note the bridge of degeneration connecting the band at the V1-V2 border with the more complex pattern of degeneration anteriorly. Symbols and abbreviations are the same as for Figure 3.

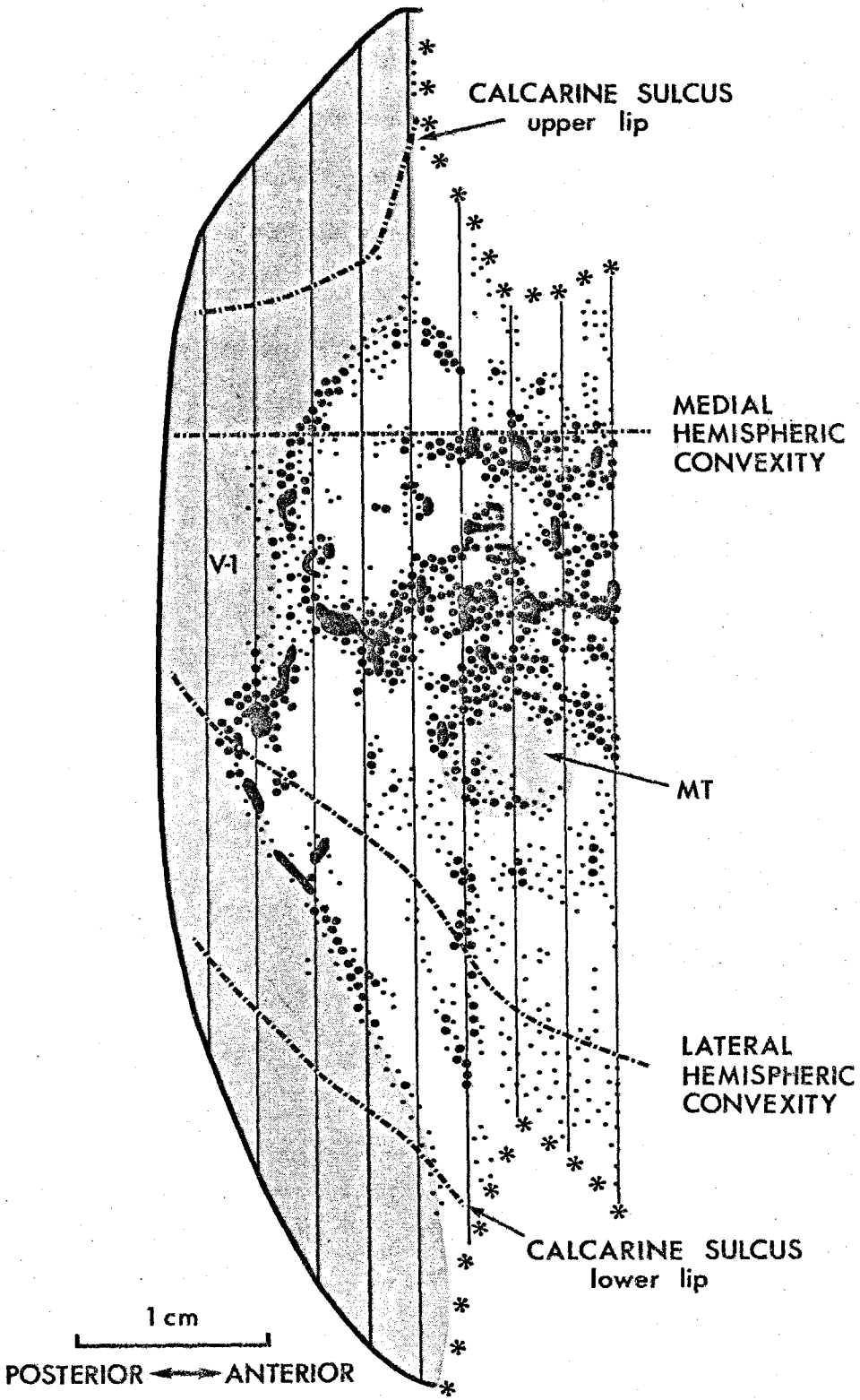
CALCARINE SULCUS
upper lip
MEDIAL
HEMISPHERIC
CONVEXITY
V-1
MT
LATERAL
HEMISPHERIC
CONVEXITY
CALCARINE SULCUS
lower lip
1 cm
POSTERIOR ANTERIOR

Figure 9. Reconstruction of visual cortex illustrating the pattern of degeneration caused by transection of the splenium of the corpus callosum (bushbaby 78-2). Once again, the discrete band of degeneration corresponding to the vertical meridian representation at the V1-V2 border is seen, and the increase in density of of degenerating axons and terminals is seen at the MT border. Note the "bridge" of degeneration connecting the band at the V1-V2 border with the complex pattern of degeneration seen anteriorly. Symbols and abbreviations are the same as in Figure 3.

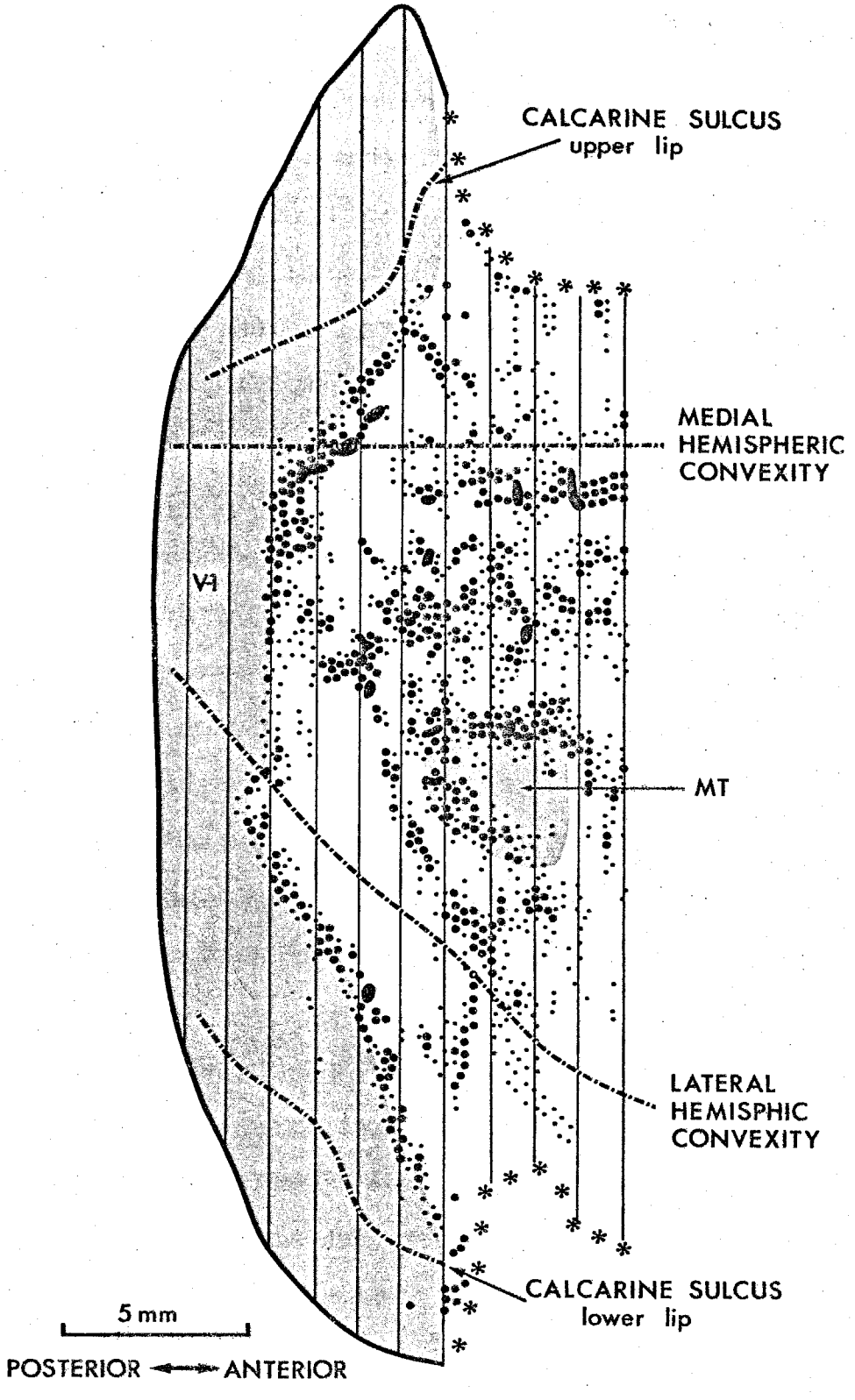
CALCARINE SULCUS
upper lip
MEDIAL
HEMISPHERIC
CONVEXITY
V-1
MT
LATERAL
HEMISPHIC
CONVEXITY
CALCARINE SULCUS
lower lip
5 mm
POSTERIOR ANTERIOR

this does not hold is along the most anterior border of the area where the visual field periphery is represented (Allman and Kaas, 1973). Thus, the precise correspondence between vertical meridian representation and callosal input at the V1-V2 border holds for both owl monkey and bushbaby, as does the more crude but still distinct correspondence at the MT boundary.

In the region of extrastriate cortex dorsal to MT, the pattern of callosal projections is very complex and does not correspond to known visual topography in the area. Figures 10 and 11 display the anatomical and physiological data on similar views of the intact cerebral hemisphere. The only extrastriate area other than V2 to be mapped entirely in this region is the dorsal visual area, D, which shares a horizontal meridian representation with V2, and whose vertical meridian representation lies anteriorly in the manner illustrated in Figure 10. There is no obvious correlation between this vertical meridian representation and the pattern of callosal input. Some extrastriate degeneration extends posteriorly as far as the vertical meridian representation of the dorsal area, but the discontinuous nature of this degeneration suggests that parts of the vertical meridian representation receive no callosal input. It seems clear that the pattern of callosal inputs has little value for determining visual area boundaries in this region of the bushbaby's cortex.

Ventral to MT, the pattern of callosal connections of extrastriate cortex seems to be simpler than the pattern found in dorsal extrastriate cortex (Figures 8, 9, and 10). It could be argued that there exists an elongated ventral patch which appears to be homologous with the discrete ventral strip observed in the owl monkey. However, close inspection shows that the degeneration on the lateral and ventral surfaces of the bushbaby cortex is of a more diffuse nature than the sharply defined strip on the owl monkey's ventral cortical surface. Degeneration ventral to MT

Figure 10. Two dorsolateral views of the right hemisphere of a bushbaby brain. The top figure illustrates the known topographic organization of visual cortex. Question marks indicate regions of uncertain boundaries. The bottom figure shows the pattern of callosal degeneration over the expanse of cortex for which the topographic organization is shown at the top. The shaded area at the occipital pole is striate cortex (V1), the shaded area on the lateral surface in extrastriate cortex is MT. The large dots signify heavy and moderate degeneration, the small dots denote light degeneration. The solid black line shows the anterior extent of the reconstruction. Note the discrete band of degeneration at the V1-V2 border and the thickening of degeneration at the MT border. (D, dorsal area; all other symbols and abbreviations are the same as in Figure 1.)

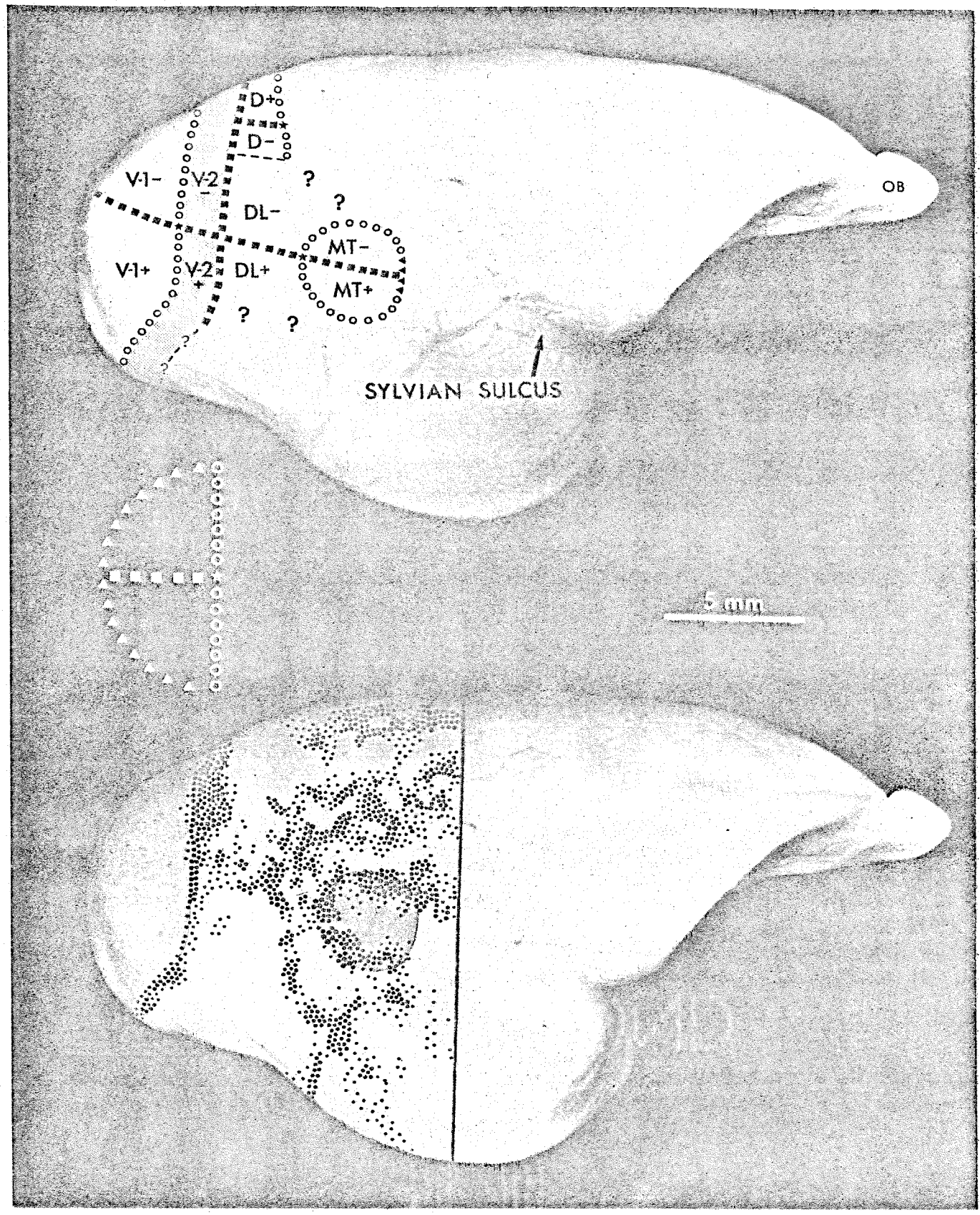
D+
D−
V-1−
V-2−
?
?
DL−
MT−
V-1+
V-2+
DL+
MT+
?
?
OB
SYLVIAN SULCUS
5 mm

Figure 11. Two ventromedial views of the left hemisphere of a bushbaby brain. The top figure illustrates the topographic organization of visual cortex. Question marks signify uncertain boundaries. The bottom figure shows the pattern of callosal degeneration over the expanse of cortex for which the topographic organization is shown at the top. The shaded area at the occipital pole is striate cortex (V1). The solid black line shows the anterior extent of the reconstruction. (D, dorsal area; OB, olfactory bulb; all other symbols and abbreviations are the same as for Figure 1.)

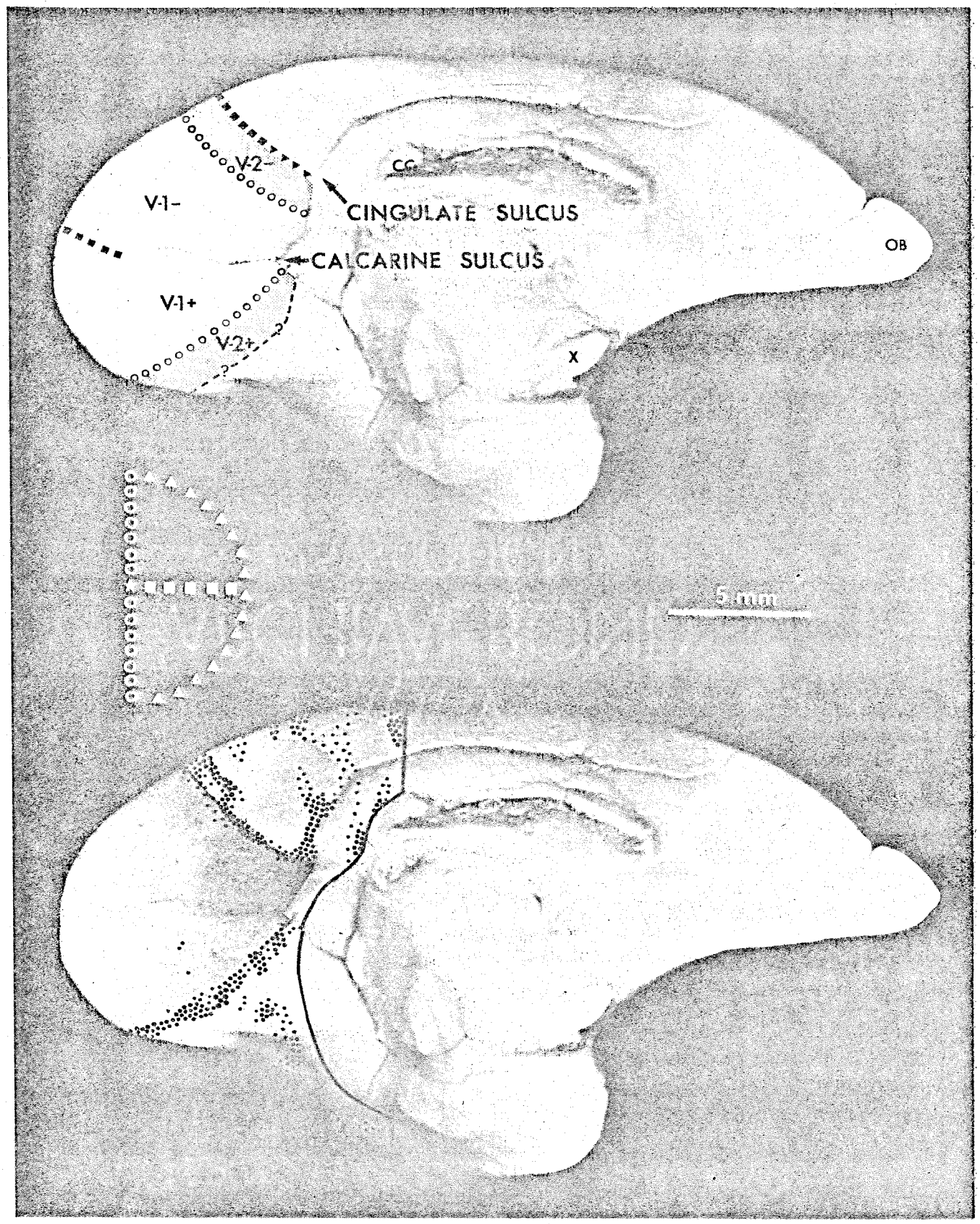
V-2-
V-1-
CG
CINGULATE SULCUS
CALCARINE SULCUS
OB
V-1+
V-2+
X
5 mm

in the bushbaby consists of a few "islands" of moderate degeneration connected by a relatively wide area of light degeneration. In histological sections, this degeneration does not appear nearly as well-defined as does the narrow, moderate-to-heavy strip of degeneration on the ventral surface of the owl monkey's cortex. Future physiological experiments should resolve this issue, but it seems unwise to make any claim for ventral surface homology between owl monkey and bushbaby on the basis of evidence presently available.

DISCUSSION

The principle goals of this study have been 1) to assess the utility of the study of callosal connections for locating boundaries of extrastriate visual areas in the owl monkey and bushbaby, and 2) to gain information concerning the existence and organization of as yet unmapped visual areas.

The experiments performed in this study demonstrate the existence of restricted regions where the correspondence between callosal connections and vertical meridian representations is precise enough to be of value in determining boundaries of visual areas. Specifically, the pattern of callosal connections has been shown to be of sufficient precision and reliability to be useful in locating the V1-V2 and MT vertical meridian representations in both owl monkey and bushbaby. In addition, there appears to be a well-defined strip of callosal input on the ventral surface of the owl monkey occipital lobe which accurately locates a vertical meridian representation.

In both species, however, the pattern of callosal connections is much less straightforward in extrastriate cortex dorsal and posterior to MT. Although there may be some correspondence in the owl monkey between degeneration extending from the termination of the Sylvian sulcus to the medial wall of the hemisphere

and the vertical meridian representation of DM and M, it is impossible to tell using the techniques of this study whether or not this correlation is of sufficient precision to be useful in locating areal boundaries. In the region of owl monkey cortex occupied by extrastriate areas DI and DL, the callosal inputs are spread diffusely over most of the interior of the visual areas (see Figure 6). Similarly, the intricate pattern of callosal connections over dorsal extrastriate cortex in the bushbaby does not, at this point, appear to correspond to known boundaries. Future functional studies of these regions may reveal physiological correlates of these complex patterns of callosal inputs. However, at present, callosal inputs to these regions of cortex are too poorly understood to be of use in drawing boundaries. It is therefore necessary for the experimenter to conduct assays of the correlation between callosal input and visual field topography before employing the pattern of connections for the subdivision of a particular region of extrastriate cortex. Examples of such assays are 1) combined physiological and anatomical experiments in the same hemisphere, and 2) the use in the same hemisphere of callosal connections and architectonic techniques which have been demonstrated to yield precise information concerning the location of vertical meridian representations. From the evidence presented here, it is anticipated that the broad patterns of interhemispheric connections within a species will be reliable enough from animal to animal to warrant regular use of the callosal technique in drawing areal boundaries once regions of useful correspondence have been located.

A major result of this study is the identification of two previously unknown visual areas, VA and VP, on the ventral surface of the owl monkey's occipital lobe. An outline of the probable topographic organization of these areas has been deduced from the pattern of callosal input to the region and from a limited number of physiological recordings in the region. The ventral posterior area, VP, lies

immediately anterior to the ventral portion of V2 and shares a common representation of the horizontal meridian with V2. At the anterior border of VP is the common representation of the vertical meridian shared by VP and the ventral anterior area, VA. This representation of the vertical meridian appears to be coextensive with a well-defined strip of callosal input to the ventral surface (see Figures 6 and 7, and Results). Interestingly, the representation of the visual field in both VA and VP is restricted largely, and perhaps completely, to the upper quadrant of the visual field. This constitutes the first major departure from the general pattern of organization of owl monkey extrastriate cortex in which each visual area has been found to contain a representation of the complete contralateral hemifield. A possible precedent for this type of organization has been found, however, in the more complex cortex of the macaque monkey. Recent studies of the projections of macaque striate cortex (Van Essen et al., 1979b) have shown that dorsal striate cortex projects to extrastriate area V3, in contrast to ventral striate cortex which does not project to V3. This evidence suggests that V3 may contain a representation of the lower visual field, but not of the upper visual field. Alternatively, V3 may contain representations of upper and lower fields, but the anatomical connections of the upper and lower fields may be different. It is not clear to what extent upper and lower visual field representations can be considered part of the same visual area if their anatomical connections (and presumably their functional properties) are radically different. Future research on the anatomical connections and physiological properties of all extrastriate visual areas should clarify this point.

With the results reported in this study, it is now possible to compare the pattern of interhemispheric connections of visual cortex in three primate species: the bushbaby, a strepsirhine primate; the owl monkey, a New World

monkey; and the macaque, an Old World monkey. In all three species, a discrete band of callosal input corresponds to the vertical meridian representation at the V1-V2 border (for macaque callosal connections, see Myers, 1962; Zeki, 1970; Van Essen and Zeki, 1978). In both owl monkey and bushbaby, an increase in the density of callosal terminals also corresponds to the vertical meridian representation at the MT border. In the macaque, a striate-receptive region of cortex in the superior temporal sulcus is, on anatomical and physiological grounds, almost certainly homologous to MT in New World monkeys (Van Essen, 1979). However, there is no simple correspondence between the boundary of macaque MT and the density of callosal terminals. This is not entirely surprising since physiological evidence indicates that, in contrast to the situation in the owl monkey and the bushbaby, the perimeter of the visual hemifield (vertical meridian and far periphery) is not always represented at the boundary of macaque MT (Maunsell et al., 1979; but see Gattas and Gross, 1979).

In extrastriate cortex on the dorsal surface of the occipital lobe, the pattern of callosal connections has little value for defining visual area boundaries in the owl monkey and the bushbaby. However, in the macaque, a consistent pattern of callosal connections corresponds to at least two representations of the vertical meridian and is a powerful aid in delineating visual area boundaries in dorsal extrastriate cortex (Van Essen and Zeki, 1978). These data in conjunction with the results of physiological mapping studies in the macaque (Zeki and Sandeman, 1976; Van Essen and Zeki, 1978) suggest organizational differences among the dorsal extrastriate areas of the macaque, owl monkey and bushbaby.

In extrastriate cortex on the ventral surface of the owl monkey's occipital lobe, a single, well-defined strip of callosal input contrasts strikingly with the complex arrangement of input dorsally. This ventral strip appears to correspond

to a vertical meridian representation shared by two newly discovered extrastriate visual areas. Recently, the callosal input to ventral extrastriate cortex in the macaque has been examined using mapping techniques which permit an accurate "unfolding" of the extensively convoluted cortex (Van Essen et al., 1979a). The resulting map shows a simple, discrete strip of callosal degeneration which traverses the ventral surface anterior to V2. This arrangement is remarkably similar to that seen in owl monkey ventral extrastriate cortex and suggests a similar topographic organization of this region in the two species. In the bushbaby, a more diffuse area of callosal input which exists on the lateral and ventral surfaces of extrastriate cortex could possibly signify an area organized similarly to ventral extrastriate cortex of the owl monkey and the macaque. Extensive physiological studies in all three species will determine the extent to which these ventral regions are strictly comparable.

A major difference in the overall pattern of callosal connections in the owl monkey and bushbaby is the existence of a continuous "bridge" of degeneration of callosal degeneration connecting extrastriate degeneration in the bushbaby with the discrete band of degeneration at the V1-V2 border (see Figures 8 and 9). This "bridge" of degeneration occurs posterior and slightly medial to MT near the center of gaze representations of V1, V2, MT and a third tier area which may be homologous to owl monkey area DL (see Figure 10). This situation contrasts with that in owl monkey where degeneration at the center-of-gaze representation of the V1-V2 border does not fuse with extrastriate degeneration. However, such a "bridge" of degeneration connecting extrastriate degeneration with the V1-V2 border does occur in the region of foveal representation of the macaque (Zeki, 1970; Van Essen and Zeki, 1978). The significance of this similarity may become apparent when detailed physiological maps of the region are available for both species.

A close examination of Figures 8 and 9 reveals an asymmetry between the upper- and lower-field vertical meridian representations of V1 in the bushbaby. If the "bridge" of callosal degeneration connecting the V1-V2 border with extrastriate degeneration approximately locates the center-of-gaze representations of V1 and V2, then the vertical meridian representation of the lower visual field (dorsal) is significantly shorter than the vertical meridian representation of the upper visual field (ventral). While the reconstructions of Figures 8 and 9 are relatively crude and point-to-point distances are sometimes distorted, this observation of upper and lower field vertical meridian asymmetry receives support from a study of topography and magnification factor in bushbaby striate cortex (Myerson and Allman, unpublished observations). In this study, three-dimensional models of bushbaby visual cortex made from physiological mapping data revealed the same asymmetry in upper and lower field vertical meridian representations. However, the total area of the striate upper and lower field representations was roughly the same despite the differences in length of the upper and lower vertical meridian representations. The functional significance of this arrangement is unclear.

If the primary function of the callosal projections to sensory areas of the cortex is to unite sensory hemifields at the midline, then the presence of callosal input over vast portions of individual visual areas, and the lack of continuous callosal input to at least one vertical meridian representation (dorsal area, D, in the bushbaby), seem mystifying. While the functions of the callosal projections are probably of sufficient complexity to defy our attempts to fully account for their appearance with a single hypothesis, several observations can be made which could partially account for the discrepancies. First, it is clear that the topographic representation of the visual field in extrastriate visual areas

is coarser than that in striate cortex. This is due to the dual effect of a drastic decrease in the amount of cortex devoted to the representation of the visual field (MT occupies about one-tenth the area of V1) and a concomitant increase in average receptive field size throughout the extrastriate areas. This means that a receptive field recorded in the interior of an extrastriate visual area has a greater chance of including the vertical meridian and thus receiving callosal input than does a receptive field recorded at a similar visual field eccentricity in V1. This effect becomes particularly acute in regions of cortex where the center-of-gaze representations of several visual areas are closely apposed. Such a region is that lying directly posterior to MT and anterior to V1 in the owl monkey. Here the central six degrees of the visual field are represented in four closely apposed visual areas, V1, V2, DL and MT (see Figure 10). As can be seen in Figure 10, this is a region of particularly complex callosal input. Thus, the presence of extensive callosal input to this region can be partially explained by the existence of large receptive fields which must involve the vertical meridian in a region of greatly expanded central representation.

Another region of particularly complex callosal input lies dorsal to DL and MT in the owl monkey in the dorsointermediate visual area, DI. Although extensive physiological recordings have been made in this area, a clear picture of its visuotopic organization has yet to emerge. Available data suggest that the internal topography of this region may be complex, with particular points in the visual field represented more than once within the area. Such complex visual topography could well lead to a complex arrangement of callosal inputs without doing violence to the idea of congruence between callosal input and vertical meridian representation. Such a situation seems to exist in area V4 of the macaque monkey where visual topography and callosal inputs appear to be very complex (Van Essen and Zeki, 1978).

Although these ideas may partially account for the complex nature of callosal connections in certain cortical regions, it appears likely that other regions of complex connections cannot be accounted for simply on the basis of visual field topography. Future research may reveal additional functions performed by callosal fibers which can account for more complex patterns of connections.

REFERENCES

Allman, J. M. (1977). Evolution of the visual system in the early primates. In Progress in Psychobiology and Physiological Psychology, Vol. 7, eds. Sprague, J. M. and Epstein, A. N. New York: Academic Press.

Allman, J. M. and Kaas, J. H. (1971a). A representation of the visual field in the caudal third of the middle temporal gyrus of the owl monkey (Aotus trivirgatus). Brain Research **31**, 85-105.

Allman, J. M. and Kaas, J. H. (1971b). Representation of the visual field in striate and adjoining cortex of the owl monkey (Aotus trivirgatus). Brain Research **35**, 89-106.

Allman, J. M. and Kaas, J. H. (1974a). The organization of the second visual area (VII) in the owl monkey: A second order transformation of the visual hemifield. Brain Research **76**, 247-265.

Allman, J. M. and Kaas, J. H. (1974b). A crescent-shaped cortical visual area surrounding the middle temporal area (MT) in the owl monkey (Aotus trivirgatus). Brain Research **81**, 199-213.

Allman, J. M. and Kaas, J. H. (1975). The dorsomedial cortical visual area: A third tier area in the occipital lobe of the owl monkey (Aotus trivirgatus). Brain Research **100**, 473-487.

Allman, J. M. and Kaas, J. H. (1976). Representation of the visual field on the medial wall of occipital-parietal cortex in the owl monkey. Science **191**, 572-575.

Allman, J. M., Campbell, C. B. G. and McGuinness, E. (1979). The dorsal third tier area in Galago senegalensis. Submitted for publication.

Allman, J. M., Kaas, J. H. and Lane, R. H. (1973). The middle temporal visual area (MT) in the bushbaby, Galago senegalensis. Brain Research **57**, 197-202.

Choudhury, B. P., Whitteridge, D. and Wilson, M. E. (1965). The function of the callosal connections of the visual cortex. Quarterly Journal of Experimental Physiology **50**, 214-219.

Ebner, F. F. and Myers, R. E. (1965). Distribution of corpus callosum and anterior commissure in cat and raccoon. Journal of Comparative Neurology **124**, 353-366.

Gattas, R. and Gross, C. G. (1979). A visuotopically organized area in the posterior superior temporal sulcus of the macaque. ARVO Annual Meeting, Abstracts. p. 184.

Hubel, D. H. and Wiesel, T. N. (1967). Cortical and callosal connections concerned with the vertical meridian of the visual fields in the cat. Journal of Neurophysiology **30**, 1561-1573.

Maunsell, J. H. R., Bixby, J. L. and Van Essen, D. C. (1979). The middle temporal area (MT) in the macaque: Architecture, functional properties and topographic organization. Society for Neuroscience, 9th Annual Meeting, Abstracts.

Mitchell, D. E. and Blakemore, C. (1970). Binocular depth perception and the corpus callosum. Vision Research **10**, 49-54.

Myers, R. E. (1962). Commissural connections between occipital lobes of the monkey. Journal of Comparative Neurology **118**, 1-16.

Myerson, J., Kaas, J. H. and Allman, J. M. (1979). The visuotopic organization of the geniculo-striate system in Galago senegalensis. In preparation.

Palmer, L. A., Rosenquist, A. C. and Tusa, R. J. (1978). The retinotopic organization of lateral suprasylvian visual areas in the cat. Journal of Comparative Neurology **177**, 237-256.

Pandya, D. N., Karol, E. A. and Heilbronn, D. (1971). The topographical distribution of interhemispheric projections in the corpus callosum of the rhesus monkey. Brain Research **32**, 31-43.

Pandya, D. N. and Vignolo, L. A. (1968). Interhemispheric neocortical projections of somatosensory areas I and II in the rhesus monkey. Brain Research **7**, 300-303.

Sanides, D. (1978). The retinotopic distribution of visual callosal projections in the suprasylvian visual areas compared to the classical visual areas (17, 18, 19) in the cat. Experimental Brain Research **33**, 435-443.

Shatz, C. J. (1977). Anatomy of interhemispheric connections in the visual system of Boston siamese and ordinary cats. Journal of Comparative Neurology **173**, 497-518.

Tusa, R. J., Palmer, L. A. and Rosenquist, A. C. (1978). The retinotopic organization of area 17 (striate cortex) in the cat. Journal of Comparative Neurology **177**, 213-236.

Tusa, R. J., Rosenquist, A. C. and Palmer, L. A. (1979). Retinotopic organization of areas 18 and 19 in the cat. Journal of Comparative Neurology **185**, 657-678.

Van Essen, D. C. (1979). Visual cortical areas. In Annual Review of Neuroscience, Vol. 2, ed. Cowan, W. M. Palo Alto: Annual Reviews, Inc.

Van Essen, D. C. and Zeki, S. M. (1978). The topographic organization of rhesus monkey prestriate cortex. Journal of Physiology (Lond.) **277**, 193-226.

Van Essen, D. C., Maunsell, J. H. R. and Bixby, J. L. (1979a). The organization of extrastriate visual areas in the macaque monkey. To be published in Multiple Cortical Areas, ed. Woolsey, C. N. Humana Press.

Van Essen, D. C., Maunsell, J. H. R. and Bixby, J. L. (1979b). Areal boundaries and topographic organization of visual areas V2 and V3 in the macaque monkey. Society for Neuroscience, 9th Annual Meeting, Abstracts.

Wiitanen, J. T. (1969). Selective silver impregnation of degenerating axons and axon terminals in the central nervous system of the monkey (Macaca mulatta). Brain Research **14**, 546-548.

Zeki, S. M. (1969). Representation of central visual fields in prestriate cortex of monkey. Brain Research **14**, 271-291.

Zeki, S. M. (1970). Interhemispheric connections of prestriate cortex of monkey. Brain Research **19**, 63-75.

Zeki, S. M. and Sandeman, D. R. (1976). Combined anatomical and electrophysiological studies on the boundary between the second and third visual areas of rhesus monkey cortex. Proceedings of the Royal Society, London, B **194**, 555-562.

II. A FUNCTIONAL LOCALIZATION OF NEURONAL RESPONSE PROPERTIES IN EXTRASTRIATE CORTEX OF THE OWL MONKEY, AOTUS TRIVIRGATUS

INTRODUCTION

In recent years it has become increasingly clear that extrastriate visual cortex in a number of mammalian species is composed of several distinct visual areas. Of particular importance in the exploration of extrastriate cortex has been the use of electrophysiological mapping techniques for the study of visual field topography. Such studies have revealed a mosaic of cortical visual areas, each of which contains a topographic representation of all or part of the contralateral visual hemifield. It is likely that such discrete cortical representations of the visual field constitute functionally distinct units for the processing of visual information.

The first topographically organized extrastriate area to be discovered was the second visual area of the cat, VII, identified in an evoked potential study by Talbot (1942). Later microelectrode recordings in the cat resulted in the discovery of an additional topographically organized extrastriate area, VIII (Hubel and Wiesel, 1965), lying lateral to VII, and also a visually responsive region in the lateral suprasylvian sulcus (Clare and Bishop, 1954). In the macaque monkey, anatomical studies of the projections of striate cortex by Cragg and Ainsworth (1969) and Zeki (1969) provided the first evidence for the existence of topographically organized extrastriate areas in primates. Striate cortex was found to project in a point-to-point fashion to two bands of surrounding cortex identified as V2 and V3. The evidence from these anatomical studies was supported and extended by Zeki's analysis of the pattern of interhemispheric connections in the macaque (Zeki, 1970). Exploiting the experimental advantages offered by the smooth cortex of the owl monkey, Allman and Kaas became the first investigators to employ microelectrode recording techniques for the systematic mapping of visual field topography over a broad expanse of extrastriate cortex. From their

studies emerged an unprecedented picture of extrastriate organization in which no fewer than seven visual areas were identified, five of which contained complete representations of the contralateral visual hemifield (Allman and Kaas, 1971a,b, 1974a,b, 1975, 1976). Combining anatomical and physiological techniques, Zeki and his colleagues have now identified five extrastriate areas in the macaque, with large regions still incompletely explored (Zeki, 1974; Zeki and Sandeman, 1976; Van Essen and Zeki, 1978). Similarly, recent work in the cat by Tusa, Palmer and Rosenquist has revealed the existence of twelve extrastriate visual areas containing topographic representation of all or some of the visual field (Tusa et al., 1978, 1979; Palmer et al., 1978). Work on other species has reinforced the conclusion that the phenomenon of multiple cortical representations of the visual field is a general feature of mammalian visual cortex. The number and arrangement of discrete areas is not the same for all species, and it remains a goal of continuing research to determine the extent to which particular visual areas can be considered homologous in the various mammalian species (for review, see Van Essen, 1979).

Given the existence of multiple visual areas in mammalian extrastriate cortex, questions naturally arise concerning the functions performed by each area in the processing of visual information. Certain clues can be obtained from the manner in which the visual field is represented in various areas. For instance, a visual area such as the medial area of the owl monkey, which has an expanded representation of the visual periphery, is probably involved in visual functions relevant to events occurring outside the center-of-gaze. However, the most fruitful approach at this time appears to be the study of functional properties of single neurons within each visual area. If a visual area can be shown to be relatively rich in neurons sensitive to a particular stimulus parameter, then it

is reasonable to assume that the visual area is preferentially involved in the analysis of that stimulus parameter. A striking example of such a localization of functional properties is in the striate-receptive region of the superior temporal sulcus (STS) of the macaque monkey. More than ninety percent of the neurons studied in this region are selective for the direction of motion of visual stimuli, while fewer than ten percent of the cells studied in other areas (V2, V3, V3A and V4) are selective for direction of motion (Zeki, 1974, 1978). Another example is the relative localization of cells which respond preferentially to the chromatic properties of visual stimuli. A third or more of the neurons in area V4 of the macaque can be considered color-coded or color-biased (Zeki, 1973, 1977; Van Essen and Zeki, 1978), while fewer than five percent of the neurons in areas V2, V3, V3A and striate-receptive STS can be so classified (Van Essen and Zeki, 1978; Zeki, 1978) (for review see Van Essen, 1979).

It has been our goal to gain information concerning the functions of extra-striate visual areas of the owl monkey by undertaking a study of the functional properties of single neurons in these areas. A summary of the topographic organization of owl monkey visual cortex as revealed by the experiments of Allman and Kaas is shown in Figure 1 (from Allman, 1978). The first visual area, or striate cortex, is located at the occipital pole of the hemisphere. The center-of-gaze representation of V1 is located laterally and the visual periphery is represented in the depths of the calcarine sulcus. Surrounding V1 on the exposed surface of the hemisphere and in parts of the calcarine sulcus is the second visual area, V2. V2 is characterized by a split representation of the horizontal meridian so that, excepting the central five degrees, the representation of the upper visual field is not physically continuous with the representation of the lower visual field. Anterior to V2 lies a third tier of visual areas, each of which shares a partial

Figure 1. Topographic organization of visual cortex in owl monkey as revealed by electrophysiological mapping studies of Allman and Kaas. At the top is a ventromedial view of the right hemisphere of the brain, at the bottom is a dorsolateral view of the whole brain. The visual field symbols on the perimeter chart are superimposed on the cerebral cortex to illustrate the representation of the visual field in the individual visual areas. The open circles symbolize representations of the vertical meridian, filled squares denote representations of the horizontal meridian, and the filled triangles locate representations of the periphery of the visual field. Pluses symbolize the upper visual field, minuses the lower field. Dashed lines are borders where visual field locations are represented other than the ones which are illustrated by symbols in the perimeter chart. The row of V's represents the approximate anterior border of visual cortex, and dotted lines broken by question marks are uncertain borders. (DI, dorsointermediate area; DL, dorsolateral crescent; IT, inferotemporal cortex; M, medial area; MT, middle temporal area; ON, optic nerve; OT, optic tectum; PP, posterior parietal cortex; T, tentorial area, as yet incompletely mapped; X, optic chiasm.) From Allman (1977).

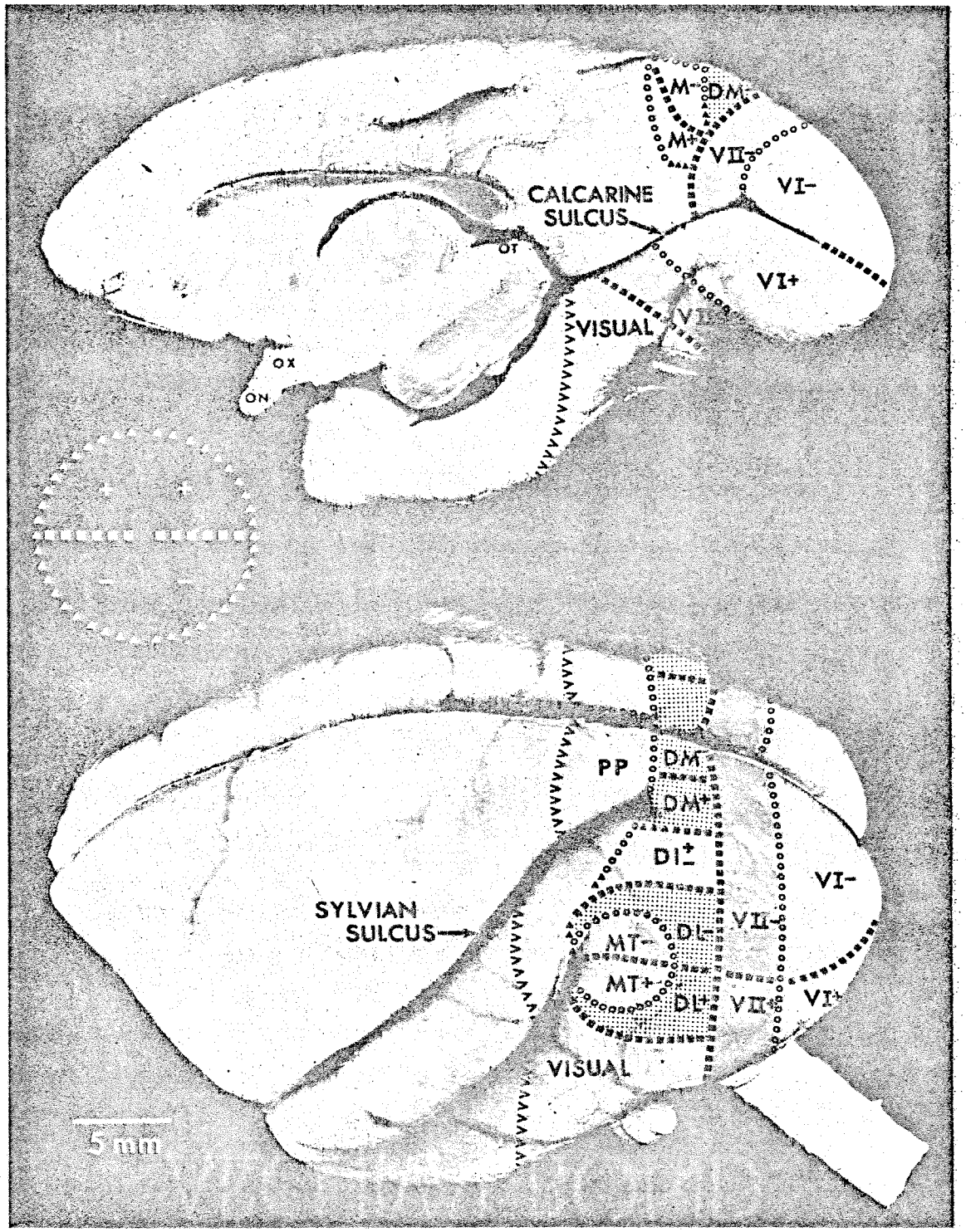
M-
DM-
M+
VII
VI-
CALCARINE
SULCUS
OT
VI+
VISUAL
VI
OX
ON
PP
DM-
DM+
DL+
VI-
SYLVIAN
SULCUS
VII
MT-
DL-
MT+
DL+
VII
VI+
VISUAL
5 mm

representation of the horizontal meridian with V2. At least three of these areas (DL, DM and M) contain complete representations of the contralateral visual hemifield. Anterior to DL lies yet another visual area, MT, which also contains a complete representation of the contralateral visual hemifield. In this study, we have examined response properties of single neurons in areas DM, M, DI, and MT in chronically prepared owl monkeys. It is hoped that by assembling preferred stimulus profiles of each of these areas, functional differences will become apparent. Special attention has been devoted to the middle temporal area, MT, because strong anatomical and now functional data suggest that MT is homologous to the striate-receptive STS area of the macaque (see Discussion).

Our approach to the study of single unit response properties in these extrastriate areas has been primarily quantitative. In the past, most physiological studies of single unit properties have relied upon the "trained ear" of the investigator to qualitatively discriminate neuronal responses to various stimuli. The final end of such studies is usually the elaboration of a scheme in which each neuron is assigned to a particular group based upon its apparent specificity for a restricted class of stimuli. Such schemes easily reinforce conclusions that such subjective categories truly correspond to unambiguous, nonoverlapping populations of cortical neurons. While such conclusions are frequently valid, recent studies indicate that single unit response properties, when quantitatively measured, do not always form unambiguous groups. Rather, neuronal response patterns tend to form continuous distributions between poles which can be described by common qualitative labels (see discussion of striate "hypercomplex" cells in Schiller et al., 1976). We have therefore employed techniques for a quantitative assessment of the distributions of neuronal responses to various visual stimuli. Presentation of such quantitatively measured distributions promotes a more realistic view of

the stimulus specificities of populations of cortical neurons. At all times, an attempt has been made to describe how the quantitative measurements correspond to, or differ from, standard qualitative descriptions of neuronal response patterns. In cases in which neuronal response patterns for a population are grouped massively toward one pole of a distribution, the results of our studies are similar to the findings of qualitative investigations.

METHODS

So that efficient use of available primates might be made, a chronic recording technique was employed which allowed multiple physiological experiments to be performed on a single animal over a period of months. Owl monkeys were prepared for surgery, and a craniotomy exposed the desired region of visual cortex. A stainless-steel chamber was cemented to the skull, covering the exposed cortex. The scalp wound was treated with disinfectant and sutured. A threaded cap at the top of the chamber allowed access to the brain for physiological recording. The dura mater remained intact throughout the sequence of recording experiments.

At the beginning of each experiment, the animal was sedated with an intramuscularly-administered dose of triflupromazine HCl (Vetame, 12 mg/kg). The sedated state was maintained throughout the twelve-hour experiment with supplemental intramuscular doses of ketamine HCl (Vetalar, 6 mg/kg/hr). The animal's head was held rigidly in place by a mechanical support which connected the implanted chamber with the structure of the primate chair in which the animal was seated. This mechanical support also held the microdrive assembly which was used to advance recording electrodes into the brain. The animal's eyes were locally anesthetized with a sterile 0.5% solution of dibucaine HCl. Each eye was fixed to a specially contoured eye ring with a commercially-obtainable tissue adhesive,

HISTOACRYL blue (n-butyl cyanoacrylate). The eyes were then positioned in the normal physiological alignment; the optic disks were situated at the same vertical elevation and 40° apart on the horizontal axis (the optic disks being located 20° from the area centralis). A series of careful adjustments was required to achieve this alignment. When the eyes were properly aligned in this manner, receptive fields as measured through the individual eyes were generally superimposed. Eye position was checked at intervals throughout the experiment by opthalmoscopically projecting the retinal image onto the tangent screen. If eye movements were found to have occurred, the eyes were readjusted to the desired position. Contact lenses of a corrective power of +4 diopters were used to focus the animal's eyes on the tangent screen 28.5 cm from the eyes. Contact lenses also prevented the eyes from drying during the experiment. Sterile, glass-insulated platinum microelectrodes (Wolbarsht et al., 1960) were used to penetrate the dura mater and record extracellularly from single cortical neurons. Electrodes were advanced by a hydraulic microdrive, and were positioned using a polar coordinate system built into the microdrive mounting assembly. An animal would serve as an experimental subject approximately once a week for as long as 6-9 months before being disimplanted and returned to a breeding colony.

Data Collection and Analysis. Extracellular signals from single neurons were amplified and displayed on an oscilloscope and audio monitor. When the amplitude and waveform of an individual neuron were large and stable enough to be reliably isolated by the oscilloscope trigger, the receptive field was mapped and the unit's response characteristics were estimated qualitatively. Visual stimuli were light and dark bars, squares, and spots focused on the tangent screen by a rear projection optic stimulator. After the initial qualitative examination, response properties were studied quantitatively using the optic stimulator in conjunction

with a Nova 2 computer (Control Data Corporation). The computer was programmed to present visual stimuli of various orientations, directions of movement, and velocities in an interleaved, pseudorandom fashion. Randomized stimulus presentations were used so as to avoid, 1) artifactual peaks in the response curves caused by a periodic waxing and waning in a cell's overall responsiveness, and 2) possible habituating effects. The computer recorded neuronal responses to the presented visual stimuli as well as the neuron's spontaneous firing rate. The data were analyzed on-line in an elementary fashion and presented to the experimenters in poststimulus-time histograms and polar plots. This on-line feedback was used to guide further study of the neuron's response properties. The data were then stored on a magnetic disk and analyzed more completely at a later date (see Results).

Identification of Extrastriate Areas. The physiological experiments were undertaken with the primary goal of obtaining data concerning the functional properties of extrastriate neurons. However, such data are useful for the investigation of functional localization of response properties only if one is able to reliably identify the extrastriate area from which one is recording. Therefore, a secondary goal of each experiment was to generate topographic maps of the cortical visual field representations so that the boundaries of particular extrastriate areas could be identified. To this end, the receptive field of each cell studied as well as receptive fields of the unresolved background activity were mapped with care and analyzed collectively to reveal the topographical organization of the area of cortex under study. In particular, transitions of receptive fields from the upper visual quadrant to the lower quadrant and reversals of progressions at the vertical and horizontal meridia were noted. The resulting map could be compared to the known topographical map of owl monkey extrastriate cortex (see Figure 1), and the cortical areas identified. Most cells could therefore be assigned to a particular extrastriate

area. However, in regions where uncertainty existed as to the exact boundaries, cells were not assigned to a particular visual area. Cells which were recorded at the boundary of areas DI and DM, or at the boundary of areas DM and M, were included in the analysis of medial third tier neurons since the results presented below are cast as a comparison of area MT and the collective medial third tier areas (DI, DM, and M) (see below and see Appendix 1). Cells recorded at other visual area boundaries were not used in the analysis.

RESULTS

Response properties of neurons in four extrastriate visual areas—middle temporal (MT), dorsointermediate (DI), dorsomedial (DM) and medial (M)—were examined in this study. Neurons in areas DI, DM and M responded similarly to the visual stimuli used in these experiments (see Appendix 1), but response properties of neurons in MT were strikingly different. For this reason, the data presented here will be cast as a comparison of response properties of neurons in MT vs. those of neurons in DI, DM, and M, collectively. Since DI, DM and M are all located medially in the third tier of visual areas (see Figure 1), they will be referred to collectively as the "medial third tier."

The overwhelming majority of cells in all four of these areas were optimally driven by simple shapes such as bars, slits and spots of varying orientation, direction of motion, velocity of motion, and stimulus size. Although more exotic stimuli were occasionally tried, extremely few convincing examples of a neuronal preference for a more complex stimulus were observed. A common feature of responses in all four extrastriate areas was a preference for moving as opposed to stationary stimuli. Frequently, cells would give a weak, transient response to a stationary stimulus, but moving stimuli were generally required for vigorous, sustained responses. In

addition, neurons in all four areas were generally stimulated through either eye alone and through both eyes simultaneously. We have quantitatively examined neuronal responses to three major stimulus parameters: form, direction of movement, and velocity of movement. The results of these quantitative studies are presented below. Evidence is also presented regarding columnar organization in MT.

Direction of Motion. Neuronal responses to systematic variations in the direction of motion of visual stimuli were examined for 277 cells, 85 in MT and 192 in the medial third tier. Responses were measured by a computer as a visual stimulus was swept through the receptive field in twelve different directions separated by 30-degree intervals. The computer initiated the stimulus sweeps so that each direction was swept five times in an interleaved, pseudorandom sequence. The stimulus form used for each cell was that which had been qualitatively determined to drive the cell best. For the majority of cells, the optimal stimulus was a light, elongate bar. Elongated stimuli were always swept through the receptive field so that the axis of orientation was perpendicular to the direction of motion. The results of two such "direction series" are shown in Figure 2. The cell at the top of the Figure is from the medial third tier and the cell at the bottom is from MT. Each oscilloscope trace represents the sum total of five stimulus sweeps through the receptive field in the direction indicated to the right of the trace. Time is represented on the horizontal axis and the strength of the neuronal response is represented by the height of the vertical columns. Spontaneous firing is shown before and after the stimulus sweep; the actual stimulus sweep is denoted by the thickened segment near the center of each oscilloscope trace. The medial third tier cell whose responses are shown at the top has a maximum response at zero degrees and another enhanced response in the opposite direction at 180 degrees. The response falls nearly to zero in the orthogonal directions at 90 and 270 degrees.

Figure 2. Responses of two extrastriate neurons to a visual stimulus swept through the receptive field in twelve directions. Each oscilloscope trace represents the sum total of five stimulus sweeps through the receptive field in the direction indicated to the right of the trace. Time is represented horizontally, and the strength of the response is indicated by the height of the vertical columns. The actual time of stimulus presentation is indicated by the thickened segment near the center of each trace. The spontaneous firing rate is shown before and after each stimulus presentation. Stimulus sweeps were conducted in an interleaved, pseudorandom order. The medial third tier neuron whose responses are shown at the top gives a response typical of an orientation-selective cell. The MT neuron whose responses are shown at the bottom gives a direction-selective response.

AIMX3180.01

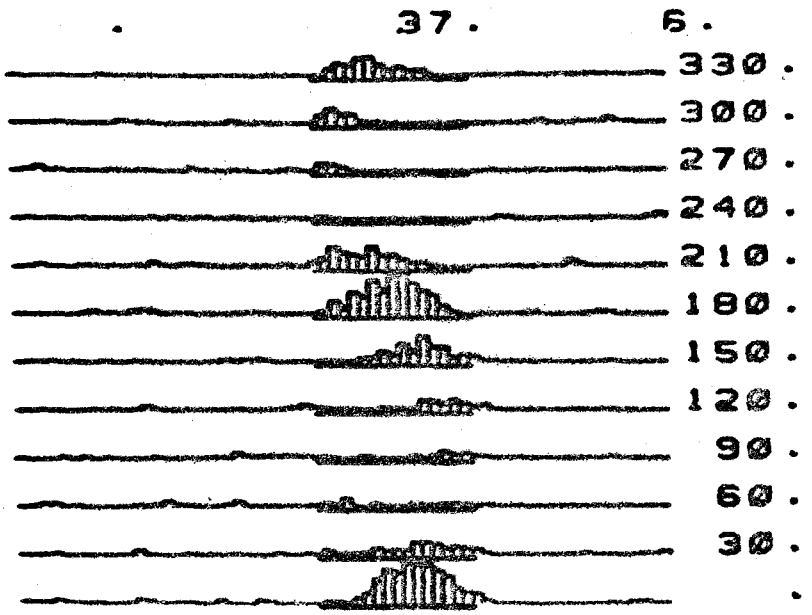

SELX4880.01

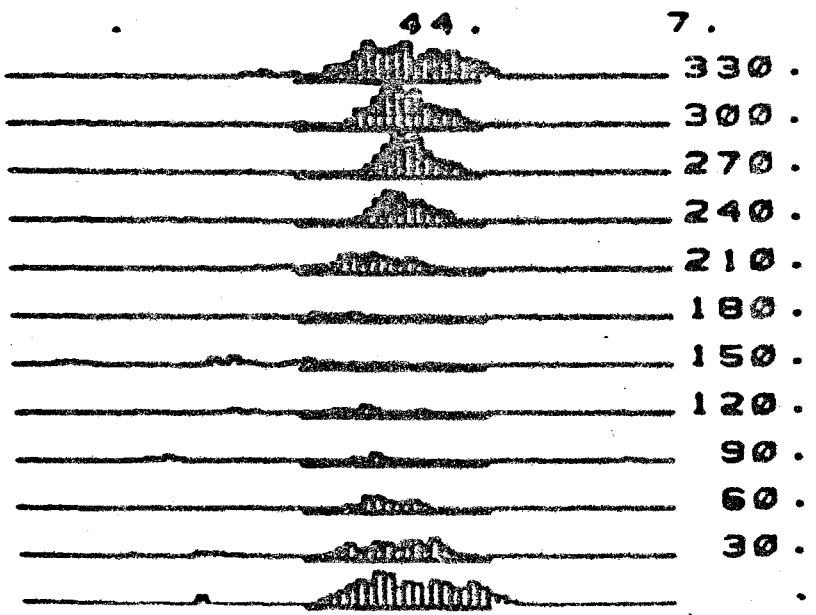

Such a response pattern to an elongated stimulus is typical of an "orientation-selective" cell which fires to elongated stimuli of a particular orientation and decreases its firing rate in response to any change in orientation from the optimum. However, cells were occasionally studied which yielded a similar response pattern to a nonoriented stimulus such as a spot (see Figure 6). Cells of this nature have been observed in the lateral suprasylvian visual areas of the cat by Spear and Baumann (1975). Such cells were termed "axially direction-selective" since they respond to motion in either direction along a 180 degree axis through the receptive field. Use of the term "orientation-selective" is inappropriate if the addition of orientation to the stimulus has no effect upon the response pattern of the cell. This point is examined in more detail below. The cell whose responses are illustrated at the bottom of Figure 2 responded optimally to a stimulus moving at 330 degrees, and not at all to one travelling in the opposite direction (150 degrees). Such a response pattern is termed "direction-selective."

From such raw data, analysis programs calculate quantitative measures of neuronal responses to the various directions of motion. A neuron's spontaneous firing rate (spikes/second) is measured in the interval immediately before the stimulus is presented, and is then subtracted from the firing rate (spikes/second) during stimulus presentation to yield the net response rate for a particular sweep. The value for the response rate (spikes/second) used in subsequent calculations is the average of the response rates for the five sweeps in a particular direction. Such quantitative analyses for the two cells shown in Figure 2 are illustrated in Figure 3. The response for each direction of motion has been normalized to a percentage of the maximum response and displayed on a graph of direction vs. response. From such data it is convenient to calculate a "direction index" for each cell which is a quantitative measure of the cell's direction selectivity. The

Figure 3. Quantitative analysis of the response patterns illustrated in Figure 2. Directions of motion at which stimuli were presented are plotted horizontally. The neuronal response for stimuli moving in each direction as a percentage of the optimal response is plotted vertically. The illustrated response in each direction is the arithmetic mean of the individual responses to the five stimulus presentations. Formulas for computation of direction and tuning indices are given at the bottom. The shaded area for each response curve is the area under the curve computed for calculation of the tuning index. For the orientation-selective cell at top: "D" index = 0.11, "T" index = 0.69. For direction-selective cell at bottom: "D" index = 1.00, "T" index = 0.33.

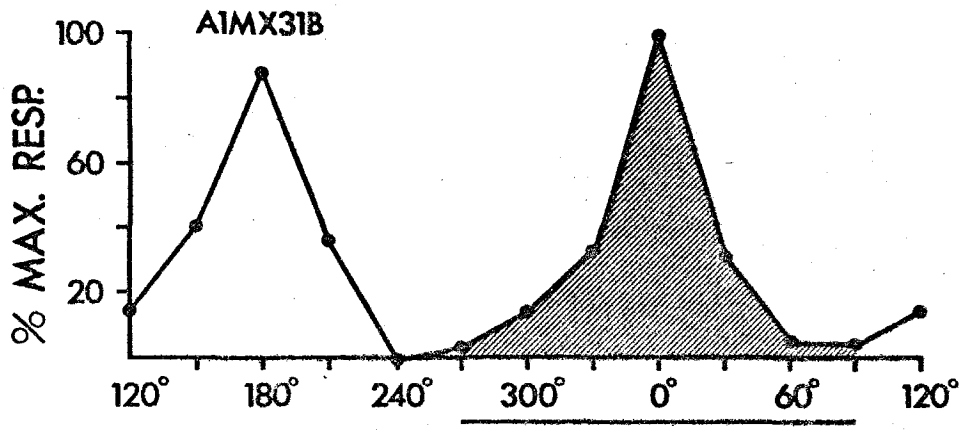

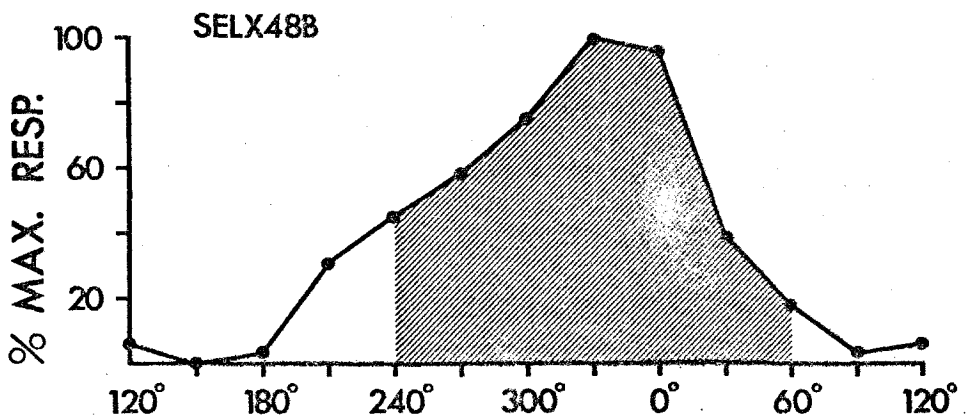

'D' INDEX = $1 - \frac{\text{OPP.}}{\text{BEST}}$ 'T' INDEX = 1 – (AREA UNDER CURVE)

formula used (shown at bottom left of Figure 3) is 1 minus the ratio of the response in the opposite direction to the response in the optimal direction. Thus, for a cell such as the one whose responses are illustrated at the top of Figures 2 and 3, the ratio of opposite response to best response is almost one, and the direction index will approach zero. For the cell whose responses are illustrated at the bottom of Figures 2 and 3, the ratio of opposite response to best response is low and the direction index approaches one. Thus, the response pattern of each cell will generate a direction index which may range from zero for orientation-selective, axially direction-selective, or pandirectional cells, to one for direction-selective cells (the direction index may be greater than one if the spontaneous firing is actually inhibited by stimuli directed opposite to the optimum direction).

Histograms illustrating the distribution of direction indices for cells of MT and of the medial third tier areas are shown in Figure 4. A striking difference is at once apparent. Neurons in MT show a strong tendency to group at the high-index end of the distribution. Thus, the great majority of MT cells exhibit a high degree of direction selectivity. In contrast, neurons of the medial third tier mass strongly at the low-index end of the distribution. Thus, the majority of medial third tier cells are of a nondirectional nature (such cells may be orientation-selective, axially direction-selective or pandirectional). The difference in the distributions is highly significant by statistical tests ($\underline{t}$ test for difference of means, $\underline{t} = 10.5$, $p << .001$). It should be noted that the segregation of direction-selective cells between MT and the medial third tier is not absolute. The data in Figure 4 demonstrate the existence of a few strongly direction-selective cells in the medial third tier and of a few orientation-selective cells in MT. It should also be emphasized that the categories of direction selectivity and orientation selectivity are not tidy boxes into which all cells unambiguously fit. Figure 4 demonstrates a continuous

Figure 4. Distributions of direction indices for MT (top) and the medial third tier areas (bottom). Direction index is plotted horizontally, the number of cells in each bin is plotted vertically. MT neurons strongly tend toward direction selectivity, medial third tier neurons strongly tend toward orientation selectivity (t-test for difference of means, $p < 0.001$).

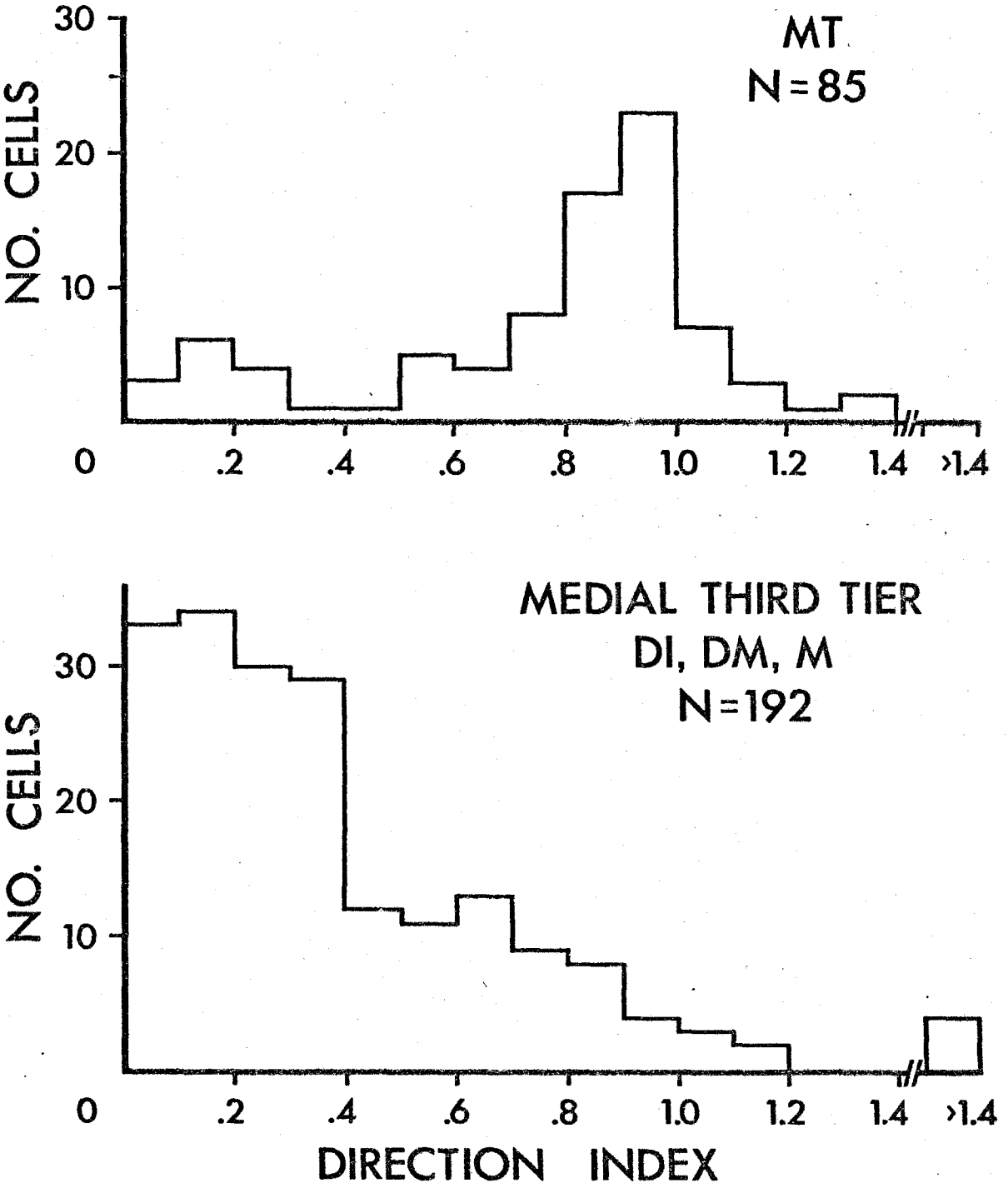
MT
N=85
NO. CELLS
30
20
10
0
.2
.4
.6
.8
1.0
1.2
1.4
>1.4
MEDIAL THIRD TIER
DI, DM, M
N=192
NO. CELLS
30
20
10
0
.2
.4
.6
.8
1.0
1.2
1.4
>1.4
DIRECTION INDEX

distribution of response patterns from completely direction-selective through various stages of direction bias to a completely "bidirectional" state of orientation-selectivity or axial direction-selectivity. Any rigid classification of response patterns to one category or the other is somewhat arbitrary. Despite these caveats, these data clearly demonstrate a localization of direction-selective cells to one of the extrastriate areas studied.

Tuning. Direction-selective cells may respond to visual stimuli moving in a range of directions on either side of the preferred direction, as does the one illustrated at the bottom of Figure 2, or they may respond to a single direction only. Neurons which respond over a narrow range are said to be "well tuned" to the preferred direction while neurons responding over a wide range are "poorly tuned." Analogously, orientation-selective cells may be well or poorly tuned to the preferred orientation. A second quantitative index which measures the degree of tuning to the optimal direction of motion was calculated for each cell for which a completed direction series was obtained. The area under 180 degrees of each response curve was calculated as a fraction of the total possible area—the area which would result if the cell had responded maximally throughout the 180 degrees of motion. The particular part of the response curve considered was the 180 degrees centered about the direction of optimal response (see shaded areas, Figure 3). The normalized area under this curve was then subtracted from 1 to yield the tuning index (see formula, lower right corner of Figure 3). The area measured was restricted to 180 degrees about the optimal direction so that tuning for orientation-selective and direction-selective cells could be measured on the same scale. For relatively well tuned cells such as the orientation-selective cell illustrated at the top of Figure 3, the response decreases quickly as the direction of motion is changed from the optimal, and the area under the relevant portion of the curve (shaded)

becomes small. Thus, the tuning index will be relatively close to one. For more poorly tuned cells such as the direction-selective cell illustrated at the bottom of Figure 3, the response decreases less rapidly as the direction of motion is changed from the optimal and the area under the relevant portion of the curve (shaded) becomes larger. Thus, the tuning index will be relatively closer to zero. Therefore, the response pattern of each cell will generate a tuning index which will be closer to one for well tuned cells and closer to zero for more poorly tuned cells. In the event that the spontaneous firing rate is inhibited in some of the relevant directions, the area under the curve is the algebraic sum of the areas above and below the zero response level (areas of inhibition being negative - see Figure 7, bottom).

The distributions of tuning indices for cells in MT and in the medial third tier are illustrated in the histograms of Figure 5. Although the difference in distributions between MT and the medial third tier is not as striking as for the direction index, it can be seen that the bulk of neurons in MT have tuning indices between 0.4 and 0.6, whereas the bulk of medial third tier neurons have tuning indices between 0.6 and 0.8. A t test for the difference of means indicates that the difference between the two distributions is very significant ($t = 3.75$, $p < .001$) with the medial third tier neurons being on the whole better tuned to the optimal stimulus than the MT neurons. For example, the well tuned medial third tier cell illustrated at the top of Figures 2 and 3 has a tuning index of 0.69, while the more poorly tuned MT cell at the bottom of the same figures has a tuning index of 0.33. It is obvious that the two distributions overlap considerably, and tightness of tuning is correspondingly less useful for distinguishing the two regions of extrastriate cortex than is direction selectivity.

Importance of Form. The form of the visual stimulus was particularly important for the responses of neurons in the medial third tier since the majority

Figure 5. Distributions of tuning indices for MT (top) and the medial third tier areas (bottom). Tuning index is plotted horizontally, the number of cells in each bin is plotted vertically. MT cells tend to be less well tuned about the optimal direction of motion than do medial third tier cells (t-test for difference of means, $p < 0.001$).

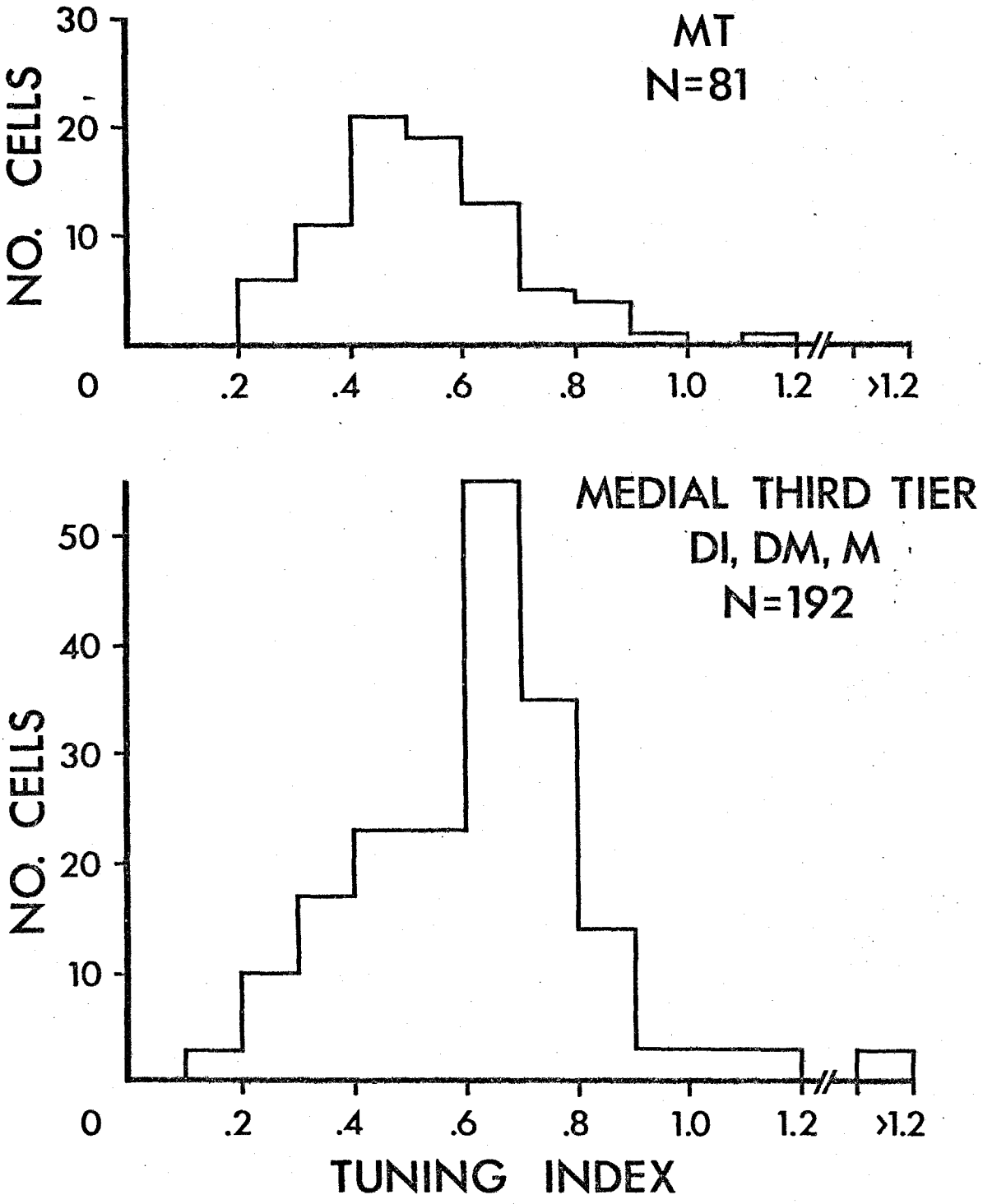
MT
N=81
NO. CELLS
30
20
10
0
.2
.4
.6
.8
1.0
1.2
>1.2
MEDIAL THIRD TIER
DI, DM, M
N=192
NO. CELLS
50
40
30
20
10
0
.2
.4
.6
.8
1.0
1.2
>1.2
TUNING INDEX

of cells were qualitatively observed to fire optimally to oriented stimuli - primarily elongate bars. However, a minority of cells in the medial third tier gave demonstrable responses to nonoriented spots of light. The response pattern of one such cell is shown in Figure 6 for two direction series, one employing a spot stimulus and one employing a bar stimulus. For this cell (from area DM), the response pattern to a spot is qualitatively similar to the response to a bar. Peak responses were obtained at 240 degrees and 60 degrees with minimum responses obtained in the orthogonal directions. Such a response pattern is typical of an orientation-selective cell, but since the same general pattern can be obtained to an unoriented stimulus, it is questionable whether the cell can be considered to be orientation-selective at all. It is possible that such an extrastriate receptive field may be composed of several small subfields, each of which is orientation-selective. If so, a relatively large spot (such as the one illustrated in Figure 6) could act as a somewhat oriented stimulus with respect to the smaller subfields. While future research on receptive field substructure may indeed verify such a hypothesis, it presently seems best to employ other, more readily interpretable, tests for orientation selectivity (see below). In MT, form was less of a critical factor since many cells responded as well to spots moving in the preferred direction as to bars. The possibility exists that such cells, in both MT and the medial third tier, may respond purely to direction of movement regardless of the form of the stimulus.

The most satisfactory experimental method for separating pure direction selectivity from orientation effects is to test the cells for orientation selectivity using stationary stimuli (Spear and Baumann, 1975). However, since neurons in MT and the medial third tier respond poorly to stationary stimuli, such an approach has not yet proven valuable. A less direct, yet informative approach is to test single neurons which give reliable responses to both oriented and nonoriented

Figure 6. Pattern of response of a single cell to a spot stimulus (top) and to a bar stimulus (bottom). Directions of motion of stimuli are plotted horizontally; the neuronal response in each direction as a percentage of the optimal response is plotted vertically. The shaded area is the area under each curve computed for calculation of the tuning index. Small visual field plots to the right of both response curves indicate the size and location of the receptive field as well as the stimulus used to obtain each response curve. A response pattern characteristic of an "orientation-selective" cell is obtained by an unoriented spot stimulus (top). Such a response pattern has been termed "axially direction-selective" (Spear and Baumann, 1975; see text for discussion). The cell still distinguishes the oriented from the unoriented stimulus by being more tightly tuned to the oriented stimulus (tuning index, bar = 0.65; tuning index, spot = 0.41).

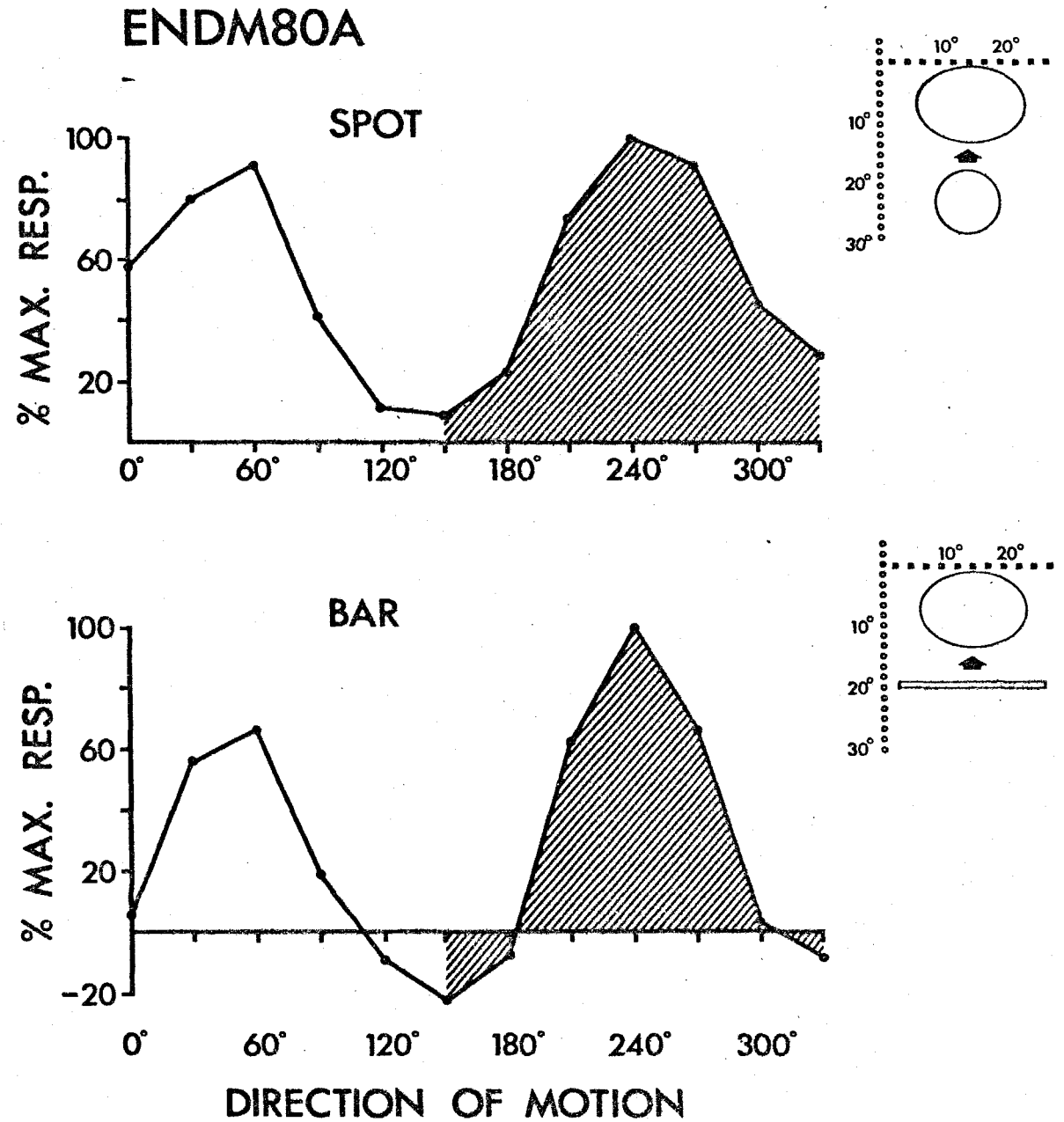

TUNING INDEX: SPOT = .41, BAR = .65

stimuli, performing two "direction series", using first a bar stimulus and then a spot. The paired data (spot vs. bar) may then be examined quantitatively for systematic differences in tuning indices. If systematic differences occur, then the cells must be affected by stimulus form as well as by direction of motion.

Forty-five cells were studied in this manner, 28 in MT and 17 in the medial third tier. The results are displayed graphically in Figure 7. Each data point on the graph represents a single neuron. The horizontal coordinate is that neuron's tuning index for the bar stimulus, and the vertical coordinate is that neuron's tuning index for the spot stimulus. The dashed line at 45 degrees is the line on which the point would fall if the tuning indices for the spot and bar were identical. For points falling below this line, the response is more tightly tuned for a bar than for a spot; for cells falling above this line, the response is more tightly tuned for the spot. It is evident that the points do not form a random distribution about the dashed line. For the medial third tier, 16 of 17 neurons fall below the line, indicating a systematically tighter tuning to bars than spots for these cells. For MT more scatter is evident, yet 20 of 28 cells fall below the dashed line indicating tighter tuning for bars. The t test for the difference of means for paired stimuli indicates that this result is highly significant in both regions ($t = 6.13$, $p < 0.001$ for medial third tier; $t = 3.57$, $p < 0.005$ for MT). For example, the neuron illustrated in Figure 6 yields a bar tuning index of 0.65 and a spot tuning of 0.41. These data show that most cells which respond well to both spots and bars in the preferred direction(s) of movement still retain the capacity to distinguish oriented from nonoriented stimuli. Therefore, even these cells can, to a certain extent, be considered orientation-selective. However, a small fraction of the cells do not discriminate form at all, or actually prefer spots to bars. More of these cells appear in MT than in the medial third tier.

Figure 7. Tuning index for bar stimulus (horizontal) vs. tuning index for spot stimulus (vertical) for 45 cells from which both sets of data were obtained. The dashed line of a 45-degree slope is the line on which a point would fall if it were equally well tuned to both stimuli. Closed circles are MT neurons, open circles are medial third tier neurons. 16 of 17 medial third tier neurons fall below the dashed line, indicating that they are more tightly tuned to an oriented stimulus. 20 of 28 MT neurons fall below the line. Both tendencies are statistically significant (t-test for difference of means, bar-tuning index means are larger than spot-tuning index means, $p < 0.001$ for medial third tier, $p < 0.005$ for MT).

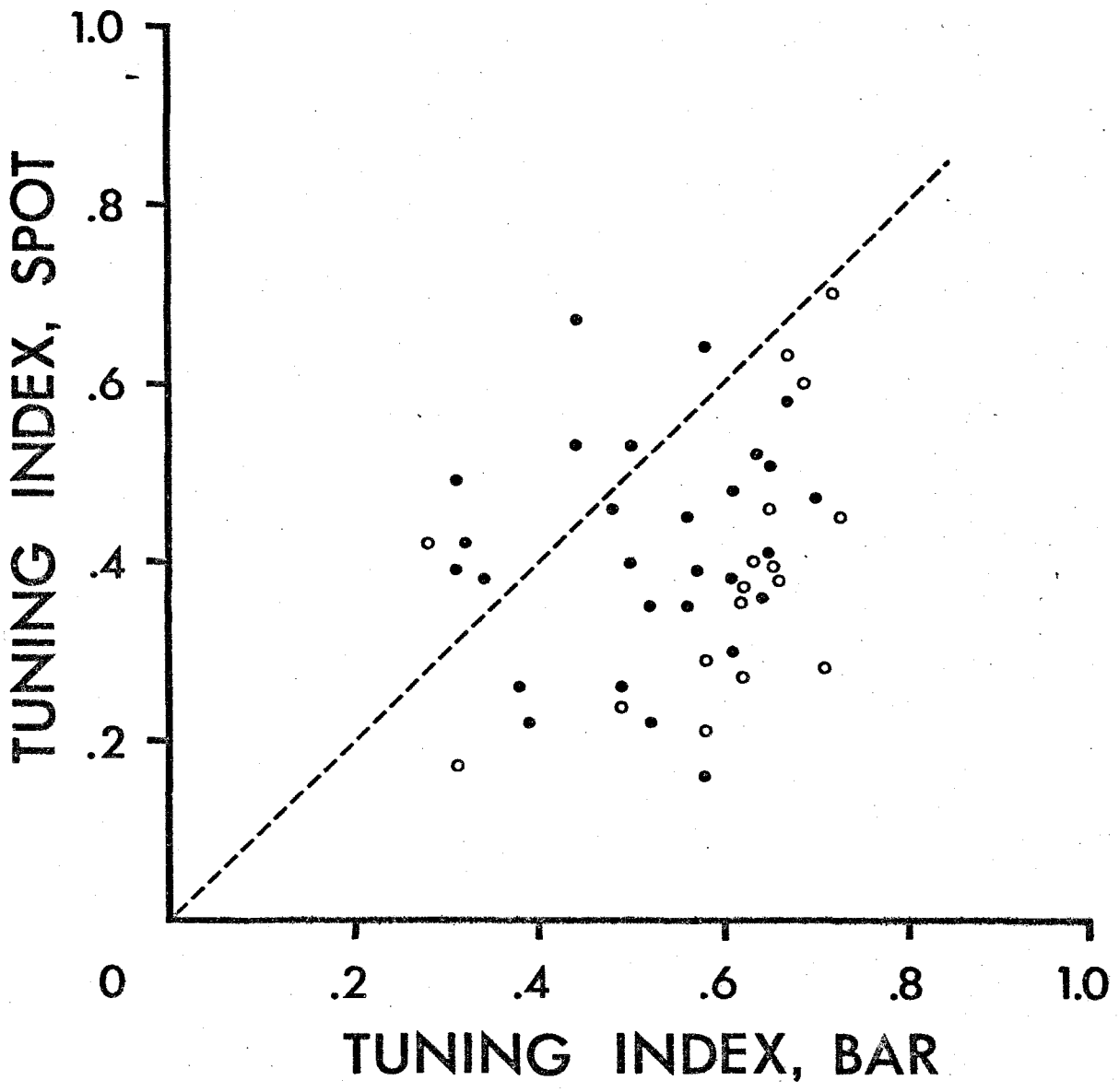

• MT, N = 28

◦ MEDIAL THIRD TIER, N = 17

Qualitative observations indicate that increasing stimulus size up to the size of the receptive field generally increases the neuronal response. Very few convincing examples were observed in which increasing size beyond the size of the receptive field resulted in any change in the cell's firing rate. Future quantitative studies may reveal such effects.

Velocity of Motion. Since virtually all cells examined in the course of this study responded optimally to moving stimuli, experiments were conducted to detect any selectivity for particular velocities of motion which might exist. Responses to moving stimuli over a wide range of velocities were examined quantitatively for 104 cells, 43 in MT and 61 in the medial third tier areas. The visual stimulus employed for a particular cell was the same stimulus which had previously been used for a direction series for that cell. The stimulus was swept through the receptive field in the direction which had been quantitatively demonstrated to yield an optimal response. A range of velocities from 1 degree/second 125 degrees/second was tested, each velocity being presented a total of five times in a pseudorandom sequence. Responses were measured by subtracting the cell's spontaneous firing rate (spikes/second) from the firing rate during stimulus presentation (spikes/second) to yield the net increase in firing rate. Many neurons exhibited strong preferences for a particular range of stimulus velocities. The data obtained from such a "velocity series" for a strongly selective MT cell are displayed graphically in Figure 8. The velocities tested are plotted linearly on the horizontal axis, while the neuronal response as a percentage of the maximum response is plotted on the vertical axis. This cell had a marked preference for a velocity of 10 degrees/second; the response decreased rapidly for stimuli moving at higher or lower velocities.

Figure 8. Response curve generated by a velocity series for an MT neuron. Stimuli are swept through the receptive field in the preferred direction. Stimulus velocities are plotted linearly on the horizontal scale; the neuronal response as a percentage of the optimal response is plotted for each velocity on the vertical scale. This cell is selective for a velocity of 10 degrees per second. The velocity tuning index is calculated by subtracting the normalized area under the tuning curve from 1. The tuning index for this cell is 0.67.

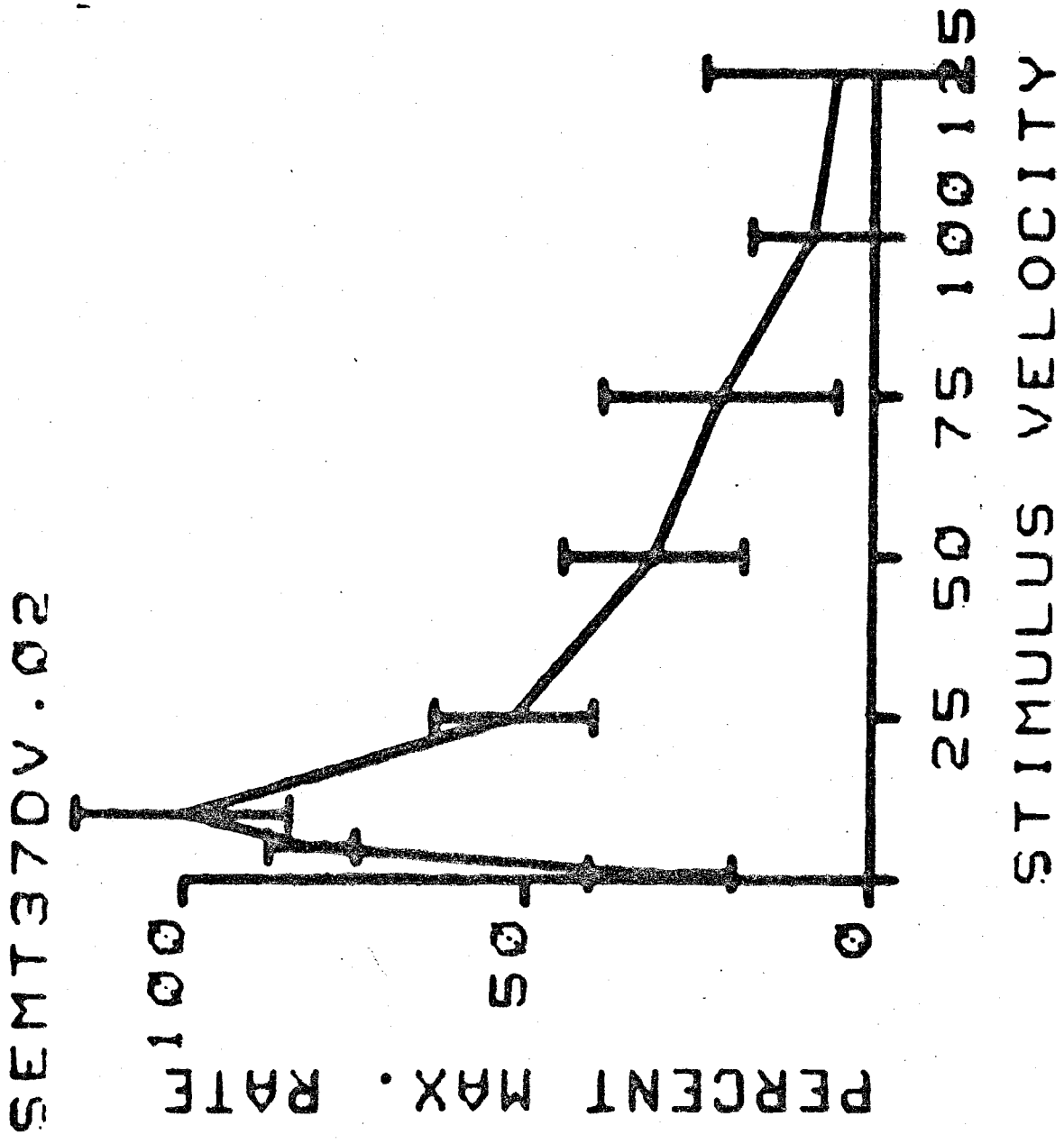
SEMT37DV.02
PERCENT MAX. RATE
100
50
0
25 50 75 100 125
STIMULUS VELOCITY

Different neurons were observed to have preferred velocities which varied over a wide range. The distributions of preferred velocities found in MT and in the medial third tier are compared in Figure 9. Clear differences in the two distributions exist ($\chi^2 = 19.68$, $p < 0.01$). MT is characterized by a distinct group of cells which exhibit preferences for relatively slow velocities (10-25 degrees/second), whereas neurons of the medial third tier areas generate a broad distribution of preferred velocities ranging from 10 to 125 degrees/second. Some neurons which appear to prefer stimuli moving at 125 degrees/second would probably have preferred higher velocities had they been tested, so the well populated bins at 125 degrees/second do not accurately reflect the fraction of the total population which actually preferred this velocity. However, it can be observed that a greater fraction of MT cells responded maximally to velocities greater than 100 degrees/second.

Response curves to velocity of motion such as the one shown in Figure 8 can also be used to calculate a quantitative index of tuning about the preferred velocity. The area under the curve is measured as a fraction of the total possible area (that area which would result if the cell were entirely unselective for velocity). The tuning index for velocity is then one minus this normalized area under the curve. Well tuned cells generated indices closer to one while poorly tuned cells result in indices closer to zero. The distributions of velocity tuning indices for MT and for the medial third tier can be seen in Figure 10. Although categorization of properties which form such a distribution is arbitrary, a qualitative guide to the tuning index might indicate that cells with indices greater than 0.5 are selective for the optimal velocity (well tuned), cells with indices from 0.3 to 0.5 are biased toward the optimal velocity, and cells with indices below 0.3 are not selective (poorly tuned). For example, the well tuned cell illustrated in Figure 8 had a velocity tuning index of 0.67. The distributions of velocity tuning indices shown

Figure 9. Distributions of preferred stimulus velocities for MT (top) and the medial third tier areas (bottom). Stimulus velocities tested are plotted horizontally; the number of cells preferring each velocity is plotted vertically. A distinct group of MT cells prefers velocities of 10-25 degrees per second. Preferred velocities of medial third tier neurons form a broad distribution from 10 to 125 degrees per second. A greater percentage of MT neurons preferred velocities greater than 100 degrees per second than was the case in the medial third tier. Distributions are significantly different (chi-square test, $p < 0.01$).

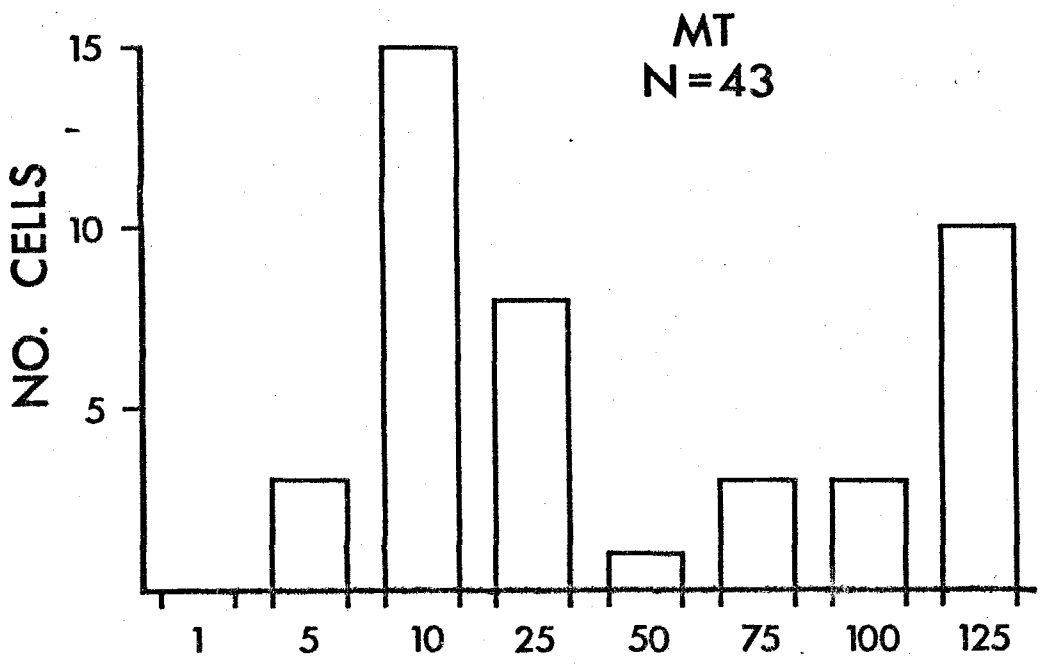
MT
N=43
NO. CELLS
15
10
5
1
5
10
25
50
75
100
125

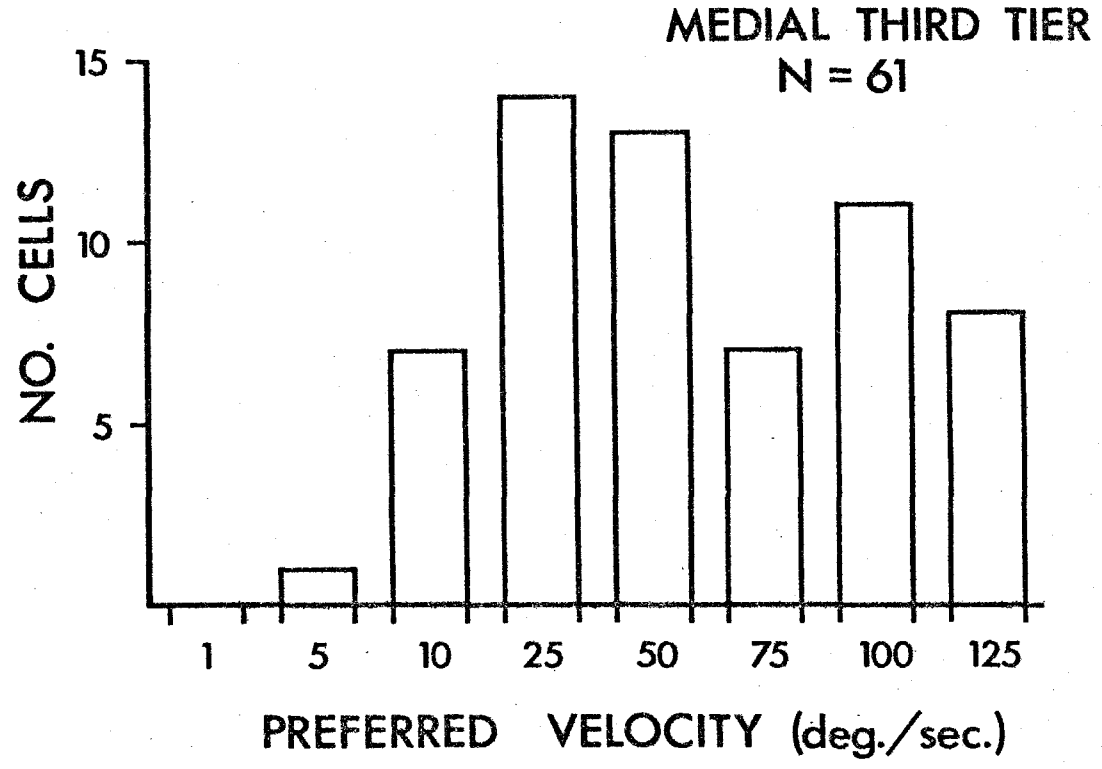
MEDIAL THIRD TIER
N = 61
NO. CELLS
15
10
5
1
5
10
25
50
75
100
125
PREFERRED VELOCITY (deg./sec.)

in Figure 10 are statistically indistinguishable (t test for the difference of means, $t = 1.37$, $p > 0.05$). Therefore, the tightness of tuning to the preferred velocity is on the whole indistinguishable between MT and the medial third tier, although the preferred velocities themselves are distinguishable.

Columnar Organization. Throughout the extrastriate areas examined, cells of similar response properties were generally encountered in clusters. The response properties of the cluster as an aggregate (as gauged by the response of the multiunit background activity) were not in general as sharply specific for particular stimulus parameters as were the individual cells within the cluster. For example, the background unit activity in MT might be broadly selective to direction of motion over a range of 180 degrees, but the individual units composing the cluster could be narrowly selective to directions of motion over a range of only 60 degrees. However, the particular 60 degrees to which individual neurons were responsive would vary within the 180-degree range to which the background was sensitive, thus accounting for the decreased specificity of the background response. Similarly, MT background activity which responded robustly in one direction and only weakly in the opposite direction (direction-biased) generally indicated the simultaneous presence of neurons which were selective for motion in the direction of the robust response, neurons which biased for motion in the direction of the robust response, and neurons which were completely orientation-selective or axially direction-selective. The point is that the multiunit activity of a cluster did not provide a precise indication of the response pattern of every cell within the cluster, but rather, defined the stimulus parameters within which the specificities of individual neurons of the cluster would fall.

It is of interest to ask whether such clusters form radial columns traversing the complete cortical depth, and whether such columns might be arranged in an

Figure 10. Distributions of velocity tuning indices for MT (top) and the medial third tier areas (bottom). The velocity tuning index is plotted horizontally; the number of cells in each bin is plotted vertically. Cells are less well tuned, on the whole, to velocity than to direction of motion. Distributions for MT and the medial third tier are not statistically different. (t-test for difference of means, $p > 0.05$).

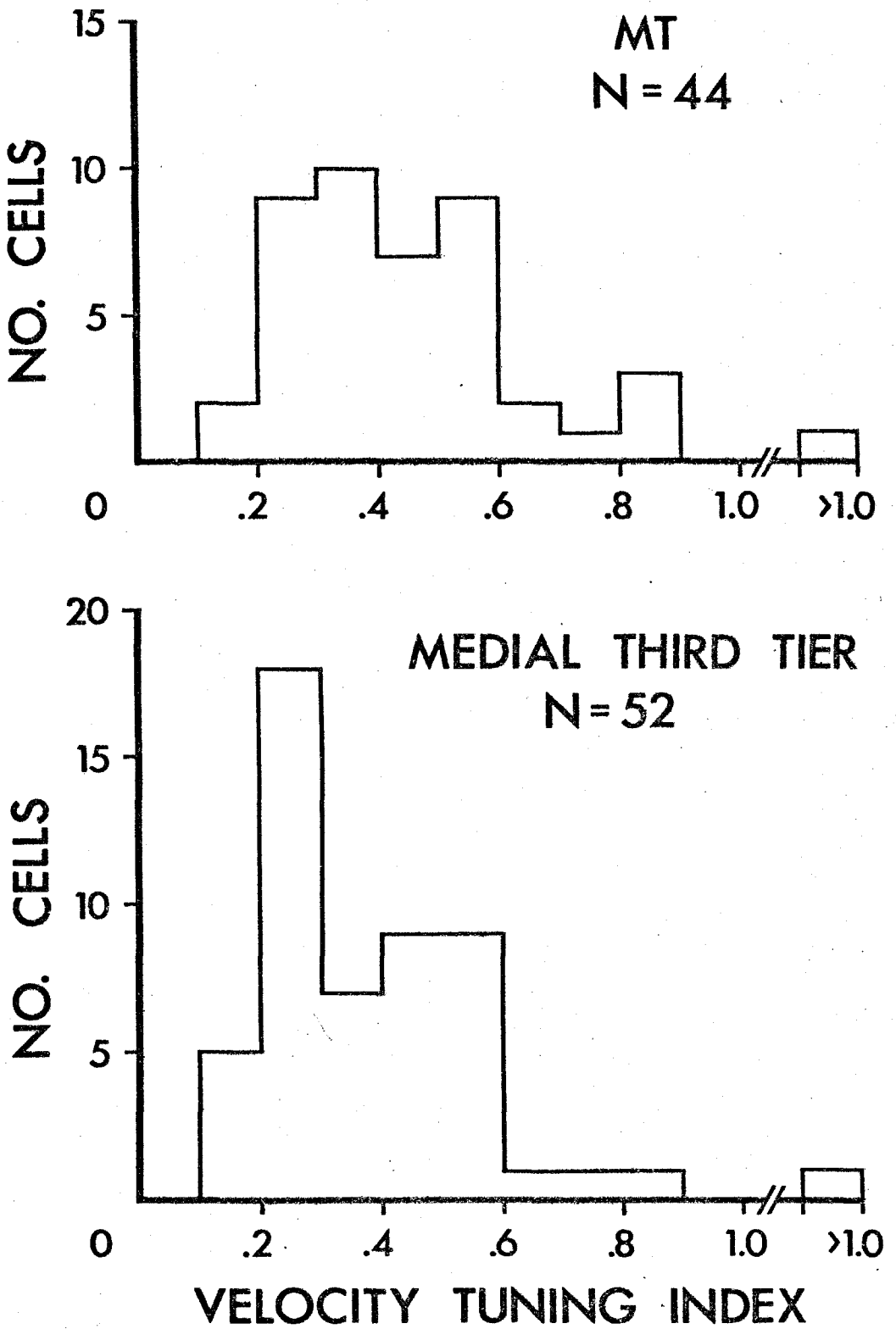
MT
N = 44
NO. CELLS
15
10
5
0
.2
.4
.6
.8
1.0
>1.0
MEDIAL THIRD TIER
N = 52
NO. CELLS
20
15
10
5
0
.2
.4
.6
.8
1.0
>1.0
VELOCITY TUNING INDEX

orderly fashion representing gradual shifts in a particular stimulus parameter. Such an orderly arrangement is known to exist for orientation columns in V1 (Hubel and Wiesel, 1975), and has been reported to exist for direction-selective columns in the striate-receptive area of the superior temporal sulcus in the macaque (Zeki, 1974a). In light of the striking anatomical and physiological similarities between MT of New World monkeys and the striate-receptive STS of the macaque (see Discussion; Van Essen, 1979), it is possible that MT of the owl monkey would contain such an arrangement of direction-selective columns. The present experiments were not specifically designed to address the question of columnar organization of MT since most penetrations were directed perpendicularly to the smooth cortical surface, and since reconstruction of electrode tracks in histological sections was not performed. However, certain observations were made which are relevant to the issue.

In Figure 11, data are presented from four penetrations in MT from which six or more sequential unit recordings were obtained. Solid vertical lines represent the individual penetrations, and the letters, representing single unit recording sites, are spaced along the length of the penetration proportional to the distance between the sites. The direction-selective or orientation-selective nature of the unit recorded at a particular site is illustrated to the right of each site. From Figure 4, it is clear that no precise dividing line can be drawn between these two cell types due to the continuous distribution of direction indices found in MT. However, for purposes of this illustration, a direction index of 0.5 was arbitrarily chosen as the deciding factor. Cells with a direction index greater than 0.5 were considered to be direction-selective, while cells with direction indices smaller than 0.5 were considered to be orientation-selective. Penetrations 2, 3, and 4 can be reasonably considered as radially-oriented penetrations due to 1) the fact that

Figure 11. Response specificities for neurons encountered in 4 MT penetrations. Distance along the penetration is plotted vertically. Capital letters represent sites of single-unit recordings. Distances between letters are proportional to distances between recording sites. The response specificity for each neuron is illustrated to the right of each recording site. The solid bar indicates the preferred stimulus orientation; arrows indicate preferred direction(s) of motion. The direction convention for text discussion is shown at the bottom right. Similar stimulus specificities of neurons in penetration 3 suggest a columnar organization. Recording sites A-F in penetration 1 suggest electrode movement across an orderly arrangement of several such columns. Penetrations 2 and 4 reflect regions of little or no columnar organization (see text for discussion).

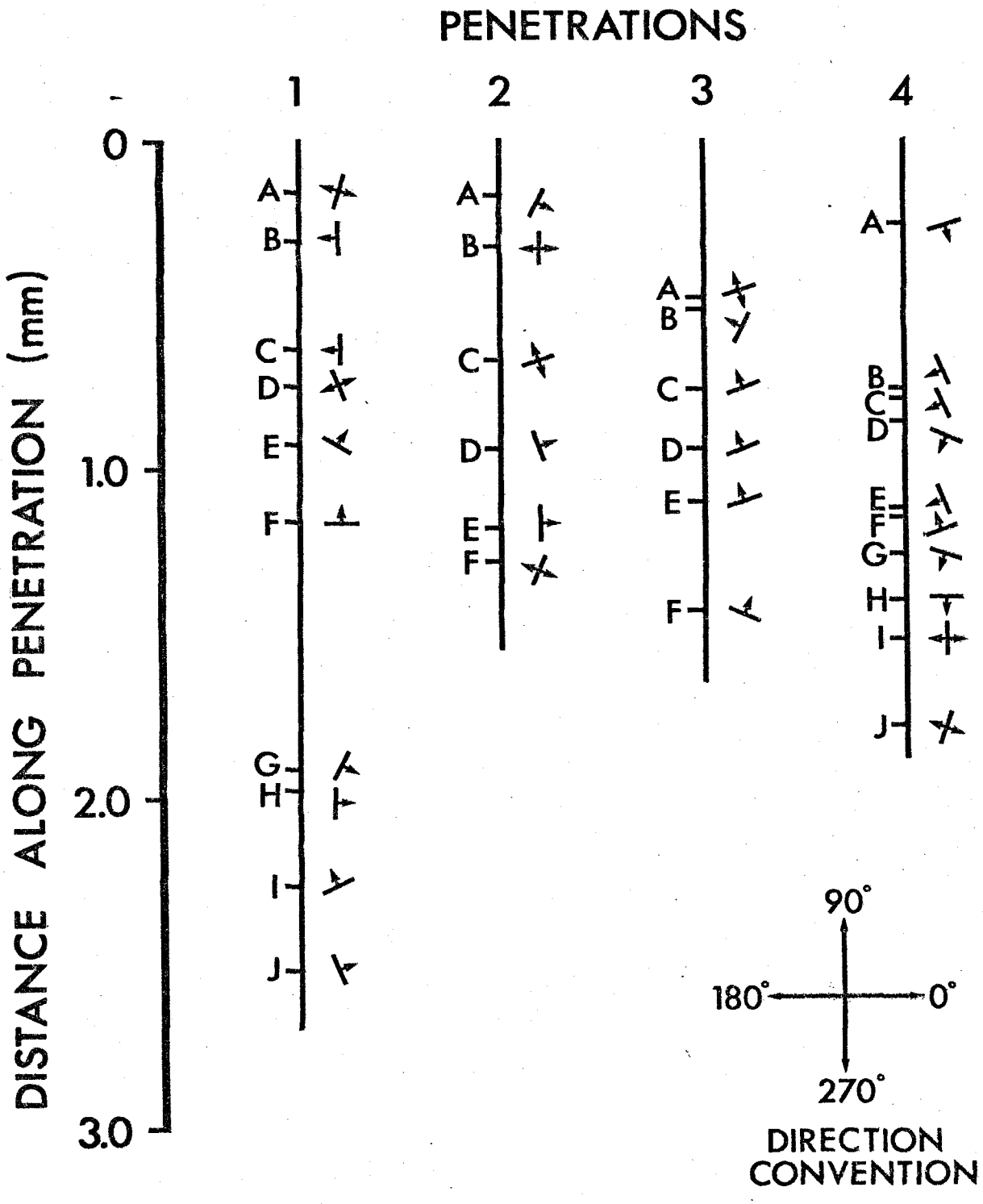
PENETRATIONS
1
2
3
4
DISTANCE ALONG PENETRATION (mm)
0
1.0
2.0
3.0
A
B
C
D
E
F
G
H
I
J
90°
180°
0°
270°
DIRECTION CONVENTION

they were perpendicularly directed to smooth, unfissured regions of MT, and 2) the fact that the length of the penetrations is within the range expected for radially-oriented penetrations (owl monkey extrastriate cortex can vary from 1.6 to 2.0 mm in thickness). Three considerations lead to the conclusion that penetation 1 ran somewhat tangentially to the cortical surface: 1) the penetration was made in the anterior part of MT near the termination of the superior temporal sulcus so that the electrode probably traversed cortex which was sloping away toward the floor of the sulcus, 2) the receptive fields encountered during this penetration formed a regular progression from about 20 degrees peripheral on the horizontal meridian to the far periphery on the horizontal meridian, as one would expect if the electrode were tangentially traversing cortex in MT near the superior temporal sulcus, and 3) the length of the penetration, 2.7 mm, is longer than the cortex is thick in a radial direction.

The overall picture which emerges from an examination of the data in Figure 11 is suggestive of a mosaic composed of some regions organized in a regular columnar manner and some regions which seem to have little or no orderly columnar organization. Evidence for a functional column of cells extending the entire thickness of the cortex can be seen in penetration 3. The preferred orientations are clustered about the 30-210 degree axis. For four of the six recording sites (A, C, D, and E), the preferred orientation is identical. In addition, five of the six cells were direction-selective with their preferred directions being similar. Evidence for orderly shifts of response properties as neighboring columns are traversed is seen in penetration 1 (a tangential penetration, see above). Recording sites A-F demonstrate an orderly progression of preferred orientation from 60 degrees through 90, 120, and 150, to 180 degrees. Within this sequence, the preferred direction of motion shifts from one direction of motion perpendicular to the axis of orientation to the opposite

direction of motion perpendicular to the axis of orientation, but these shifts in preferred direction are compatible with an orderly progression in the axis of orientation (or axis of bidirectional response for cells which lack any orientation selectivity). Evidence for regions in MT lacking columnar organization can be seen in penetrations 2 and 4. In penetration 2, the preferred axis of orientation shifts in a manner which is not obviously orderly. It could be that units were not recorded at sufficiently close intervals to reveal the columnar organization which exists, but all available evidence indicates that this penetration was nearly radial, and very narrow intervals should not be required to demonstrate columnar organization. However, disorderly shifts in preferred stimulus parameters are shown conclusively in penetration 4. Although recording sites B through E appear to belong to a homogeneous cluster, the unit recorded at F, less than 50 microns from the unit recorded at E, had a preferred direction completely orthogonal to unit E. That this is not an isolated case is clear from the fact that units at H and I in the same penetration, separated by only 100 μm, also had completely orthogonal preferred axes of orientation. These results are based on only four penetrations and should be considered tentative, but the observation is valid that certain regions of MT appear to be organized in a regular columnar manner while other regions appear relatively disorganized. The extent to which one of these conditions predominates over the whole of MT should become clear with further experimental evidence.

DISCUSSION

The major result of this study is the demonstration of a striking localization of direction-selective cells to extrastriate area MT of the owl monkey. Neurons responded maximally to moving stimuli in all four of the extrastriate areas examined,

but MT neurons preferred stimuli tuned about a single optimal direction whereas neurons of DI, DM, and M generally preferred oriented stimuli moving in either of two directions perpendicular to the optimal axis of orientation. This segregation of response properties is evident after a few penetrations in each region, and can now be used as a powerful aid in determining the particular extrastriate area from which one is recording.

Other differences in response properties were noted between MT and the medial third tier. There was a systematic difference in the tightness of tuning to the optimal stimulus direction. Neurons in MT tended to be less well tuned to the optimal direction than did neurons of the medial third tier. Neurons in MT also exhibited a different pattern of preferences for stimulus velocities than did the neurons of the medial third tier. A distinct group of MT cells had a preference for velocities of 10-25 degrees/second while cells in the medial third tier had a broad distribution of preferred velocities ranging from 10-100 degrees/second. However, a greater fraction of MT neurons preferred velocities greater than 100 degrees/second than was the case for the medial third tier. There was no systematic difference in tuning to the preferred velocity for the two regions.

The majority of cells tested in owl monkey extrastriate cortex responded better to elongate, light bars light than to nonoriented stimuli such as spots. Such cells were considered to be orientation-selective if they showed a preference for motion in either or both directions perpendicular to a particular axis of orientation. A minority of extrastriate cells responded as well to spots moving in the preferred direction as to bars. Most such cells could still distinguish oriented from nonoriented stimuli on the basis of the degree of tuning to the optimal direction of motion. These cells were generally more tightly tuned for bar stimuli than for spot stimuli and could thus be considered orientation-selective, albeit in a

weaker sense than those cells which clearly preferred oriented stimuli in the best direction. A few cells failed completely to discriminate orientation and responded in all ways similarly to a spot as to a bar. Such cells are properly considered purely direction-selective or axially direction-selective (Spear and Baumann, 1975). The response of most extrastriate cells increased with increasing stimulus size up to the width of the receptive field. Qualitatively, very few convincing cases were observed in which increasing stimulus size beyond the receptive field size had any effect upon the neuron's firing rate. Future quantitative studies may be more successful in demonstrating such effects.

The present experiments show that neuronal response properties, when quantitatively studied, place a cell at a particular location on one or more scales, each of which varies continuously from one type of response specificity to a second type. Thus, trigger feature labels such as "direction-selective," "orientation-selective," "velocity-selective," etc., do not define a neuron's response properties unambiguously, but rather define a range of values within which a measured response may fall. For example, the distribution of direction indices shown in Figure 4 does not provide an unambiguous demarcation between direction-selective and non-direction-selective cells. Arbitrarily designating dividing points, one might say that any cell with a direction index greater than 0.6 should be considered direction-selective, cells with direction indices between 0.4 and 0.6 are direction-biased, and cells falling below 0.4 are not direction-selective (such cells may be axially direction-selective, orientation-selective, or pandirectional depending upon tuning indices). From such a classification, one would conclude that 76% of the cells in MT are direction-selective, 8% are direction-biased, and 16% are not direction-selective. Similarly, one would conclude that 22% of the cells in the medial third tier are direction-selective, 12% are direction-biased, and 66% are not direction-selective.

Similarly, one might choose points on the tuning scale (Figure 5) which would group non-direction-selective cells into pandirectional (low tuning index), orientation-biased (moderate, 0.3 to 0.5, indices), and orientation-selective (high indices, may also be axially direction-selective) groups. As described earlier (see Results), arbitrary division of velocity tuning indices yields relative frequencies for velocity-selective, velocity-biased and non-velocity selective neurons. While such figures are useful for qualitative guides, the percentages will vary depending upon the particular division that is chosen. Such divisions are made by "ear" in experimental studies in which nonquantitative data collection techniques are employed. Such techniques have yielded perfectly valid results in situations where differences between populations of cells are dramatic, but quantitative techniques give a more realistic picture of the properties of a population of neurons and are almost certainly required to reliably detect more subtle variations.

The middle temporal visual area (MT) has been shown to exist in several primate species. It has been characterized by dense myelination, reception of striate projections, and its location near the boundary of the occipital and temporal lobes in the marmoset (Spatz, 1975, 1977; Spatz and Tigges, 1972) and in the squirrel monkey (Spatz et al., 1970). In addition, MT has been demonstrated to contain a complete representation of the contralateral visual hemifield in the owl monkey (Allman and Kaas, 1971a) and the bushbaby, a prosimian primate (Allman et al., 1973). Given such broad similarities, it seems safe to conclude that MT is a homologous visual area in each of these species.

Whether or not any visual area homologous to MT exists in Old World monkeys is a more complex issue. The extensive convolution of the macaque cortex has retarded the study of topographic organization, and has made comparisons with extrastriate cortex of smooth-brained primate species difficult.

The striate-receptive visual area of the superior temporal sulcus became a prime candidate for an Old World primate homologue of MT when a unique pattern of striate connections was found to occur in both structures. Using the technique of retrograde transport of HRP, Spatz (1975, 1977) showed that the striate projection to MT in the marmoset (a New World monkey) originated from layer IVb and from the solitary cells of Meynert at the boundary between layers V and VI. Lund et al. (1976) have also used the retrograde transport of HRP to demonstrate an identical origin of striate projections to the striate-receptive STS in the macaque. This pattern of projections in the two species is particularly striking since the projection of the solitary cells of Meynert to MT and to the striate-receptive area of the STS is the first firmly identified cortico-cortical projection of striate cortex which originates in the deep layers (V and VI). Such a projection from the deep layers of striate cortex to MT was reported in the squirrel monkey (Spatz et al., 1970), but was not observed in a later study (Martinez-Milan and Hollander, 1975). However, both of these studies relied upon the restriction of proline injections or lesions to particular laminae of striate cortex, and are therefore more suspect than the previously mentioned studies using retrograde transport of HRP.

Recent results have made the case for homology between MT and the striate-receptive STS compelling. The striate-receptive area of the STS has been shown to be coextensive with a region of heavily myelinated fibers (Ungerleider and Mishkin, 1979; Maunsell et al., 1979) as is MT in New World monkeys. Striate-receptive STS of the macaque has also been shown to be topographically organized (Ungerleider and Mishkin, 1979; Weller and Kaas, 1978) although the topography may be somewhat more complex than for MT of New World monkeys (Maunsell et al., 1979). Zeki (1974) has shown that neurons of the striate-receptive STS are overwhelmingly direction-selective, and this result has received confirmation

from other investigators (Gattas and Gross, 1979; Van Essen et al., 1979). The results reported in the present study indicate a preponderance of direction-selective cells in MT of a New World monkey, the owl monkey. In this light, it is interesting to note that Dow (1974) has reported a concentration of direction-selective cells in layer IVb of macaque striate cortex, which in turn projects to the striate-receptive STS. It now seems highly probable that MT is an extrastriate visual area which is present throughout the primate order. Interestingly, Allman (1977) has pointed out the observation made by Flechsig during the course of his pioneering myelogenetic studies, that an early and heavily myelinating region of cortex exists in the human near the junction of the occipital and temporal lobes. It is an intriguing possibility that such an early myelinating center might be a human homologue of MT.

No clear homologues of MT exist outside the primate order. A possible candidate is the lateral suprasylvian region of the cat in which a concentration of direction-selective cells has been found (Spear and Baumann, 1975; Camarda and Rizzolatti, 1976). However, this region is not characterized by heavy myelination as is primate MT, and its connections with striate cortex do not conform to the peculiar pattern of such connections found for primate MT (Gilbert and Kelly, 1975). Definite conclusions concerning nonprimate homologues of MT must await future studies of the embryological origins and functional roles of possible homologues.

REFERENCES

Allman, J. M. (1977). Evolution of the visual system in the early primates. In Progress in Psychobiology and Physiological Psychology, Vol. 7, eds. Sprague, J. M. and Epstein, A. N. New York: Academic Press.

Allman, J. M. and Kaas, J. H. (1971a). A representation of the visual field in the caudal third of the middle temporal gyrus of the owl monkey (Aotus trivirgatus). Brain Research **31**, 84-105.

Allman, J. M. and Kaas, J. H. (1971b). Representation of the visual field in striate and adjoining cortex of the owl monkey (Aotus trivirgatus). Brain Research **35**, 89-106.

Allman, J. M. and Kaas, J. H. (1974a). The organization of the second visual area (VII) in the owl monkey: A second order transformation of the visual hemifield. Brain Research **76**, 247-265.

Allman, J. M. and Kaas, J. H. (1974b). A crescent-shaped cortical visual area surrounding the middle temporal area (MT) in the owl monkey (Aotus trivirgatus). Brain Research **81**, 199-213.

Allman, J. M. and Kaas, J. H. (1975). The dorsomedial cortical visual area: A third tier area in the occipital lobe of the owl monkey (Aotus trivirgatus). Brain Research **100**, 473-487.

Allman, J. M. and Kaas, J. H. (1976). Representation of the visual field on the medial wall of occipital-parietal cortex in the owl monkey. Science **191**, 572-575.

Allman, J. M., Kaas, J. H. and Lane, R. H. (1973). The middle temporal visual area (MT) in the bushbaby, Galago senegalensis. Brain Research **57**, 197-202.

Camarda, R. and Rizzolatti, G. (1976). Visual receptive fields in the lateral suprasylvian area (Clare-Bishop area) of the cat. Brain Research **101**, 427-443.

Clare, M. H. and Bishop, G. H. (1954). Responses from an association area secondarily activated from optic cortex. Journal of Neurophysiology **17**, 271-277.

Cragg, B. G. and Ainsworth, A. (1969). The topography of the afferent projections in circumstriate visual cortex of the monkey studied by the Nauta method. Vision Research **9**, 733-747.

Dow, B. M. (1974). Functional classes of cells and their laminar distribution in monkey visual cortex. Journal of Neurophysiology **37**, 927-946.

Gattas, R. and Gross, C. G. (1979). A visuotopically organized area in the posterior superior temporal sulcus of the macaque. ARVO Annual Meeting, Abstracts. p. 184.

Gilbert, C. D. and Kelley, J. P. (1975). The projections of cells in different layers of the cat's visual cortex. Journal of Comparative Neurology **163**, 81-106.

Hubel, D. H. and Wiesel, T. N. (1965). Receptive fields and functional architecture in two non-striate visual areas (18 and 19) of the cat. Journal of Neurophysiology **28**, 229-289.

Hubel, D. H. and Wiesel, T. N. (1974). Sequence regularity and geometry of orientation columns in the monkey striate cortex. Journal of Comparative Neurology **158**, 267-294.

Lund, J. S., Lund, R. D., Hendrickson, A. E., Bunt, A. H. and Fuchs, A. F. (1976). The origin of efferent pathways from the primary visual cortex, area 17, of the macaque monkey as shown by retrograde transport of horseradish peroxidase. Journal of Comparative Neurology **164**, 287-304.

Martinez-Milan, L. and Hollander, H. (1975). Cortico-cortical projections from striate cortex of the squirrel monkey (Saimiri sciureus). A radioautographic study. Brain Research **83**, 405-417.

Maunsell, J. H. R., Bixby, J. L. and Van Essen, D. C. (1979). The middle temporal area (MT) in the macaque: Architecture, functional properties and topographic organization. Society for Neuroscience, Abstracts (submitted).

Palmer, L. A., Rosenquist, A. C. and Tusa, R. J. (1978). The retinotopic organization of lateral suprasylvian visual areas in the cat. Journal of Comparative Neurology **177**, 237-256.

Schiller, P. H., Finlay, B. L. and Volman, S. F. (1976). Quantitative studies of single-cell properties in monkey striate cortex. I. Spatiotemporal organization of receptive fields. Journal of Neurophysiology **39**, 1288-1319.

Spatz, W. B. and Tigges, J. (1972). Experimental-anatomical studies on the "middle temporal visual area (MT)" in primates. I. Efferent cortico-cortical connections in the marmoset, Callithrix jacchus. Journal of Comparative Neurology **146**, 451-464.

Spatz, W. B. (1975). An efferent connection of the solitary cells of Meynert. A study with horseradish peroxidases in the marmoset Callithrix. Brain Research **92**, 450-455.

Spatz, W. B. (1977). Topographically organized reciprocal connections between areas 17 and MT (visual area of the superior temporal sulcus) in the marmoset (Callithrix jacchus). Experimental Brain Research **27**, 559-572.

Spatz, W. B., Tigges, J. and Tigges, M. (1970). Subcortical projections, cortical associations, and some intrinsic interlaminar connections of the striate cortex in the squirrel monkey (Saimiri). Journal of Comparative Neurology **140**, 155-174.

Spear, P. D. and Baumann, T. P. (1975). Receptive-field characteristics of single neurons in lateral suprasylvian visual area of the cat. Journal of Neurophysiology **38**, 1403-1420.

Talbot, S. A. (1942). A lateral localization in cat's visual cortex. Federation Proceedings 1, 84.

Tusa, R. J., Palmer, L. A. and Rosenquist, A. C. (1978). The retinotopic organization of area 17 (striate cortex) in the cat. Journal of Comparative Neurology 177, 213-236.

Tusa, R. J., Rosenquist, A. C. and Palmer, L. A. (1979). Retinotopic organization of areas 18 and 19 in the cat. Journal of Comparative Neurology 185, 657-678.

Ungerleider, L. G. and Mishkin, M. (1979). The striate projection zone in the superior temporal sulcus of Macaca mulatta: Location and topographic organization (submitted for publication).

Van Essen, D. C. (1979). Visual cortical areas. In Annual Review of Neuroscience, Vol. 2, ed. Cowan, W. M. Palo Alto: Annual Reviews, Inc.

Van Essen, D. C., Maunsell, J. H. R. and Bixby, J. L. (1979). The organization of extrastriate visual areas in the macaque monkey. To be published in Multiple Cortical Areas, ed. Woolsey, C. N. Humana Press.

Van Essen, D. C. and Zeki, S. M. (1978). The topographic organization of rhesus monkey prestriate cortex. Journal of Physiology (Lond.) 277, 193-226.

Weller, R. E. and Kaas, J. H. (1978). Connections of striate cortex with the posterior bank of the superior temporal sulcus in macaque monkeys. Society for Neuroscience, 8th Annual Meeting, Abstracts. p. 650.

Wolbarsht, M. L., MacNichol, E. F. and Wagner, H. G. (1960). Glass insulated platinum microelectrode. Science 132, 1309-1310.

Zeki, S. M. (1969). Representation of central visual fields in prestriate cortex of monkey. Brain Research 14, 271-291.

Zeki, S. M. (1970). Interhemispheric connections of prestriate cortex in monkey. Brain Research 19, 63-75.

Zeki, S. M. (1973). Colour coding in rhesus monkey prestriate cortex. Brain Research **53**, 422-427.

Zeki, S. M. (1974). Functional organization of a visual area in the posterior bank of the superior temporal sulcus of the rhesis monkey. Journal of Physiology (Lond.) **236**, 549-573.

Zeki, S. M. (1978). Uniformity and diversity of structure and function in rhesus monkey prestriate cortex. Journal of Physiology (Lond.) **277**, 273-290.

Zeki, S. M. and Sandeman, D. R. (1976). Combined anatomical and electrophysiological studies on the boundary between the second and third visual areas of rhesus monkey cortex. Proceedings of the Royal Society, London, Series B **194**, 555-562.

APPENDIX 1

Statistics, medial third tier areas

A. Area breakdown of medial third tier neurons

Total neurons recorded from medial third tier areas	190
Neurons recorded from dorsointermediate area, DI	25
Neurons recorded from dorsomedial area, DM	84
Neurons recorded from medial area, M	28
Neurons recorded from medial third tier but not definitely located to one area (close to border between DM and DI or between DM and M - see Figure 1)	53

B. Direction Index, t-test for difference of means, two-tailed

	N	mean	std. dev.		t value	p value
DI	25	0.427	0.423	DI vs. DM	0.843	p>0.1
DM	84	0.405	0.395	DI vs. ME	0.821	p>0.1
ME	28	0.349	0.229	DM vs. ME	0.917	p>0.1

C. Tuning Index, t-test for difference of means, two-tailed

	N	mean	std. dev.		t value	p value
DI	25	0.610	0.350	DI vs. DM	0.313	p>0.1
DM	84	0.670	0.257	DI vs. ME	0.501	p>0.1
ME	28	0.570	0.203	DM vs. ME	2.104	p<0.05

D. Velocity Tuning Index, t-test for difference of means, two-tailed

	N	mean	std. dev.		t value	p value
DI	4	0.480	0.302	DI vs. DM	0.691	p>0.1
DM	20	0.383	0.164	DI vs. ME	0.389	p>0.1
ME	14	0.409	0.266	DM vs. ME	0.200	p>0.1

APPENDIX 1 (cont.)

E. Preferred Velocity, chi squared test, two-tailed

	1°/sec	5°/sec	10°/sec	25°/sec	50°/sec	75°/sec	100°/sec	125°/sec
DI	0	0	0	3	1	0	0	0
DM	0	1	4	5	9	3	4	3
ME	0	0	1	4	2	2	4	1

$\chi^2 = 10.23$ $p>0.1$

APPENDIX 2

Statistics, MT vs. Medial third tier

A. Direction Index, t-test for difference of means, two-tailed

	N	mean	std. dev.	
MT	85	0.781	0.319	$t = 9.24$
Medial third tier	190	0.383	0.349	$p < 0.001$

B. Tuning Index, t-test for difference of means, two-tailed

	N	mean	std. dev.	
MT	81	0.530	0.170	$t = 3.35$
Medial third tier	190	0.637	0.270	$p < 0.001$

C. Velocity Tuning Index, t-test for difference of means, two-tailed

	N	mean	std. dev.	
MT	44	0.448	0.207	$t = 1.37$
Medial third tier	52	0.392	0.189	$p > 0.1$

D. Preferred Velocity, Chi squared test, two-tailed

	1°/sec	5°/sec	10°/sec	25°/sec	50°/sec	75°/sec	100°/sec	125°/sec
MT	0	3	15	8	1	3	3	10
Medial third tier	0	1	7	14	13	7	11	8

$\chi^2 = 19.682$ $p < 0.01$

E. Tuning - Spot vs. Bar, t-test for difference (d) of paired stimuli, one-tailed

for MT: $\bar{d} = 0.107$ std. dev. = 0.159

$t = 3.56$ $p < 0.005$

for Medial third tier: $\bar{d} = 0.211$ std. dev. = 0.142

$t = 6.13$ $p < 0.001$